The IgG Paradox:
Unraveling Pro- and Anti-Inflammatory Mechanisms
in Neuroinflammatory Disease

Dissertation

zur

Erlangung der naturwissenschaftlichen Doktorwürde
(Dr. sc. nat.)

vorgelegt der

Mathematisch-naturwissenschaftlichen Fakultät

der

Universität Zürich

von

Isaak Josef Quast

aus

Österreich

Promotionskomitee

Prof. Dr. rer nat. Christian Münz (Vorsitz)
Prof. Dr. med Jan D. Lünemann
Prof. Dr. rer nat. Burkhard Becher

Zürich, 2015

Disclaimer

This thesis was based on and partly adapted form the following manuscripts:

Quast I., Lünemann JD. *Fc glycan-modulated immunoglobulin G effector functions*
J Clin Immunol. 2014 Jul;34 Suppl 1:S51-5. doi: 10.1007/s10875-014-0018-3.

Quast I., Cueni F., Nimmerjahn F., Tackenberg B., Lünemann JD. *Deregulated Fcγ Receptor Expression in Patients with CIDP*
Neurology: Neuroimmunology & Neuroinflammation. Accepted June 2015

Quast I., Keller CW., Maurer MA, Giddens JP., Tackenberg B., Wang L-X., Münz C., Nimmerjahn F., Dalakas M., Lünemann JD. *IgG Fc-sialylation impairs complement-dependent cytotoxicity*
Under review

Acknowledgement

This thesis would not have been written without the support of many people.

First and foremost I would like to thank Jan Lünemann for giving me the opportunity to work in his lab. I am particularly grateful for your guidance in the beginning of my PhD, for giving me the freedom to develop my own ideas and projects and for enabling me the attendance to scientific meetings..

To Christian Münz: thank you for all your contributions of time, ideas and funding, for always-welcoming discussions and for being member of my PhD committee.

To Burkhard Becher: thank you for your scientific advice, in particular concerning animal experiments, and for being member of my PhD committee.

Special thanks go to Rosa Barreira da Silva, Johannes vom Berg and Miguel Maurer for a very warm welcome when I arrived to the lab and for ensuring a good life-work balance by introducing me to all the bars, clubs and restaurants of Zürich.

To Miguel Maurer and Christian Keller: discussing experiments with you was definitely one of the most joyful aspects of my time as a PhD student. Your support and contributions to my experiments were really important for me. Also, many thanks for all the concert-evenings we`ve been to!

To Patrick Weber: thank you for your precise work, for teaching me how to do animal experiments and automate protein purification, for science-free coffee breaks and for your enthusiasm and willingness to improve the quality of reagents and experiments!

To Flavio Cueni: supervising others has to be learned and you were my first experiment of that kind. I am very thankful for your patience, your work and the nice time with you in the lab!

To Michael Hohl, Markus Seeger and Damien Morger: thank you for answering all my questions about proteins, HPLC, columns, vectors, tags,…

Thanks to the past and present members of the Institute of Experimental Immunology for a great working environment! In particular, thank you Kristina Kakalacheva, Christina Sina, Ana Raykova, Vanessa Landtwing, Olga Antsiferova, Carol Sze Ki Leung, Sonja Rämer, Danusia Vanoaica, Anne Müller, Monique Gannage, Susana Romao, Heike Nowag, Bithi Chatterjee, Iva Lelios, Margit Lanzinger, Bettina Schreiner, Paulina Klug, Melissa Vrohlings, Anne Buttgereit, Kathrin Nussbaum, Sabine Spath, Melanie Greter, Maries van den Broek, Laura Surace, Donal McHugh, Obinna Chijioke, Patrick Rämer, Stanislav Pantelyushin, Felix Hartmann, Vinko Tosevski, Andrew Croxford, Tom Hartwig, Florian Mayr, Andreas Müller and Kay Hänggi for your personal and professional contributions.

I thank our collaborators Lai Xi Wang, John Giddens, Björn Tackenberg, Falk Nimmerjahn and Marinos Dalakas for providing essential reagents and patient material and for discussing experimental results.

Thanks Catañoles for all the great evenings together talking about everything but science.

Lluïsa, Josep i Jordi: moltes gràcies per una benvinguda tan agradable a la vostra vida, casa i cuina!

An meine Brüder: Danke für die Gewissheit, dass ihr da seit wenn ich etwas brauche und dass ich mir (obwohl ich nicht mehr auf euch aufpassen kann) keine Sorgen um euch machen muss.

An meine Eltern: Danke für die Unterstützung meiner Ziele, Wünsche und Träume sowie die bedingungslose Freiheit diese selbst zu bestimmen und den Weg dorthin zu finden.

To Eva: thank you for coming to Zürich to be with me, for making me happy even when I think work just doesn’t allow me to be, for supporting my dream to continue with science and for all the love and encouragement you give to me.

Summary

Immunoglobulin gamma (IgG) molecules are preeminent effector proteins of the humoral immune system. Their antigen-binding fragment, Fab, recognizes cognate antigens with high specificity and their constant region (Fc) conveys pro-inflammatory effector functions such as recruitment and activation of leukocytes through engagement with Fcγ receptors (FcγRs) and complement activation. However, high doses of pooled, monomeric IgG depict anti-inflammatory activity as reflected by the therapeutic efficacy of intravenous immunoglobulins (IVIG) in several autoimmune diseases. The underlying mechanisms that confer these anti-inflammatory activity are incompletely understood. Experimental data provide evidence that IgG Fc-linked glycan structures regulate antibody-mediated effector functions. As such, the presence of terminal sialic acid acts as a molecular switch shifting IgG activity from a pro-inflammatory to an anti-inflammatory pathway. We investigated mediators and regulators of IgG functions such as FcγR expression and Fc-linked glycan structures in patients with chronic inflammatory demyelinating polyneuropathy (CIDP), an autoimmune disease of the peripheral nervous system in which humoral immune responses are central in mediating tissue damage. Compared to healthy individuals, patients with CIDP showed increased expression levels of activating FcγRs and decreased expression of inhibitory FcγRIIB indicating that the FcγR regulatory system is disturbed. Clinically effective IVIG therapy partially restored deregulated FcγR expression. In addition, induction of IgG Fc-sialylation was associated with clinical disease remission over time. We demonstrate that IgG Fc sialylation does not affect antibody-dependent cell-mediated cytotoxicity (ADCC) but impairs the efficacy of IgG molecules to activate complement by inhibition of C1q binding to galactosylated IgG. We conclude from these data that inhibition of CDC represents an FcγR-independent mechanism by which Fc-sialylated glycovariants might limit pro-inflammatory IgG effector functions. Thus, our data support the development of strategies that target increased Fc-sialylation for the treatment of human autoimmune diseases. In addition, we found that dimeric antigen-binding fragments, $F(ab')_2$, are sufficient to prevent disease development in a murine model of T cell mediated autoimmunity, indicating that more than one mechanism is responsible for the clinical efficacy of IVIG.

Zusammenfassung

Immunoglubulin-gamma (IgG) Antikörper sind wichtige Effektor-Proteine des humoralen Immunsystems. Über ihre antigen-bindenden Regionen (Fab) erkennen sie Zielstrukturen mit hoher Spezifität und die konstante Region (Fc) vermittelt Effektormechanismen wie die Aktvierung von Leukozyten über Fcγ-Rezeptoren (FcγR) oder Komplementaktivierung. Darüber hinaus wirken hohe Dosen intravenös appliziertem IgG (IVIG) anti-inflammatorisch, eine Eigenschaft die zur Behandlung von Autoimmunerkrankungen eingesetzt wird. Welche Mechanismen allerdings dafür verantwortlich sind, ist unzureichend bekannt. Untersuchungen haben gezeigt, dass die Struktur des Zuckers in der Fc-Region die Funktionalität von Antikörpern beeinflusst. So wird der Anwesenheit von Sialylsäure zugeschrieben, dass sie als molekularer Schaltmechanismus von pro- auf anti-inflammatorisch fungiert. Wir haben FcγR und IgG-Fc Zuckerstrukturen in Patienten mit Chronischer Inflammatorischer Demyelinisierender Polyneuropathie (CIDP) untersucht, einer Erkrankung des peripheren Nervensystems in der humorale Immunantworten von zentraler Bedeutung sind. Im Vergleich zu gesunden Individuen hatten CIDP Patienten mehr aktivierende FcγR auf der Zelloberfläche und weniger inhibitorische FcγRIIB, was ein regulatorisches Ungleichgewicht suggeriert. Behandlung mit IVIG führte zu einer teilweisen Normalisierung der FcγR Expression. Ausserdem konnten wir zeigen, dass die vermehrte Präsenz von Sialylsäure am IgG-Fc Zucker mit klinischer Remission der Erkrankung korreliert. Die Analyse von Antikörpern mit unterschiedlichen Fc-Zuckervarianten zeigte, dass komplement-vermittelte (CDC), nicht aber zell-vermittelte Zytotoxizität (ADCC) durch die Anwesenheit von Sialylsäure verringert wird. Wir schlussfolgern daraus, dass Sialylsäure die pro-inflammatorische Aktivität von IgG durch Reduktion von Komplement-Aktivierung vermindert. Dies empfiehlt die Entwicklung von therapeutischen Strategien zur Induktion von IgG-Fc Sialylierung. Zusätzlich konnten wir in murinen modellsystems für T Zell vermittelte Autoimmunität nachweisen, dass isolierte antigen-bindende Fragmente anti-inflammatorisch wirken können. Dies zeigt, dass die therapeutische Wirksamkeit von IVIG wahrscheinlich nicht auf einen einzelnen Mechanismus zurückzuführen ist sondern auf der Kombination mehrerer beruht.

Table of contents

1. Introduction

1.1 Basic concepts and components of the immune system

In biology, immunity is defined as the resistance to develop a pathologic condition.
The fight against biological invasion needs to be balanced with maintenance of immune homeostasis to avoid overwhelming inflammation and autoimmune disease. An important implication to fulfill this function is the ability to distinguish “normal” self from non-self, a property that even the most primitive eukaryotes possess [1]. Physical barriers such as the skin are the first preventive measures against the invasion of foreign organisms. If they fail, an active immune response is initiated by cellular and humoral components of the innate immune system through recognition of pathogen associated molecular patterns (PAMPs). Joint host-pathogen evolution led to the development of germline-encoded PAMP-recognizing molecules however, in parallel, pathogens evolved to avoid recognition and actively interfere with the immune system. As a result, innate immunity is insufficient for host protection.
This led to the development of a second line of defense found in all jawed vertebrates: the adaptive immune system [2]. One important feature of adaptive immunity is that its specificity is not restricted by the germline, instead somatic DNA modification allows for the directed generation of novel antigen binding receptors. Besides inactivation of invading organisms, the phagocytes of the innate immune system process and present pathogen-derived components to lymphocytes (T and B cells), the cellular members of the adaptive immune system. Whereas T cells developed to recognize mostly linear protein epitopes presented on the cell surface of antigen presenting cells and virus or tumor transformed cells, B cells recognize antigens in their native confirmation. A complex selection process prevents the development of cells reactive to self-antigens while enabling specific high-affinity recognition of foreign antigens. The second cardinal feature of adaptive immunity is the transition of successfully developed antigen-specific T or B cells into a pool of long-lived cells. Re-encounter of the same antigen (for example by a second infection with the same pathogen) leads to reactivation and subsequent proliferation of the respective cells thereby enabling a more rapid secondary response. The communication between innate and adaptive immunity is bidirectional and both systems depend on each other for functionality. A list of the basic components of the immune system is given in table 1.1.

	Type	Mediator		Function
Innate immunity	Barriers	Physical barrier		Prevention of microbe entry
		Antibiotics (defensins, cathelicidins)		Prevention of microbe entry
		Intraepithelial leukocytes		Prevention of microbe entry
	Cells	Granulocytes		Phagocytosis and killing of microbes
		Macrophages		Phagocytosis and killing of microbes
		NK cells		Killing of infected and tumor transformed cells
		Dendritic cells		antigen presentation to T & B cells
	Soluble mediators	Complement		Killing of microbes, opsonization of microbes, activation of leukocytes
		Mannose-binding lectin		Opsonization of microbes, activation of complement
		C-reactive protein		Opsonization of microbes, activation of complement
		Cytokines & chemokines		Inhibition of microbial spread, regulation of leukocyte homing, differentiation and proliferation
Adaptive immunity	Cells	B cells	Conventional B cells	Antibody production
			Regulatory B cells	Regulation of adaptive immune responses (maintenance of self-tolerance)
		T cells	$CD4^+$ T cells	Activation of macrophages and dendritic cells, stimulation and regulation of B & T cell responses
			$CD8^+$ T cells	Killing of infected and tumor transformed cells
			$FoxP3^+$ T cells	Suppression of T cell function (maintenance of self-tolerance)
	Soluble mediators	Antibodies		Neutralization, opsonization and phagocytosis of microbes, CDC, ADCC
		Cytokines & chemokines		Inhibition of microbial spread, regulation of leukocyte homing, differentiation and proliferation

Table 1.1 Components of the immune system
Adapted from [3, 4].

1.2 Antibodies

1.2.1 The history of antibodies: From serum therapy to clonal selection and monoclonal antibodies

At the end of the 19th century, Emil Behring and Shibasabura Kitasato made the landmark finding that transfer of serum from animals immunized with diphtheria toxin can be used to protect animals from an otherwise lethal dose of toxin [5]. This was the first confirmed description of passive immunization and the basis for a new field of research: immunology [6]. The protective effect was found to be specific as immunization with one toxin would only lead to protection against the very same toxin. The urgent need for treatment of diphtheria resulted in rapid attempts to translate this finding into clinical use. Immunization of sheep and horses

were the first sources of serum and treatment showed promising results but fever, rashes and also serious anaphylactic reactions frequently occurred. Soon after, the protein fraction of the serum was identified to mediate protection [5] and 1897 Paul Ehrlich proposed a molecular mechanism, the side-chain theory. In brief, this theory is based on the presence of cell-surface molecules (side-chains) with different structural properties normally used for the uptake of products. Coincidental recognition of a toxin induces the cell to produce more of the side-chain resulting in its release into the circulation. These soluble side-chains would then be able to bind the toxin before it can bind to other cells and thereby render it innocuous [7, 8]. Using our current wording, cell-surface bound side-chains would be called B cell receptors (being a cell-surface bound antibody) and soluble side-chains would be secreted antibodies.

But it still took a few years until the chemical nature of antibodies was elucidated. Michael Heidelberger unequivocally proved that antibodies are proteins [9] and in 1939 his student Elvin Kabat found that smaller and larger antibodies exist (referring to IgG and IgM) [10, 11]. Subsequently, purification of a human serum fraction enriched for immune gamma globulin (IgG) largely reduced the side effects and was used for the first time in 1944 to treat measles [12, 13]. Soon after, plasma cells were identified as a cellular source of gamma globulins [14]. Finally Rodney Porter recognized the presence of an antigen-binding region (Fab, fragment antigen binding) and an Fc (fragment crystallizable) [15] and Gerald Edelman solved the basic structure of antibodies being composed of two heavy and two light chains linked by disulfide bonds [16-18]. At the same time, Macfarlane Burnet formulated the “clonal selection theory”, anticipating many of the basic aspects of our current understanding about the development of antibody diversity [19]. He postulated that antibodies are selected from a pre-existing pool and are purposefully modified in order to recognize a target antigen [19,20].

One of the most significant advances for modern research and medicine was made in 1975 when Köhler and Milstein developed the hybridoma technique allowing the continuous culture of an antibody-secreting cell with defined specificity [21]. First attempts for clinical use resulted in the development of Muronomab-CD3, the first mouse anti-human monoclonal antibody approved for the application in humans to treat leukemia [22, 23]. However, like animal serum transfer at the turn of the 19th century, treatment of humans with murine antibodies led to serious side effects including anaphylactic shock [24] and the development of human-anti-mouse antibodies abrogated therapeutic efficacy [23, 25]. Advances in molecular cloning and expression techniques allowed the generation of monoclonal antibodies with a human constant region (chimeric antibodies) [26] and later fully human antibodies were established [27]. More than 100 years after Paul Ehrlich`s idea of developing a “magic bullet” to specifically target a molecular structure [28] we are now able to do so and continuous efforts are made to select new targets and optimize the therapeutic properties of antibodies.

1.2.2 The role of antibodies within the immune system

Immunoglobulins are amongst to the most abundant proteins found in serum [29]. Producing these vast amounts is a huge investment of the body which highlights the essential role of antibodies in the immune system. During a primary infection, pre-existing mostly germline-encoded low-affinity antibodies (natural antibodies) work in an innate-like manner and recognize PAMPs. This can neutralize toxins or microbes by blocking the structures required for their toxic or pathologic action. In addition, antibody-driven activation of the complement system (discussed in more detail below) and cytotoxic cells can kill invading organisms [30]. At the same time, immunoglobulins increase the visibility of the pathogen for the body, a process called opsonization. Thereby, pathogens and infected cells are "marked" by antibodies and complement components leading to the activation of phagocytes such as macrophages and DCs which engulf, destroy, process and transport the pathogen to secondary lymphoid organs for the initiation of an adaptive immune response. This results in the generation of B cells producing more potent, higher affinity antibodies and antigen-specific T cells which both may enter the memory pool and provide superior protection upon re-encounter of the same pathogen (see chapter 1.1.4). The protective mechanisms mediated by different types of antibodies are discussed in more detail in chapters 1.2.5 and 1.3.

1.2.3 Antibody structure

Antibodies are closely related glycoproteins that consist of four polypeptide chains consisting of two identical heavy chains (HC) and two identical light chains (LC) (figure 1.1) [31]. Differences among the antibody variants (isotypes) are discussed later. The tertiary protein structure of both HC an LC is characterized by the immunoglobulin (Ig-) fold, which is composed of two disulfide-bond stabilized β-sheets that form a barrel-like structure (β barrel) [32]. The N-terminal Ig domain of each HC and LC contains the variable regions (complementary determining regions, CDRs) in charge of the diversity and specificity of antigen recognition. These Ig domains are called V_H (variable region; heavy chain) and V_L (variable region; light chain). The remaining Ig domain of the LC is called C_L and those of the HC C_H1 to C_H3 (and C_H4 for some isotypes). Disulfide bonds in between the two HCs as well as the HCs and LCs covalently link the individual polypeptides and stabilize their quaternary structure. Several genes encode for different HC sequences that significantly impact the antibody structure and function (see chapter 1.2.5). In contrast, only two light chain genes (κ an λ) exist and no major differences have been identified. Based on early proteolytic and structural studies, antibodies are traditionally divided into two regions. Each of the two identical fragment antigen binding

(Fab) regions consists of a complete LC and the two N-terminal Ig domains of a HC. If the two Fab regions are still linked to each other by the hinge-region disulfide bonds, the fragment is called F(ab')$_2$. The C-terminal fragment cristallyzable (Fc) encompasses C_H2 and C_H3 (and C_H4) and varies based on the antibody isotype (see chapter 1.1.4). Fab and Fc are joined by the hinge region (except for IgM and IgE) which provides conformational flexibility to the antibody. Another important structural component are glycans which account for 4-18 % of the total weight [31]. At least one N-glycan is located in the constant region of each HC [1]. V_H and C_H regions can occasionally contain glycans and some antibody subclasses possess O-glycans [33].

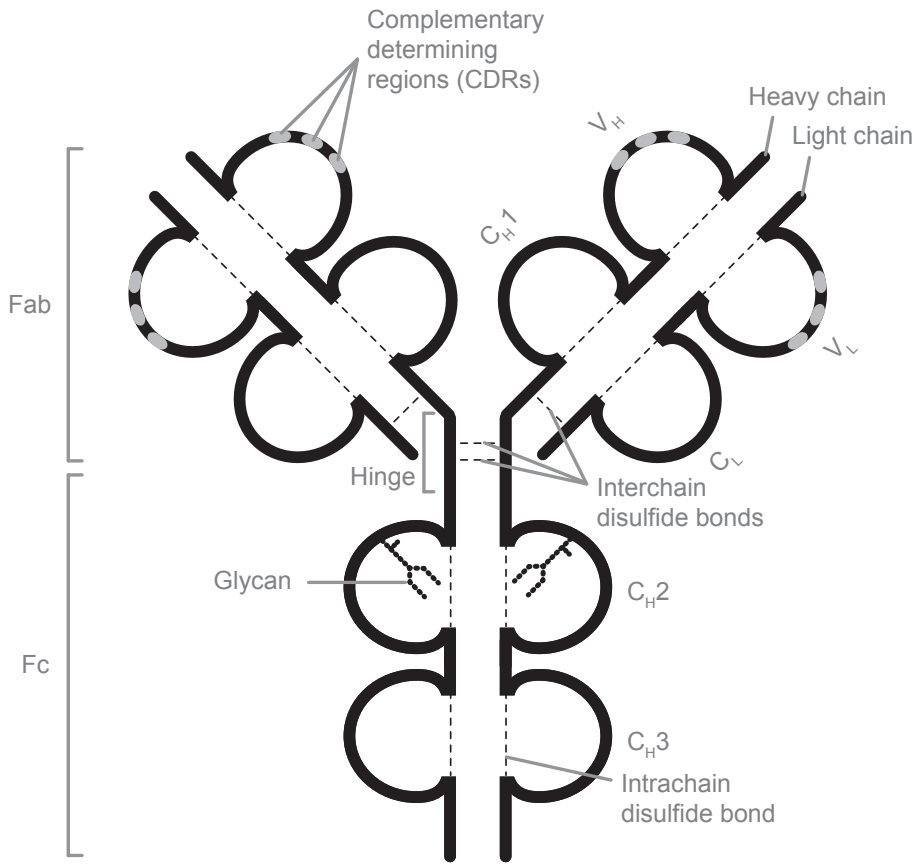

Figure 1.1 Basic antibody structure
A prototypic (IgG1) antibody composed of two heavy and light chains and two glycans is shown. Structural and functional components are indicated in grey. Modified from [1, 31].

1.2.4 B cell maturation: Generation of antibody diversity and memory

B lineage cells are the cellular origin of antibodies. They arise from hematopoietic progenitor cells and develop in the bone marrow until the immature B cell stage when they leave the bone marrow, enter circulation and home to the spleen or other secondary lymphoid organs. In the periphery, B cells further differentiate towards the mature naïve B cell stage [3]. The human immunoglobulin repertoire of naïve (pre-immune) B cells is estimated to exceed 10^{12} different antibody molecules [34]. Encoding this diversity in the genome would not leave much space for anything else [5]. This seemingly paradox situation made Dreyer and Bennett postulate that "immunologically competent cells have evolved a pattern of somatic genetic behavior which is radically different from anything normally found in modern molecular genetics" [35]. Their suggested mechanism involved "a kind of genetic scrambling process" [35] and the subsequent combination of the antibody variable regions with a constant region [35]. Today, the genetic scrambling process is called V(D)J recombination referring to the three genomic segments V, D and J which together encode the antibody variable region. D is in brackets because these segments exist only in the heavy chain sequences and not in the light chains [3, 36, 37]. Several copies of each segment, each composed of a different nucleotide sequence, are present in the genome. Combination of different segments with each other results in the diversity of the immature B cell receptor (BCR) [3, 36]. Expression of a functional non self-reactive immature B cell receptor (cell-surface bound IgD and IgM) allows the cell to exit the bone marrow. In the spleen, B cells are again positively and negatively selected for a functional but non self-reactive BCR expression [38-40] before they enter the mature naïve B cell stage [41, 42]. Further development is only induced by the recognition of a cognate antigen and depending on the nature of the antigen as well as the anatomic location within the body. Two distinct developmental pathways can occur: T cell independent maturation in the gut and marginal zone of the spleen resulting in B cells producing antibodies which recognize mainly polymeric non-protein antigens, or T cell dependent maturation in a germinal center as typically induced by protein antigens [3, 43]. The latter is characterized by further diversification of the BCR repertoire via affinity maturation. During this process, antigen and helper-T cell activated B cells migrate from the outer regions ("T cell zone") of secondary lymphoid organs into the follicle and proliferate extensively. This usually happens 4 to 7 days after the first antigen encounter and marks the beginning of a germinal center reaction. The induction of activation-induced deaminase (AID) by CD40-CD40L interactions between T and B cells results in the generation of cytosine (C) to uracil (U) mutation preferentially in the three highly susceptible regions (complementary determining regions 1-3, CDR1-3) of the rearranged heavy and light chain immunoglobulin V(D)J DNA. During DNA replication Us (usually only present in RNA and not DNA) are exchanged for thymidines (Ts) generating C to T mutation or Us may be excised

by uracil N-glycosylase following error-prone repair resulting in substitution by any of the four DNA bases [3]. This is called somatic hypermutation (SHM) and aims to generate antibodies which recognize their cognate antigen with increased affinity. Following proliferation and SHM in the "dark zone" of the germinal center, newly developed B cells migrate to the light zone where they encounter antigen presented on the surface of follicular DCs. Only those B cells which recognize the antigen with high affinity are positively selected and survive, all others undergo apoptosis. Positive selection can either result in another round of SHM and selection or B cells exit the germinal center and further differentiate [44]. Before this happens they undergo yet another diversification: the constant region of the antibody HCs is responsible to combine the specific antigen recognition with humoral and cellular effector functions. Depending on the requirements of the immune response, the functional properties of an antibody can be changed by a process called "class switching" or "isotype switching". Thereby, the genomic region encoding for the desired antibody constant region (isotype) is joined to the variable region by DNA recombination. This allows keeping the specificity unchanged while adjusting the functional properties (see next chapter for functional properties of isotypes) [1]. As a final step of maturation to become an antibody-producing cell, the cytoplasmic tail and transmembrane region of the BCR is removed by alternative mRNA processing resulting in the secreted form of the BCR, now called antibody. This process enables a B cell to produce secreted and membrane-bound Ig at the same time allowing it to still be responsive to BCR stimuli and adapt the antibody production depending on the needs of the immune system [3]. Besides immediate antibody production following a successful germinal center reaction, few cells become long-lived plasma cells or quiescent long-lived memory B cells. Upon reencounter of a pathogen, such a memory B cell can again enter the germinal center reaction, undergo further SHM, isotype switching and differentiation in memory- or plasma cells. This secondary B cell response happens much faster than the primary response because of pre-existing high-affinity antibodies and memory B cells (in addition to enhanced T cell responses, not discussed here). Both germinal-center derived B cell populations from the primary response contribute to accelerate the secondary response. Bone-marrow resident, germinal-center derived long-lived plasma cells are providing enhanced protection by continuously secreting antibodies and long-lived memory B cells reside in or recirculate between the spleen and secondary lymphoid organs where, upon encounter of their cognate antigen and stimulation by helper T cells, they mount a potent secondary immune response [3].

1.2.5 Classification and function of human antibody isotypes

Based on major structural differences, five isotype classes (IgG, IgM, IgA, IgE and IgD) can be distinguished. IgG can be further subdivided in the subclasses IgG1-4 and IgA in IgA1 and

IgA2 [1] (table 1.2). IgM is the first isotype produced during a primary immune response. It comprises the major pool of germline-encoded "natural antibodies" which have a limited affinity but broad antigen specificity [30]. Pentamerization (or sometimes hexamerization) by means of association with an additional polypeptide, the J chain produced by antigen secreting cells, allows increasing the avidity for repetitive structures. This reflects the essential role of IgM in the first line of defense against invading microbes by activation of the complement system [45] and for tissue homeostasis by the clearance of apoptotic cells [46]. IgA is found in body fluids such as the mucous, saliva, teers and breast milk but also in serum [47]. In order to enter mucosal secretions, IgA needs to dimerize or oligomerize with the J chain, which allows its transfer across mucosal epithelial cells by means of the polymeric immunoglobulin receptor [48, 49]. Mucosal IgA neutralizes pathogens and toxins without the initiation of an inflammatory response due to its limited ability to activate the complement system and plays an important role in establishing a mutual relationship with commensal bacteria [50-53]. Both IgA1 and IgA2 are found in the mucosa whereas in serum IgA is mainly restricted to monomeric IgA1 [53, 54]. Circulating IgA can bind to several receptors including FcαRI expressed on various innate immune cells but the functional consequence is poorly understood [53]. IgA concentration in colostrum exceeds 12 mg/ml reflecting its important role in protecting newborns via the breast milk against various microorganisms [47, 55]. IgE is mainly known for its protective effect against helminths as well as its pathophysiological significance in type I hypersensitivity and allergy [56]. IgE effector functions are mediated via the high-affinity IgE-Fc receptor (FcεRI) expressed on mast cells and basophils as well as human macrophages and DCs [57]. Antigen induced FcεRI cross-linking on mast cells and basophils induces the release of inflammatory mediators such as histamins, proteases and heparin in addition to the production of cytokines and chemokines [58]. FcεRI expression on antigen presenting cells was suggested to influence antigen presentation to, and phenotypic development of T cells [57]. Cell-surface bound IgD constitutes together with IgM the initial B cell receptor of a mature B cell and its function as secreted antibody is still enigmatic. IgD class-switched plasmacytoid B cells were found in the upper respiratory mucosa and secreted IgD bound to myeloid cells via an unknown receptor. It was therefore suggested that IgD plays a role in enhancing immunity to airborne pathogens [59]. The last antibody class, IgG, is of particular importance for this work and will be discussed in more detail below.

Class	IgD	IgM	IgG				IgA		IgE
Subclass			IgG1	IgG2	IgG3	IgG4	IgA1	IgA2	
Molecular weight (kDa)	188	970 (pentamer)	146	146	165	146	160 (monomer)	160 (monomer)	184
Serum concentration (mean adult mg/ml)	0.03	1.5	9	3	1	0.5	3	0.5	5×10^{-5}
Half-life in serum (days)	3	10	21	20	7 to 21*	21	6	6	2
Palcental transfer			+++	+	+ to +++*	++			
Mucosal transfer		+					+++	+++	

* depends on allotype.

Table 1.2: Basic characteristics of human antibody isotypes
Adapted from [3, 31, 49, 60].

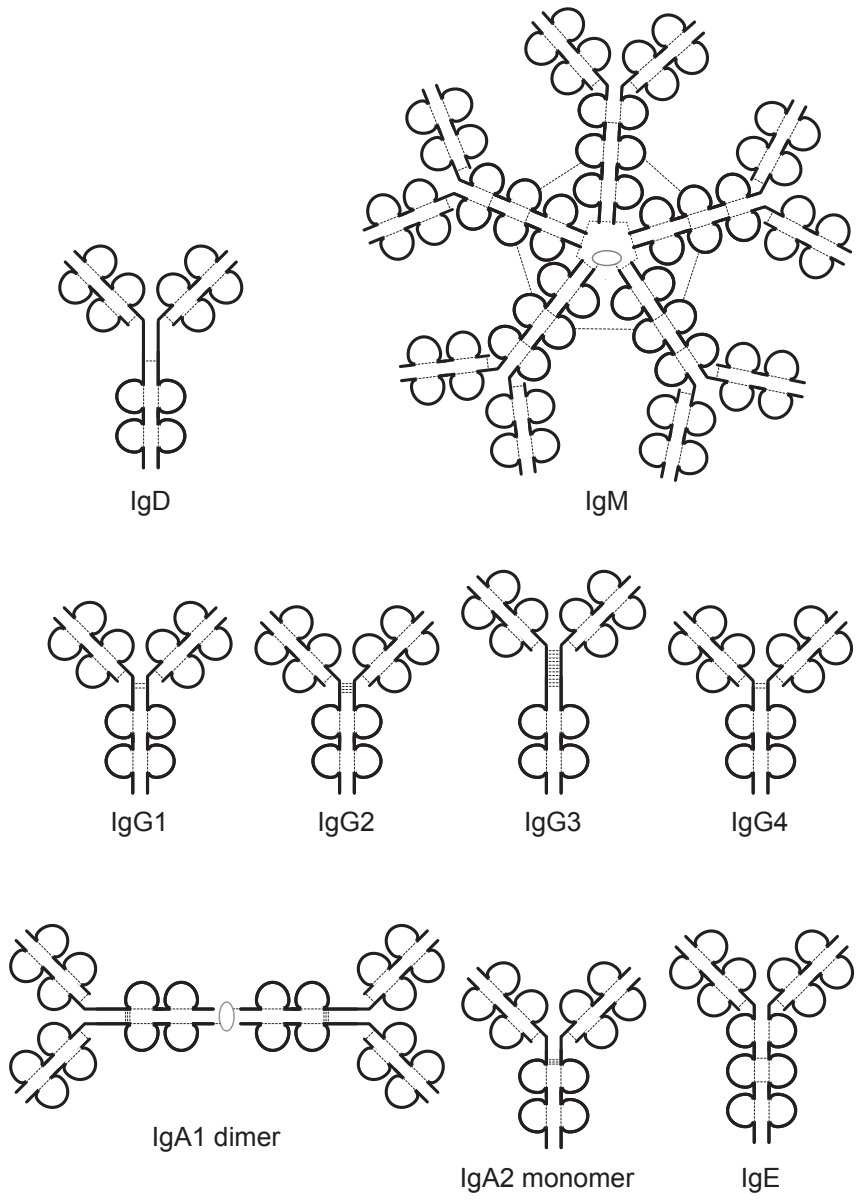

Figure 1.2 Structure and function of human antibody isotypes.
The structure of all human antibody isotypes is shown. IgM and IgA represented in their most frequently occurring polymeric form in association with the J chain (grey circle). Disulfide bonds are indicated as dotted lines. The number of disulfide bonds of IgG3 depends on the allotype. Modified from [1, 31, 47, 61-64].

1.3 Immunoglobulin G

1.3.1 The structure and function of human IgG subclasses

IgG is the prototypic antibody isotype and the predominant antibody in serum. IgG HCs are encoded by four closely related genes, the translation of which results in the isotypes IgG1, IgG2, IgG3 and IgG4 (figure 1.2). The numbering of the isotypes is not based on their genomic location but on relative abundance in serum (table 1.2) [65, 66]. Although 90% homologous in amino acid sequence, differences in the regions containing the binding sites for mediators of cellular and humoral effector mechanisms result in important functional differences. One area of high diversity is the hinge region which contains the inter-HC disulfide bonds. The length of the hinge, its amino acid composition and the amount of disulfide bonds varies between the four subclasses and results in major differences in Fab arm flexibility. IgG3 is most flexible followed by IgG1, IgG4 and IgG2 [67]. Besides the hinge region, the amino acid composition of the C_H2 domain is the most diverse IgG region [31]. IgG mediated complement activation (C1q binding) is strongly influenced by hinge and C_H2 structure resulting in IgG3 being the most potent complement activator followed by IgG1. IgG2 only weakly binds C1q and IgG4 does not activate the complement system [31]. The influence of the IgG subclass on FcγR binding is summarized in figure 1.5.

1.3.2 IgG glycosylation

An estimated 50 % of the proteins in our body carry glycans making glycosylation the most frequently occurring post-translational modification (PTM). In addition, the large variety of different combinations of sugars results in glycosylation also being the most complex PTM [68]. The glycosylation of IgG is unique among all antibody classes because it consists only of a single, highly conserved asparagine-linked glycan (N-glycan) in the C_H2 domain of the HC of all subclasses [33]. In addition 15 to 20 % of circulating IgG contain N-glycans in the variable regions of HC and/or LC due to the generation of glycosylation sites during somatic mutation of antigen-binding regions [69-72]. As suggested by their location, Fab glycans influence the antigen binding property of antibodies [72]. For reasons of completeness it has to be mentioned that a rarely glycosylated, non-classical N-glycosylation site has also been observed in the C_H1 domain of IgG [73]. In contrast to these additional glycosylations, the Fc glycan is indispensable for IgG to be successfully produced. During protein translation a pre-formed lipid-linked glycan is transferred and covalently attached to asparagine at position 297 in the lumen of the endoplasmatic reticulum (ER). This initial glycan is composed of two N-acetylglucosamines (GlcNAc) followed by branched mannose (Man) residues. Its structure

is highly conserved in eukaryotes and serves as an important mechanism for protein folding and quality control of proteins carrying N-glycans [74]. If successfully produced and folded, the IgG polypeptide is transferred from the ER to the Golgi network where glycosyl-hydrolases and -transferases can modify the core glycan leading to such diverse and highly complex glycans as seen in the IgG-Fc. The monosaccharide composition of the glycan is impacted by the amino acid sequence as well as glycan modifying enzyme- and substrate availability [75]. The presence of glycosylhydrolases and glycosyltransferases in the Golgi is regulated at the level of transcription and location within the secretory pathway [76]. Peptide-glycan interactions and the three-dimensional structure of the Fc are thought to limit the glycan variability and the extent of galactosylation and sialylation by limiting the accessibility of the glycan to glycosyltransferases [75, 77]. A total of more than 30 different glycan structures is found in the IgG-Fc pool [33, 78]. Compared to the Fab glycans, reduced bisecting GlcNAc, less galactose and less sialylation is found on the Fc glycans [71, 77]. The restricted glycan diversity may be essential to enable directed IgG-Fc glycan modifications and use them for shaping antibody functionality. How and which immunological factors such as cytokines influence antibody glycosylation is yet to be defined but much progress has been made in understanding the structural and functional consequences of the presence or absence of different sugar moieties on the IgG-Fc carbohydrate. In addition to the oligosaccharide core, more than 95 % of the bi-antennary complex type structure of the final IgG glycan carries a N- acetylglucosamine on both arms [78, 79] and 85 % are fucosylated [80]. In contrast, the presence of galactose is less homogenous with 40 % of glycans carrying one galactose (G1 glycan) and the frequency of non-galactosylated (G0) or bi-galactosylated glycans (G2) ranging between 20 and 40 % depending on age and gender [79, 81]. Additional heterogeneity is conferred by the presence of a bisecting N-acetylglucosamine present on approximately 10 to 15 % of total IgG-Fc glycans [82]. Based on the structure of the glycan, the conformation of the IgG-Fc homodimer in the binding interface to Fc-receptors and the complement protein C1q (C_H2 domain) changes from an open (maximal C2-C2 domain distance) to a closed conformation (minimal C2-C2 domain distance) [83, 84]. Analysis of crystal structures revealed that removal of terminal galactose and N-acetylglucosamine residues favors a closed conformation which impacts thermal stability and accessibility for IgG binding molecules [84-86]. The most distal sugar on the glycan is sialic acid (neuraminic acid, Neu5Ac). Around 10 % of glycans carry sialic acid on one arm and bi-sialylated glycans are found only in trace amounts. The linkage of sialic acid to the penultimate galactose is found in either α2-3 or α2-6 confirmation with a strong preference for the latter [33]. Galactose is added mainly to the 1-6 arm of the glycan, whereas sialic acid is almost exclusively found on the 1-3 arm [77]. While the 1-6 arm bias of galactose may be largely explained by accessibility [77] the 1-3 arm specific addition of sialic acid by human sialyltransferase is retained even *in vitro* using the released Fc glycan, substrate and recombinant human sialyltransferase arguing

for an enzyme-intrinsic bias [87]. The opposing glycan arm-bias of galactose and sialic acid provides a rationale for the inefficient addition of sialic acid. The functional consequences of the different glycan structures will be discussed in chapter 1.3.4)

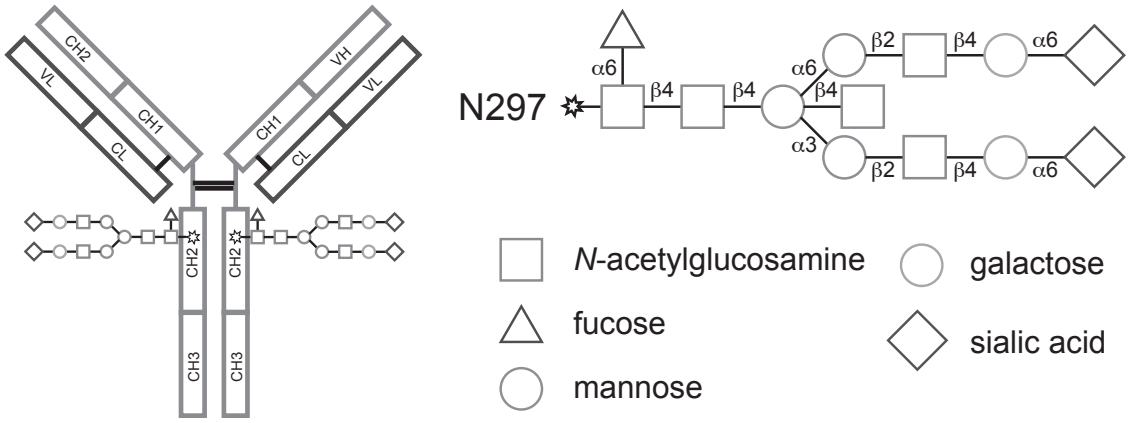

Figure 1.3 Structure of the IgG-Fc N-glycan
An IgG antibody containing two glycan residues and a fully processed N-glycan, galactosylated, sialylated and containing a bisecting N-acetylglucosamine is shown. Modified from [88].

1.3.3 IgG effector functions

Immunoglobulin G (IgG) represents 75 % of the immunoglobulins in serum reflecting its role in defending us against bacteria and viruses which have penetrated beyond epithelial and mucosal barriers [3]. Like for other antibodies, the Fab region of IgG can directly neutralize pathogens. Additionally, IgG can be bound by receptors specific for the antibody's Fc region (FcγRs), which allows FcγR-expressing cells to use the specificity of the Fab and combine it with their functional capabilities. Examples therefore are antibody-dependent cell-mediated phagocytosis (ADCP) and antibody-dependent cell-mediated cytotoxicity (ADCC) (figure 1.4). Also, IgG (IgG1 and IgG3) and IgM are the most potent antibodies in terms of activation of the complement system.

1.3.3.1 Cellular effector functions of IgG: The role of FcγRs

Receptors binding the Fc region of IgG, Fcγ-Receptors (FcγRs), are crucial for the functionality of antibodies. They contribute to clearance of pathogens and virus- or tumor-transformed cells by facilitating their uptake, inactivation and processing for antigen presentation.

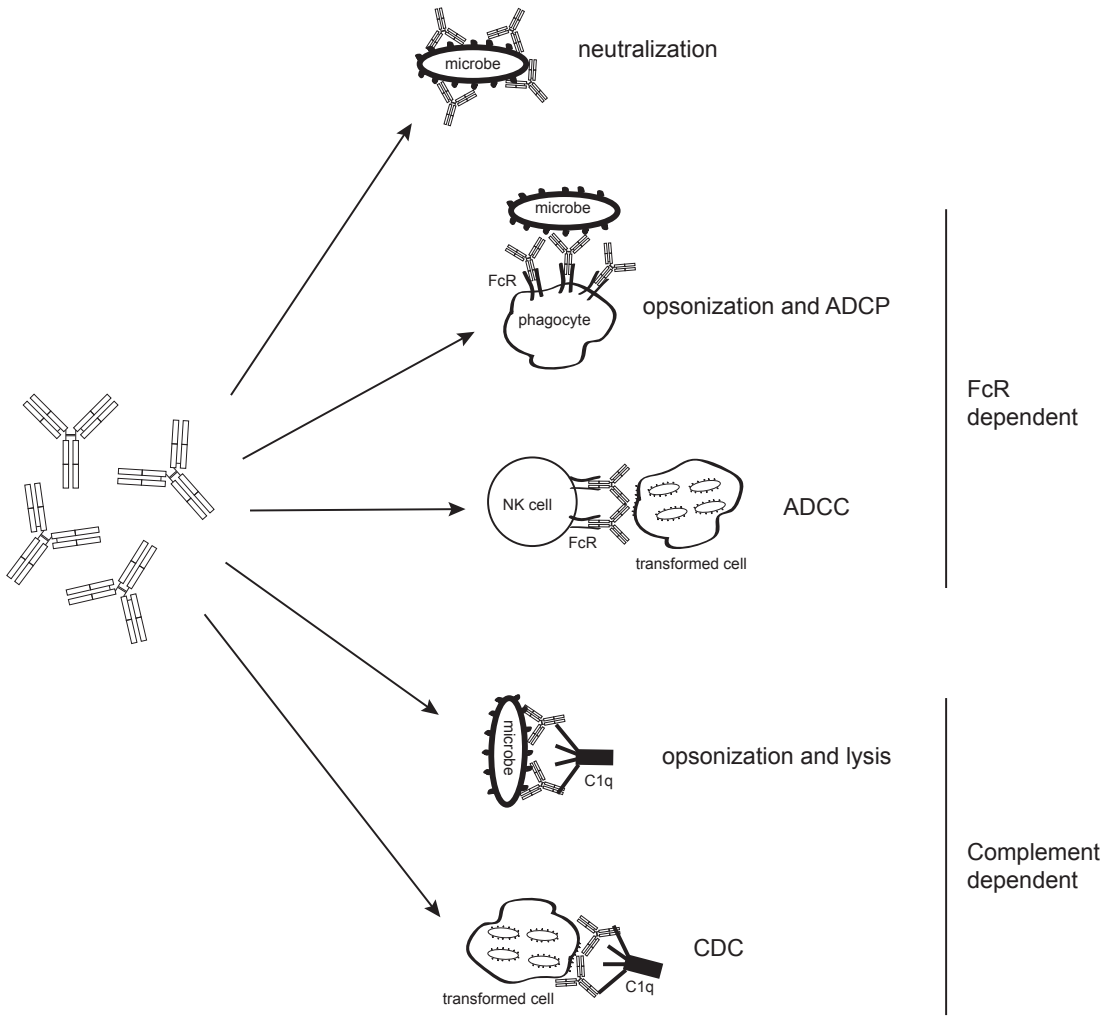

Figure 1.4 Effector functions of IgG
Schematic depiction of the main IgG effector functions. ADCP (Antibody-dependent cell-mediated phagocytosis); ADCC (Antibody-dependent cell-mediated cytotoxicity); CDC (Complement-dependent cytotoxicity). Modified from [3].

Traditionally, these receptors are divided into two groups based on their inhibitory or activating function (figure 1.5) reflected by the presence of either an immunoreceptor tyrosin-based inhibitory (ITIM) or -activation motif (ITAM) sequences in their intracellular domain or their signaling adaptor molecules. All classical FcγRs (FcγRI, FcγRII-A, -B, -C, FcγRIII-A, -B) bind to the upper C_H2 and hinge region of IgG [89-93]. The receptor`s affinity for IgG determines if the antibodies bind in a monomeric form and cells expressing the respective FcγR are therefore constantly associated with surface-bound antibodies. Alternatively, formation of an immune complex is required to allow FcγR binding. Innate immune cells such as monocytes, macrophages and DCs express several FcγRs on their cell surface and can co-express activating FcγRs (FcγRI, FcγRIIA and FcγRIIIA) with the inhibitory FcγRIIB. Relative expression levels of activating versus inhibitory receptors have been shown to influence the response towards

immune complexes and set the threshold for DC activation [94]. FcγRIIA is particularly important for ADCP mediating the internalization of immune complexes for antigen processing, presentation and degradation [95, 96].
Similarly to its function on myeloid cells, FcγRIIB negatively regulates signaling in B cells via the BCR resulting in decreased antigen-induced proliferation and antibody production [97, 98]. Its expression on plasma cells controls their persistence in the bone marrow [99] and the deletion of FcγRIIB was found to result in increased frequencies of auto-reactive plasma cells in transgenic mouse model expressing a DNA-specific immunoglobulin heavy chains [100].
FcγRIIIA is the main FcγR found on natural killer (NK) cells where it is essential for the lysis of tumor- or virus-transformed cells by ADCC. Through FcγRIIIA, NK cells bind to antibodies bound to the surface of a pathogen or transformed cell and lyse the target by releasing pre-formed cytotoxic granules [3, 101]. About 20% of individuals additionally express FcγRIIC on NK cells which may also have important implications for NK cell functions [102].
Fc-receptors also contribute to the exceptionally long half-life of IgG antibodies (see table 1.2). The neonatal FcR (FcRn) cycles between the cell surface and acidic endosomal compartments where low pH allows its binding to internalized IgG. FcRn-IgG complexes are then transported back to the cell surface and physiological pH leads to the dissociation of the FcRn-IgG complex and IgG's release back to circulation [103]. This process not only increases the half-life of IgG up to five fold but also allows trans-epithelial transport [104, 105].

1.3.3.2 Humoral effector functions of IgG: The complement pathway

The complement system is traditionally seen as an innate defense mechanism against invading pathogens. Accordingly, initiators of the complement system such as mannose-binding lectin (MBL), ficolins and C1q are potent pattern-recognition molecules. Upon target surface binding of MBL, ficolins or C1q, associated serine proteases get activated and cleave C4 into C4a and C4b. This in turn leads to the exposure of a thioester group in C4b resulting in its covalent surface deposition. Thereby, C4b turns into an active protease and cleaves C2 into C2a and C2b. C4b and C2b form together the C3 convertase C4b2b. C3 is the central molecule for all complement pathways. Again, if C3 is cleaved by its convertase, a reactive thioester is exposed leading to the covalent binding of C3b to amines and carbohydrates on target surfaces. In the classical and lectin pathway, C4b, C2b and C3b form the C5 convertase, which in turn associates with C6 and C7 and inserts into the surface of the target cell. Finally, this complex interacts with C8 and several units of C9 to form the membrane attack complex, a lytic pore in the cell membrane [3, 108]. In addition to this lytic process, C3b opsonizes targeted cells

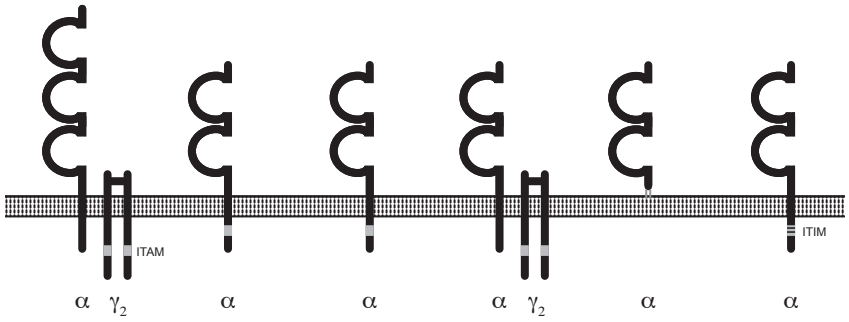

Name		FcγRI	FcγRIIA		FcγRIIC		FcγRIIIA		FcγRIIIB	FcγRIIB	
CD		CD64	CD32A		CD32C		CD16A		CD16B	CD32B	
Expression	Lymphoid	not expressed	not expressed		NK cells		NK cells		not expressed	B cells, plasma cells	
	Myeloid	Monocytes, DCs, macrophages	Monocytes, DCs, macrophages		not expressed		Monocyte, DC macrophage		not expressed	Monocytes, DCs, macrophages	
	Granulocyte	Neutrophils, eosinophils	Neutrophils		not expressed		not expressed		Neutrophils, mast cells, eosinophils	Neutrophils, baso-phils, mast cells	
IgG binding affinity	FcγR allele	-	H_{131}	R_{131}	Q_{13}	$stop_{13}$	V_{158}	F_{158}	-	I_{232}	T_{232}
	IgG1	$6x10^7$	$5x10^6$	$3x10^6$	$1x10^5$	-	$2x10^5$	$1x10^5$	$2x10^5$	$1x10^5$	ND
	IgG2	-	$5x10^5$	$1x10^5$	$2x10^4$	-	$7x10^4$	$3x10^4$	-	$2x10^4$	ND
	IgG3	$6x10^7$	$9x10^5$	$9x10^5$	$2x10^5$	-	$1x10^7$	$8x10^6$	$1x10^6$	$2x10^5$	ND
	IgG4	$3x10^7$	$2x10^5$	$2x10^5$	$2x10^5$	-	$2x10^5$	$2x10^5$	-	$2x10^5$	ND

Figure 1.5 Human FcγRs
Schematic depiction of human FcγRs γ-chains and the major signaling adaptor molecule for FcγRI and FcγRIIIA, the common gamma chain dimer (γ2). Immune-tyrosine based activation (ITAM) - or inhibition (ITIM) sequences in the intracellular domain or adaptor molecule are indicated. FcγR expression pattern and binding affinity of allelic FcγR variants to IgG isotypes is shown [106, 107]. FcγRIIC is only expressed by 20 % of individuals [102]. The three known allelic variants of FcγRIIIB are not indicated as they have shown no differences in FcγR binding properties. Modified from [106, 107].

for phagocytosis via receptors on macrophages and DCs (such as CR1, 3 and 4) [108]. It also lowers the threshold for B cell stimulation (via CR2), facilitating antigen presentation and initiation of an adaptive immune response [108, 109]. This process is further amplified by anaphylatoxins C3a and C5a, the small proteolytic fragments of C3 and C5, which act as potent chemoattractants for antigen presenting cells and trigger proinflammatory signaling via binding to C3aR, C5aR and C5L2 [110, 111]. The importance of the complement system for the defense against microbes is demonstrated by C3 deficiency, which leads to recurrent and life-threatening bacterial infections [112]. In addition, complement is involved in the removal of apoptotic cells and deficiency in components of the classical complement pathway, in particular C1q, is associated with autoimmunity [113]. This highlights the importance of the complement system not only for the defense of the body but also for its homeostasis.

Depending on the isotype, IgG antibodies are potent initiators of the complement cascade. Three ways of IgG-mediated complement activation have been described. First, antigen-bound IgG is a high-affinity binding partner for C1q [83, 114]. Second, mannose-binding lectin (MBL)

can bind IgG containing non-galactosylated IgG-Fc glycans [115, 116]. Third, spontaneously activated C3b has a certain affinity for IgG and forms $C3b_2$-IgG complexes [117-119]. The C1q-dependent pathway is presumably most important for IgG function and best understood. It enables IgG-mediated lysis of both microbes and cells by formation of the membrane attack complex, a process called complement-dependent cytotoxicity (CDC) (figure 1.6).

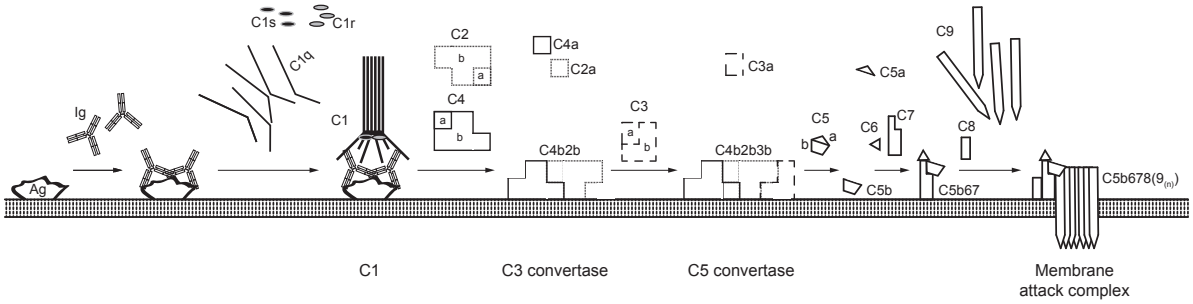

Figure 1.6 The classical complement pathway.
Binding of an antibody to its cognate antigen induces the assembly of C1 which in turn results in the induction of the complement cascade culminating in the insertion of the membrane attack complex in the cell membrane and lysis of the cell. Modified from [1, 3]

1.3.4 Regulation of IgG effector functions by the IgG-Fc glycan

The IgG-Fc glycan is located in the C_H2 region in proximity to the FcγR and C1q binding sites suggesting its involvement in their intermolecular interaction [93, 114]. In accordance with that, absence of the IgG-Fc N-glycan results in the abrogation of effector-FcγR binding [120] as well as C1q binding [86, 121, 122]. In contrast, the binding of IgG to FcRn and therefore serum half-live was found to be hardly affected by the presence or absence of the IgG-Fc N-glycan. This is likely explained by the distinct position of the FcRn binding site located between the C_H2 and C_H3 domain of IgG-Fc [123, 124].

From the three variable sugar residues galactose, sialic acid and fucose, the latter has the most pronounced effect on antibody functionality. Its presence largely reduces the affinity of IgG for FcγRIIIA [92] and therefore NK cell mediated ADCC. This finding is currently assessed for its clinical applicability with at least 12 de-fucosylated antibodies being evaluated as anti-cancer therapeutics in clinical trials [125] and mogamulizumab (non-fucosylated humanized mAb recognizing CCR4) already approved for relapsed or refractory CCR-4-positive adult T cell leukemia-lymphoma in Japan [126].

The reduced frequency of galactose in the IgG-Fc glycan during inflammation due to autoimmunity or infection was reported in numerous studies [78, 127-131]. However, very little evidence exists for a functional consequence. Agalactosylated IgG was found to depend on FcγRs for *in vivo* functionality [116] although in the absence of galactose, IgG gains the

ability to interact with mannose-binding lectin (MBL) [115] and could therefore activate the complement system via the lectin pathway [115, 116]. Also, the presence of galactose favors C1q binding [116] but suppresses C5aR signaling via dectin-1 and FcγRIIB cross-linking [132]. An additional important aspect to consider when looking at the functional impact of galactose is that it provides the basis for the addition of sialic acid, the most distal sugar moiety on the IgG-Fc glycan. But again, very little is known about the significance of sialic acid for antibody functionality. It was suggested that IgG-Fc sialylation may reduce both activating and inhibitory FcγR [133] binding as well as ADCC [134], but further investigations, in particular for human antibodies and receptors have to be carried out to confirm that effect. Conflicting results exist whether sialylated IgG gains the ability to bind the adhesion and antigen capture molecule DC-SIGN or its murine ortholog SIGN-R1 [135-138]. The most convincing data about a functional role of sialic acid were found for its role in mediating the anti-inflammatory effect of pooled human antibodies [133, 139]. This will be discussed in more detail in chapter 1.3.6.2.

1.3.5 Anti-inflammatory IgG: intravenous immunoglobulin (IVIG)

In 1981, Paul Imbach made a surprising discovery, which should turn out to become one of the most efficient and best-tolerated treatments for several human autoimmune diseases. A patient suffering from both hypogammaglobulinemia and immune thrombocytopenia (ITP) received intravenous injections of high-dose polyclonal antibodies purified and pooled from numerous serum donors as immunoglobulin replacement therapy to complement his IgG deficiency. Unexpectedly, not only the serum-immunoglobulin levels increased but also the number of platelets [140, 141]. This led to the idea that IgG may have anti-inflammatory properties in addition to the well-established pro-inflammatory functions. Since then successful clinical studies prompted the approval of IVIG in the autoimmune diseases ITP, Kawasaki`s disease, chronic inflammatory demyelinating polyneuropathy (CIDP) and multifocal motor neuropathy (MMN) [142]. Furthermore, IVIG has applications in many other neuromuscular, hematologic or dermatologic disorders. Examples are Guillain-Barré syndrome, myasthenia gravis, relapsing-remitting multiple sclerosis, graft-versus-host disease and pemphigus vulgaris [142].

1.3.5.1 Properties of IVIG and clinical regimen

The purification of IgG from pooled serum for immunoglobulin replacement therapy has been developed in the 1940 and was based on cold ethanol preparation. With a few adaptations, this is still today the core method except for one company using caprylate precipitation [143]. The IgG subclass distribution in IVIG reflects what is found in healthy human serum being 68 % IgG1, 29 % IgG2, 4-8 % IgG3 and 1 % IgG4 [144, 145]. Besides, small amounts of IgA and

IgM are also present [143]. IVIG is prepared as physiologic salt solution, the pH varies between 4 and 7.2 depending on the preparation and in order to avoid aggregates, sugars (either glucose, sorbitol, mannose or maltose) are added in most preparations [143]. IgG concentration in the infusion solution is usually between 50 and 100 g/l [143]. The treatment regimen depends on the disease and the individual patient. A standard application for the treatment of autoimmunity would be 2 g/kg initially and 1 g/kg maintenance infusion every 3-6 weeks [145, 146].

1.3.6.2 The anti-inflammatory mechanisms of IVIG

Despite IVIG`s clinical efficacy in a wide range of autoimmune diseases, it has not been possible to find a uniform mechanism of action yet, suggesting that various aspects of IgG play a role. Possible mechanisms identified so far (table 1.3) can be divided in two groups based on their association with the functional components of IgG, Fab or Fc. The large variety of antigen specificities contained within the IVIG preparation and the high dose given to patients potentially allows rare antigen specificities to block, remove and neutralize components of the immune system as well as environmental factors such as microbes. Exemplary mechanisms are interference of cell homing and interaction by blocking of integrins [147], immune modulation by blocking of cytokines [148-150], neutralization of pathogenic autoantibodies by anti-idiotype antibodies [151, 152] and modulation of host-bacteria (commensals and pathogens) interaction by anti-carbohydrate antibodies [153]. In addition, the constant region of $F(ab`)_2$ fragments was shown to neutralize anaphylatoxins C3a and C5a by physical association [154]. Unlike $F(ab`)_2$ mediated anti-inflammatory properties which were so far only demonstrated *in vitro* or in animal models, a clinical trial showed efficacy of Fc fragments in ITP [155]. Numerous follow-up studies investigated the protective mechanism of Fc. Obtained results include FcγR blocking [156], modulation of FcγR expression [157] and signaling [158], increased autoantibody clearance by FcRn saturation [159], suppression of immunoglobulin production [160], modulation of antigen presenting cell activation by induction of inhibitory FcγRIIB [161] as well as blockade of complement proteins [162]. Interference with the function of antigen presenting cells [161, 163] can shape adaptive T and B cell responses. Similarly, peptide epitopes contained within the constant regions of the IgG heavy chain were shown to be recognized by regulatory T cells which may in turn suppress autoreactive T cells [164]. Because an extremely high dose of IVIG is required for its efficacy (1-2 g per kg), it was speculated that the beneficial effect may be mediated by a small sub-fraction of IVIG. Jeffrey Ravetch and colleagues identified the presence of the IgG-Fc glycan to be essential [133]. In particular, the most terminal sugar moiety, α2-6 linked sialic acid, was found to be the anti-inflammatory mediator of IVIG in the K/N experimental arthritis model [133, 165]. Collectively, studies in

murine models and human autoimmune diseases suggest that the IgG-Fc portion is sufficient to mediate the anti-inflammatory action of IVIG [133, 155] possibly via sialic acid [133, 139, 165-167] and FcγRIIB [139, 157, 158]. In addition, $F(ab`)_2$ mediated immune-modulation may play a role by blocking of inflammatory mediators [147, 149].

Mechanism	Reference
Anti-idiotypic antibodies	[151] [152]
Modulation of immunomodulatory molecules (cytokines, chemokines, receptors, adhesion molecules)	[147-150, 168-172]
Neutralization of pathogens and superantigens	[153, 173]
Interference with FcγR signaling and expression	[139, 156, 157, 174-176]
Interaction and signaling via DC-SIGN (SIGN-R1)	[136, 161]
Modulation of complement activity	[154, 177, 178]
Modulation of maturation and function of DCs	[163]
Blockade of FcRn	[159]
Regulatory T cell activation via “Tregitopes”	[164]
Suppression of immunoglobulin production by B cells	[160]
Improvement of steroid signaling	[179]

Table 1.3 Suggested anti-inflammatory mechanisms of IVIG

1.4 Chronic inflammatory demyelinating polyneuropathy (CIDP)

1.4.1 Clinical manifestation of CIDP

CIDP is an acquired autoimmune disease of the peripheral nervous system and represents the most common chronic autoimmune neuropathy with a prevalence between 1.9 and 8.9 per 100 000 individuals [180, 181]. The disease usually develops insidious over the course of weeks to years and is characterized by progressive, symmetric motor and sensory deficits in the limbs as well as paresthesia and impaired balance with large inter-patient variation as to the involvement of the individual characteristics [181-185]. In its most severe form CIDP can lead to complete immobilization and eventually death [186, 187]. CIDP is more common in elderly individuals, but onset can occur from early childhood on throughout life with males being more often affected than females [182]. The disease course can be chronic progressive or contain relapses with various degrees of remaining disability [182, 187].

1.4.2 CIDP treatment and disease pathology

At least two thirds of patients with CIDP respond to immunotherapy [181, 188]. Randomized controlled clinical trials showed an overall similar efficacy of corticosteroids [189], IVIG [190-192] and plasma exchange [193-195]. Steriods (prednisolone) and IVIG are considered first-line treatments but the exact treatment regimen has to be individually tailored based on the disease severity, age and general health status [196]. If patients do not respond, immunosuppressants and CD20-monoclonal antibody mediated B cell depletion is sometimes used but no controlled clinical trial has shown usefulness so far [188, 196]. Treatment success was found to correlate with age of onset [197] and the involvement of proximal or distal muscle weakness [198]. Juvenile CIDP patients are likely to respond well to treatment and achieve complete recovery whereas most elderly patients do not show complete recovery [197].

CIDP is regarded as an autoimmune disease and disease pathology is thought to involve autoantibodies, T cells, macrophages and complement. The main immune cells found in active lesions are macrophages and few T cells [181, 183, 186]. Successful treatment by plasmapheresis, which depletes the blood of soluble factors such as cytokines, chemokines and antibodies, suggests that humoral immune mediators play an important role [181]. The cerebrospinal fluid (CSF) of CIDP patients contains increased overall protein concentration [199] and elevated chemokine and cytokine levels [172, 199-202]. In addition, deposits of antibodies and complement on the surface of myelin sheaths [203] and transferability of demyelination by the intraneural injection of serum or IgG from CIDP patients into rodents [204] supports the relevance of antibodies for disease pathology. Both complement and macrophages could contribute to the neuropathology of antibodies but also antibodies on their own could be disease-relevant by modulation of signaling via receptors and soluble mediators [205].

Despite increasing evidence for antibodies as mediators of immunopathology in CIDP, the nature of a potential autoantigen is still largely elusive. Small subgroups of patients were found to have antibodies binding to neurofascin [206] or contactin-1 [207] and myelin-reactive antibodies are only present in rare cases [208]. In addition, higher than normal titers of β-tubulin reactive antibodies are found in less than half of CIDP patients but their significance for disease pathology remains unknown [209, 210]. The diversity of CIDP disease pathology may also be the result of several target autoantigens involved and identification of such would have a great potential to differentiate CIDP subtypes and optimize the treatment.

1.5 Experimental autoimmune encephalomyelitis (EAE) - T cell mediated neuro-inflammation of the central nervous system

1.5.1 History of EAE

Louis Pasteur used repeated injections of dried spinal cord of rabies infected rabbits as post-exposure vaccine [211]. Despite its clinical success against rabies, temporal neurologic impairments such as facial palsy or paresis of limbs were frequently occurring side-effects [212]. In its most severe form, progressive paralysis started from the lower extremities, ascended to the upper limbs and neck and finally affected breathing and swallowing culminating in death [213-215]. In the beginning, the neurological impairments were attributed to the virus until it was found that repeated injections of rhesus macaques with uninfected rabbit brain also resulted in impaired movement and myelin degeneration [216, 217]. The first hint that the immune system may play a role originated from the observation that brain-specific antibody titers correlated with the appearance of paralysis [218]. A logic consequence was that stimulation of the immune system by use of an adjuvant should exacerbate the pathogenicity of brain injections. This was the starting point for the development of experimental autoimmune encephalomyelitis (EAE), the immunization of animals with brain extracts emulsified in oil containing heat-killed *Mycobacterium tuberculosis* (the so-called complete Freund's adjuvant, CFA) [212]. Although details in the disease phenotype vary, the organ-specific neurological phenotype of EAE was replicated in numerous animals including pigs, rabbits, goats, rats, dogs, chicken and mice [212]. Efforts to identify the antigenic components led to a stepwise simplification of the model until only a single antigenic peptide replaced the whole brain lysate. Although antibodies were the first indicators of a role for the immune system in disease pathology, the use of peptides resulted in a T cell dependent model of autoimmune neuroinflammation [219, 220] with a critical involvement of many other cell types and inflammatory mediators strongly depending on the species, strain and epitope used [221, 222]. The most commonly used peptides for EAE in mice are derived from either myelin basic prvotein (MBP) or myelin oligodendrocyte glycoprotein (MOG). The next chapter briefly introduces the distinctive features of T cells as well as their subsets and effector mechanisms before going into further details about the pathology of EAE.

1.5.2 T cells: Basic properties and comparison to B cells

T cells are, besides B cells, the second cellular component of the adaptive immune system. Both subsets develop from a common pluripotent bone-marrow derived lymphocyte progenitor cell but whereas B cells undergo a large part of their development in the bone marrow, early T cell

progenitors home to the thymus. T cells have an antigen receptor composed of an alpha and beta chain and accessory signaling molecules. Also the basic principles of antigen receptor repertoire development by somatic gene segment rearrangement, V(D)J recombination, as well as positive and negative selection (although involving different tissues and cell types) are very similar among B and T cells. However, there are some important differences. First, additional diversity by somatic hypermutation does not exist in T cells. Second, T cells do not recognize native antigens but peptides presented by "major histocompatibility complex" (MHC) molecules of other cells. Third, the TCR remains membrane-bound and T cells themselves are the cellular mediators of effector functions such as target cell lysis and stimulation of innate and adaptive immune responses by the secretion of cytokines [3]. The next chapter briefly summarizes the different subsets of T cells and their respective functions in the immune system.

1.5.2.1 T cell subsets and their effector functions

Naïve mature T cells can be divided in two subsets based on their expression of either CD4 or CD8. These TCR co-receptors are essential for the interaction with antigen-bound MHC. They functionally restrict CD4 T cells to recognize peptides in the context of MHC class II (MHC-II) and CD8 T cells in the context of MHC class I (MHC-I) [223]. MHC-I is expressed on almost all nucleated cells and presents peptides derived from intracellular origin. Intracellular (cytosolic) proteins, host or pathogen-derived, are degraded by the proteasome, loaded on MHC-I in the ER and finally presented on the cell surface [3]. This mechanism is of particular importance for the immune system to detect virally transformed cells by the recognition of virus-derived peptides via $CD8^+$ T cells [3]. Activation of $CD8^+$ T cells leads to cytokine production and lysis of the target cell. This subset is therefore called cytotoxic T lymphocyte (CTL). MHC-II molecules are mainly expressed on so-called professional antigen presenting cells (e.g. DCs) as well as B cells and present peptides derived from extracellular proteins. Endocytic vesicles fuse with specialized MHC-II loading compartments and the peptide-associated MHC-II molecules are transported to the cell surface. Recognition of the cognate antigen by a $CD4^+$ T cell (also called helper T cell) usually does not result in lysis of the presenting cell but rather in stimulation of its ability to destroy the phagocytosed microbe. In addition, the secretion of cytokines and chemokines recruits other immune cells and stimulates the capacity of antigen presenting cells to amplify the primary immune response and initiate a secondary immune response. Based on their expression of specific transcription factors and secretion of cytokines, several subsets of T cells can be distinguished [224]. The best-characterized subsets are shown in table 1.4. $CD4^+$ T cells also have an essential function during the induction and recall of antigen-specific antibody responses by the recognition of pathogen-derived peptides on MHC-II molecules on the surface of B cells. T - B cell interaction in the lymph node results in the migration of B cells into the

primary follicle where, upon antigen recognition, they start to proliferate and initiate a germinal center reaction [3]. Again, T cells are indispensable. The production of IL-21 and CD40 - CD40-ligand interaction with germinal-center B cells is essential to maintain the germinal center reaction as well as differentiation of high affinity non-self reactive B cells into long lived memory and plasma cells by a yet to be defined mechanism [225, 226]. A specialized subset of $CD4^+$ T cells expressing the transcription factor FoxP3 has important functions in regulating peripheral T cell tolerance by inhibition of T cell activation and modulation of their effector functions [227]. In addition, γδ T cells and mainly lipid-recognizing natural killer T (NKT) cells exist which will not be discussed here. Both $CD4^+$ and $CD8^+$ T cells can differentiate into memory T cells and provide superior protection upon a secondary infection [3].

Th cell subset	Differentiation stimulated by	Lineage-defining transcription factors	Signature cytokines	Responsive cells	Major fucntions
Th1	IL-12, IL-27	STAT4, T-bet	IFN-γ, TNF-α, TNF-β, IL-3, GM-CSF	DCs, macrophages, neutrophils, NK cells, B cells	Cell-mediated immunity (defense against intracellular bacteria & viruses)
Th2	IL-4, IL-25	STAT6, GATA3	IL-3, IL-4, IL-5, IL-9, IL-10, IL-13, GM-CSF	DCs, macrophages, eosinophils, mast cells, basophils, B cells	Humoral immunity (defense against extracellular parasites such as helminths), mucosal immunity, allergy, asthma
Th17	TGF-β, IL-6, IL-21	STAT3, ROR-α, ROR-γt	IL-17A, IL-17F, IL-21, IL-22	Neutrophils, macrophages, endothelial cells, epithelial cells	Cell-mediated inflammation, defense against extracellular pathogens and fungi, autoimmune diseases
Treg	TGF-β	Foxp3	TGF-β, IL-10	DCs, macrophages, B cells	Immunoregulation (peripheral tolerance)
Tfh	IL-6, IL-21	STAT3, Bcl-6	IL-4, IL-10, IL-21	Germinal center B cells	B cell maturation, regulation of peripheral tolerace in the germinal center

Table 1.4 Characteristics of conventional T cell subset
Adapted from [3, 224, 226, 227]

1.5.3 Disease pathology of MOG_{35-55} peptide induced EAE in C57BL/6 mice

EAE is induced in C57BL/6 mice (B6 mice) by subcutaneous immunization with the immunodominant MOG_{35-55} peptide emulsified in CFA [228]. This results in a continuous release of adjuvant and peptide. In addition, mice receive pertussis toxin, which is thought to facilitate the development of clinical symptoms by aiding to open the blood-brain barrier and modulation of APCs and T cells [229, 230]. MOG protein expression is largely restricted to the central nervous system (brain and spinal cord) where it is present on the myelin sheath of oligodendrocytes [231-233]. The disease pathology in the B6 mouse is usually chronic progressive and can have phases of partial remission [222, 228]. The disease onset typically starts between day 9 and 15 after immunization with tail paralysis, which subsequently ascends

to the hind- and sometimes also forelimbs [228]. Histologically, MOG-induced EAE in B6 mice is characterized by perivascular infiltration of mononuclear cells and demyelination in the cortex, spinal cord and cerebellum [228, 234]. DCs are thought to pick up the antigen and transfer it to the skin-draining lymph node where antigen-specific T cells recognize the peptide and are primed in the context of the danger signal provided by the adjuvant. This results in the generation of MOG_{35-55} peptide-specific, encephalitogenic T cells which migrate to the CNS where they recognize their cognate antigen presented in the context of MHC-II ($H\text{-}2^b$). Myeloid cells and T cells mediate the pathogenesis but other cell types may also be critically involved [228]. By comparison, B cells, antibodies and complement play an insignificant role during demyelination in MOG protein or MOG_{35-55} peptide-induced EAE in B6 mice due to an inability to mount a MOG-specific antibody response capable of recognizing the native protein [221]. EAE in the B6 mouse provides an adequate model to study autoantigen- and tissue-specific T cell responses and, therefore, became one of the most widely used animal models for investigating T cell-mediated immunopathologies in autoimmune disease conditions [222].

2. Results

2.1 FcγR expression in CIDP

2.1.1 Deregulated inhibitory and activating FcγR expression in patients with CIDP

Humoral immune responses are thought to play a crucial role in mediating peripheral nerve damage and represent important pharmacological targets in CIDP [184, 204, 235]. IgG-mediated effector functions require the interaction of the antibodies' Fc fragment with their cognate cellular Fc-gamma receptors (FcγR) expressed by innate immune cells and B lymphocytes. Most hematopoietic cells express both activating and inhibitory FcγR and the *in vivo* activity of an IgG antibody therefore results from the net effect of engaging both classes of receptors. Compared to demographically matched healthy controls, patients with CIDP were previously reported to express lower FcγRIIB levels on B cells. IVIG therapy led to increased levels of FcγRIIB and, in some patients, on $CD14^+$ monocytes [157]. Here, we investigated the expression profile of activating and inhibitory FcγRs in patients with CIDP before and during IVIG therapy.

Expression of the activating FcγRI and FcγRIIA and the inhibitory FcγRIIB was determined on circulating $CD19^+CD27^-$ naïve and $CD19^+CD27^+$ memory B cells and additionally on classical $CD14^{high}CD16^-$ and inflammatory $CD14^{low}CD16^+$ monocytes in untreated patients with CIDP (n = 24) compared to demographically matched healthy blood donors (n = 19) (table 4.1). No statistically significant differences were detectable in the frequencies of the aforementioned immune cell subsets (data not shown). Consistent with earlier reports [157], patients with CIDP showed reduced expression levels of FcγRIIB on B cells (figure 2.1A). The reduction in FcγRIIB expression was stronger in the $CD19^+CD27^+$ memory ($p = 0.002$) compared to $CD19^+CD27^-$ naïve ($p = 0.009$) B cell compartment due to a failure of CIDP patients to upregulate or to maintain upregulation of FcγRIIB when B cells become memory cells. FcγRIIB expression was also reduced in classical $CD14^+CD16^-$ monocytes ($p = 0.046$) and tended to be lower in $CD16^+$ monocytes ($p = 0.216$). Expression of the high-affinity activating FcγRI, not expressed on B cells, was increased in both monocyte subsets in patients with CIDP (figure 2.1B). Expression of the low-affinity FcγRIIA was increased on $CD14^{low}CD16^+$ monocytes. Thus, expression levels of inhibitory versus activating FcγRs are deregulated in untreated patients with CIDP.

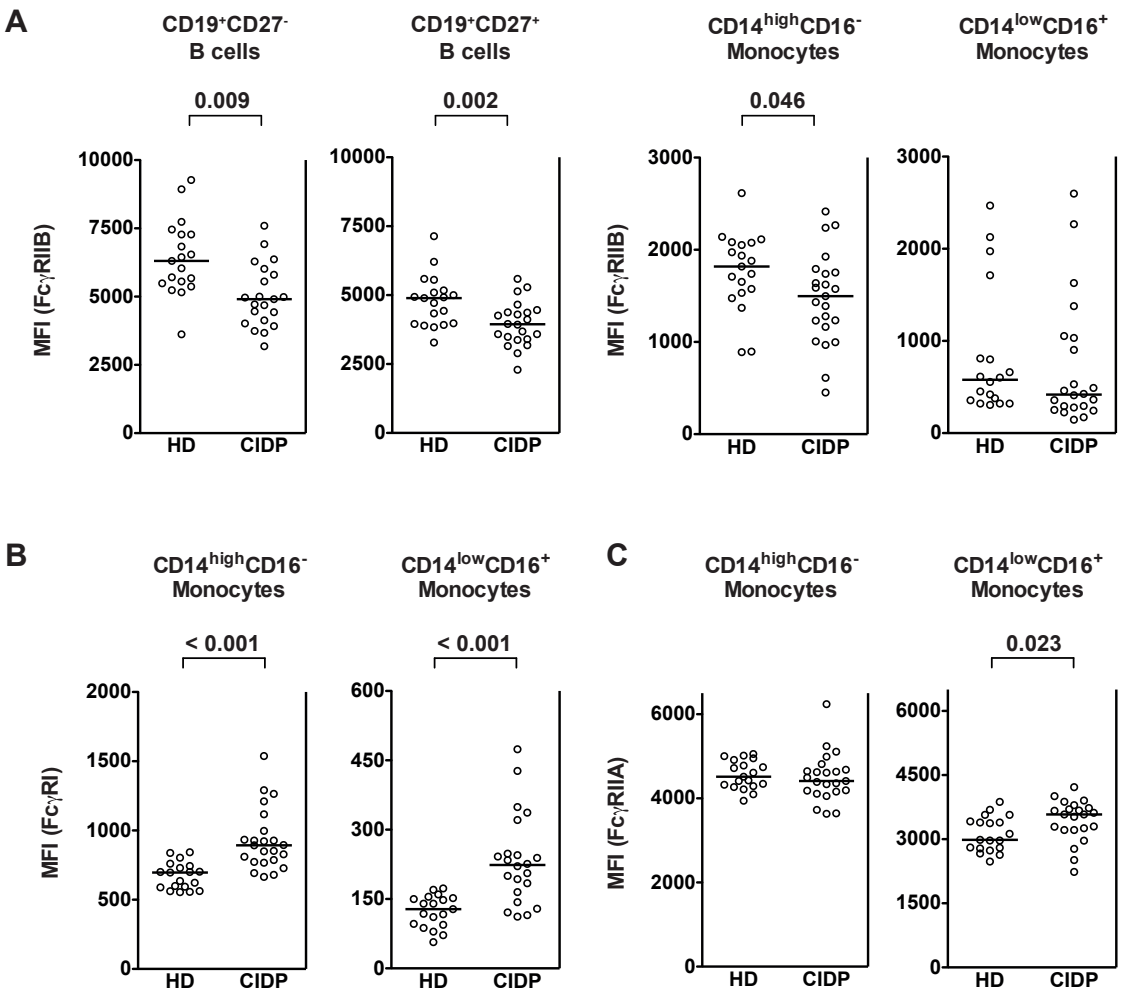

Figure 2.1 Deregulated inhibitory and activating FcγR expression in CIDP
PBMC of CIDP patients and demographically matched healthy controls were stained with fluorochrome-coupled antibodies. FcγR expression levels were measured on B cell and monocyte subsets by flow cytometry. Median fluorescence intensity (MFI) of FcγRIIB **(A)** on naïve ($CD27^{-}$) and memory ($CD27^{+}$) B cells, and classical ($CD14^{high}CD16^{-}$) and non-classical ($CD14^{low}CD16^{+}$) monocytes. **(B)** FcγRI and **(C)** FcγRIIA MFI on classical ($CD14^{high}CD16^{-}$) and inflammatory ($CD14^{low}CD16^{+}$) monocytes. Statistics were performed using the Mann-Whitney U test.

2.1.2 Effect of IVIG therapy on deregulated FcγR expression

Studies in various mouse autoimmune disease models provided solid evidence that the anti-inflammatory activity of IVIG depends on the presence and upregulation of the inhibitory FcγRIIB [190, 236, 237]. We analyzed expression levels of FcγRIIB compared to the activating FcγRI and FcγRIIA in patients with CIDP before and 2 or 4-8 weeks after IVIG therapy. The clinical response rate to IVIG therapy was 87.5 % as defined by improvement of disability within 4 weeks after IVIG therapy [184, 238]. Only samples where >100 cells could be detected in the final gate were included in the analysis. FcγRIIB expression was induced on both naïve

and memory B cells 2 weeks after IVIG therapy ($p = 0.007$ and 0.004 for naïve and memory B cells, respectively) (figure 2.2A). After 4-8 weeks, no further induction of FcγRIIB expression on B cells was observed for most patients (Naïve B cells: further induction in 7/20; 35.0 %. memory B cells: further induction in 5/17; 29.4 %), but levels remained significant compared to baseline values ($p = 0.002$ and 0.047 for naïve and memory B cells, respectively). On monocyte subsets, FcγRIIB expression was upregulated in some patients ($CD14^{high}CD16^{-}$: 16/23; 69.6 % after 2 weeks; 15/22; 68.2 % after 4-8 weeks; $CD14^{low}CD16^{+}$: 10/19; 52.6 % after 2 weeks; 9/20; 45.0 % after 4-8 weeks), but the overall difference was not statistically significant (figure 2.2A). IVIG therapy was associated with a transient downregulation of the activating FcγRI on inflammatory $CD14^{low}CD16^{+}$ monocytes after 2 weeks ($p < 0.001$) (figure 2.2B). After 4-8 weeks, FcγRI levels did not differ significantly from baseline values ($p = 0.18$). Monocyte expression levels of the low affinity activating FcγRIIA were not significantly regulated by IVIG therapy (figure 2.2C).

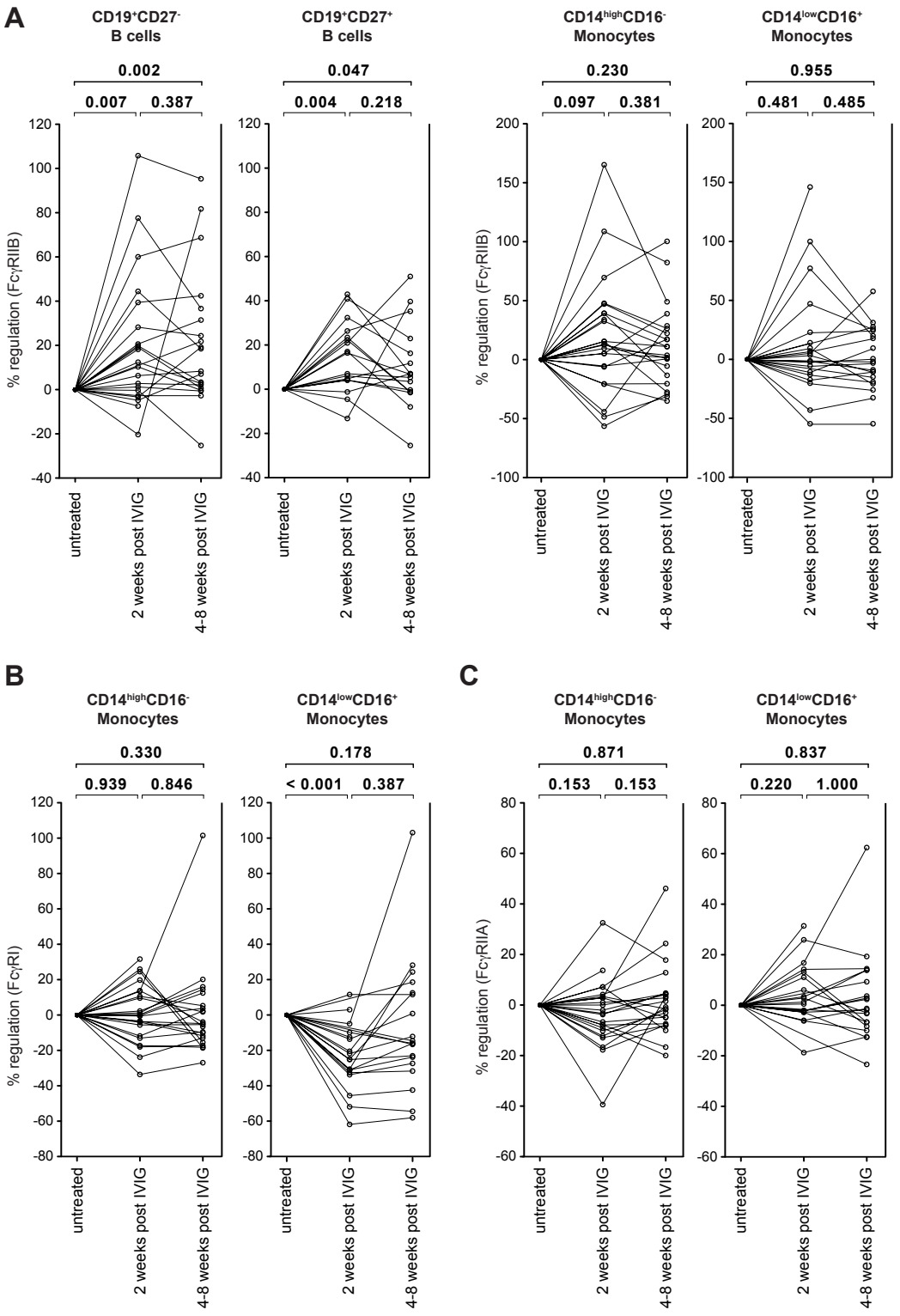

Figure 2.2 IVIG therapy partially restores FcγR expression on B cells and monocytes.

Flow cytometry analysis of FcγR expression on PBMC of treatment-naïve CIDP patients before and 2 or 4-8 weeks after a single-dose of IVIG (2 g/kg) treatment. Data points for individual patients are connected by lines. For some patients not all data points were available. Changes of FcγRIIB **(A)**, FcγRI **(B)** and FcγRIIA **(C)** MFI following IVIG treatment are shown relative to baseline (untreated). Statistics were performed using the Wilcoxon signed rank test.

2.2 IgG-Fc glycosylation in patients with CIDP

Studies in murine models of antibody-mediated autoimmunity suggested that IgG-Fc sialylation conveys anti-inflammatory properties to IgG [133, 139]. Therefore, we were interested in the regulation of antibody sialylation in human autoimmunity. High-performance chromatography with fluorescence detection (HPLC-FL) and lectin blotting were used for the specific detection of IgG-Fc glycoforms.

2.2.1 Frequency of IgG-Fc glycoforms in CIDP patients

According to the number of terminal galactose residues, *N*-glycans are classified as G0 (no galactose residue and, consequently, no sialic acid residue), G1 (one galactose residue), and G2 (both branches carry a galactose residue) groups. The frequency of these IgG-Fc glycoforms was evaluated by high performance anion-exchange chromatography (figure 2.3A) in 19 previously untreated patients with CIDP included in the ICE trial [192] (see capter 4.2.1 for further details) before randomization to IVIG or placebo treatment and compared to 20 healthy individuals matched by age (median age (range): 55 (22-74) for CIDP and 53.5 (21-73) for HD) and gender (male to female ratio: 1.7 for CIDP and 1.9 for HD). Total serum IgG levels were similar in patients and controls (data not shown).

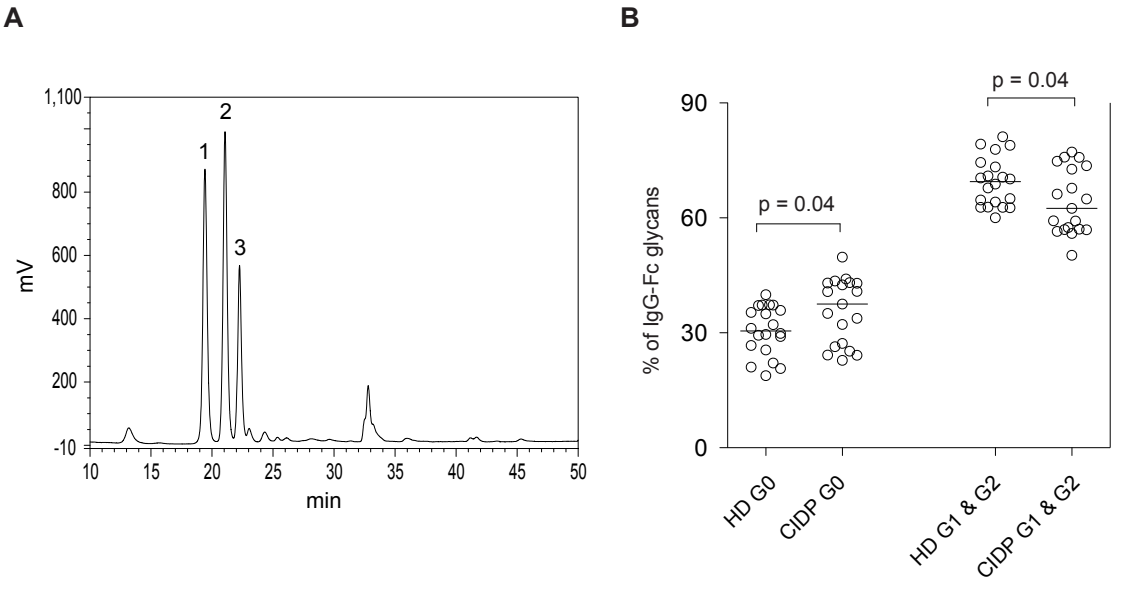

Figure 2.3 Serum IgG-Fc galactosylation.
(A) Representative HPLC-FL chromatogram of IgG-Fc glycan analysis. The three major IgG-Fc glycoforms G0 (no galactose), G1 (one galactose), G2 (two galactoses) are indicated with 1, 2 and 3, respectively. **(B)** Frequency of agalactosyl (G0) and galactosylated (G1 and G2) IgG-Fc glycans in healthy donors (HD) as compared to CIDP patients. GlcNAc, N-Acetylglucosamine; Man, mannose; Gal, galactose; Fuc, fucose; Sial, sialic acid. p values by Mann-Whitney U test.

The frequency of agalactosyl IgG-Fc was significantly increased in patients with CIDP (figure 2.3B). Conversely, galactosylated glycoforms were less frequently detected and the ratio of galactosyl to agalactosyl IgG-Fc was decreased in CIDP sera. Both G1 and G2 groups were reduced in CIDP patients and contributed to the overexpression of agalactosyl *N*-glycans. Next, we analyzed IgG-Fc glycosylation longitudinally in patients with CIDP by Lectin-blotting for the detection of individual glycan residues.

2.2.2 Longitudinal analysis of serum IgG-Fc glycosylation in CIDP patients

2.2.2.1 Serum IgG concentration

We longitudinally analyzed serum from CIDP patients, who had been were treated with IVIG. As we analyzed antibody glycosylation, it was important to assess the influence of IVIG on total serum IgG concentration. In the ICE trial cohort, total serum IgG levels in samples obtained before and 24 weeks after placebo (n = 18) and IVIG treatment (n = 17) were analyzed. Unlike in patients receiving placebo, IVIG treated patients showed a consistent increase in serum IgG-Fc levels (figure 2.4A). This was not the case in an additional cohort of 33 CIDP patients ("Marburg cohort", see capter 4.2.1 for further details) in whom post-treatment samples were taken 3-5 weeks following the last infusion of IVIG (mean ± SD: 4 ± 0.6) and total serum IgG levels after IVIG therapy were not significantly increased as compared to pre-treatment samples (figure 2.4B).

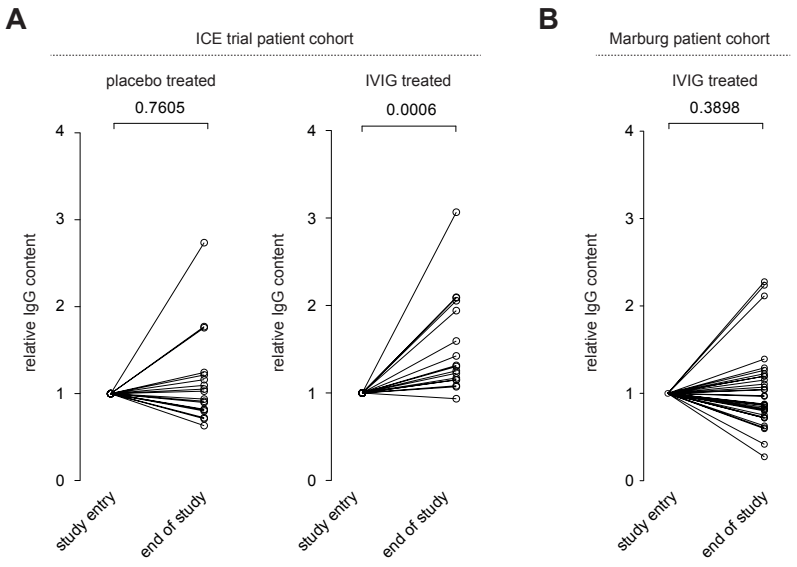

Figure 2.4: IVIG treatment leads to an increase of serum IgG content.
Serum IgG content was measured by ELISA. Relative IgG content compared to study entry is shown. **(A)** Serum of CIDP patients participating in the ICE trial was taken before and 2 weeks after the last treatment with IVIG (left) or placebo (right) **(B)** Patients from an independent cohort ("Marburg cohort") all received IVIG. Serum was taken 3-5 weeks following the last infusion of IVIG (mean +/- SD: 4.0 +/- 0.6). (IVIG, intravenous immunoglobulin). Statistics were performed by Wilcoxon matched pairs test.

2.2.2.2 Induction of IgG-Fc sialylation is associated with disease remission in CIDP

First, patients from ICE cohort were analyzed. We found that patients with clinical disease remission during placebo therapy could be distinguished from those with stable or worsened disease by the induction of Fc-sialylation (figure 2.5A). Changes in Fc-galactosylation and fucosylation were similar in patients with disease remission compared to stable or worsened disease. In contrast, IgG-Fc glycosylation in patients who received IVIG was not associated with successful treatment (figure 2.5A). The detected increase of total IgG serum levels 2 weeks after the last infusion compared to baseline levels (figure 2.4A) precluded profiling of endogenous IgG in this cohort. We therefore analyzed serum samples from an independent cohort of 33 CIDP patients ("Marburg cohort", see table 4.3 for further details). In this cohort, reduction in clinical disease severity scores upon IVIG therapy was significantly associated with an induction of IgG-Fc sialylation. No significant correlation was observed for IgG-Fc galactosylation and fucosylation and the reduction of disease severity (figure 2.5B).

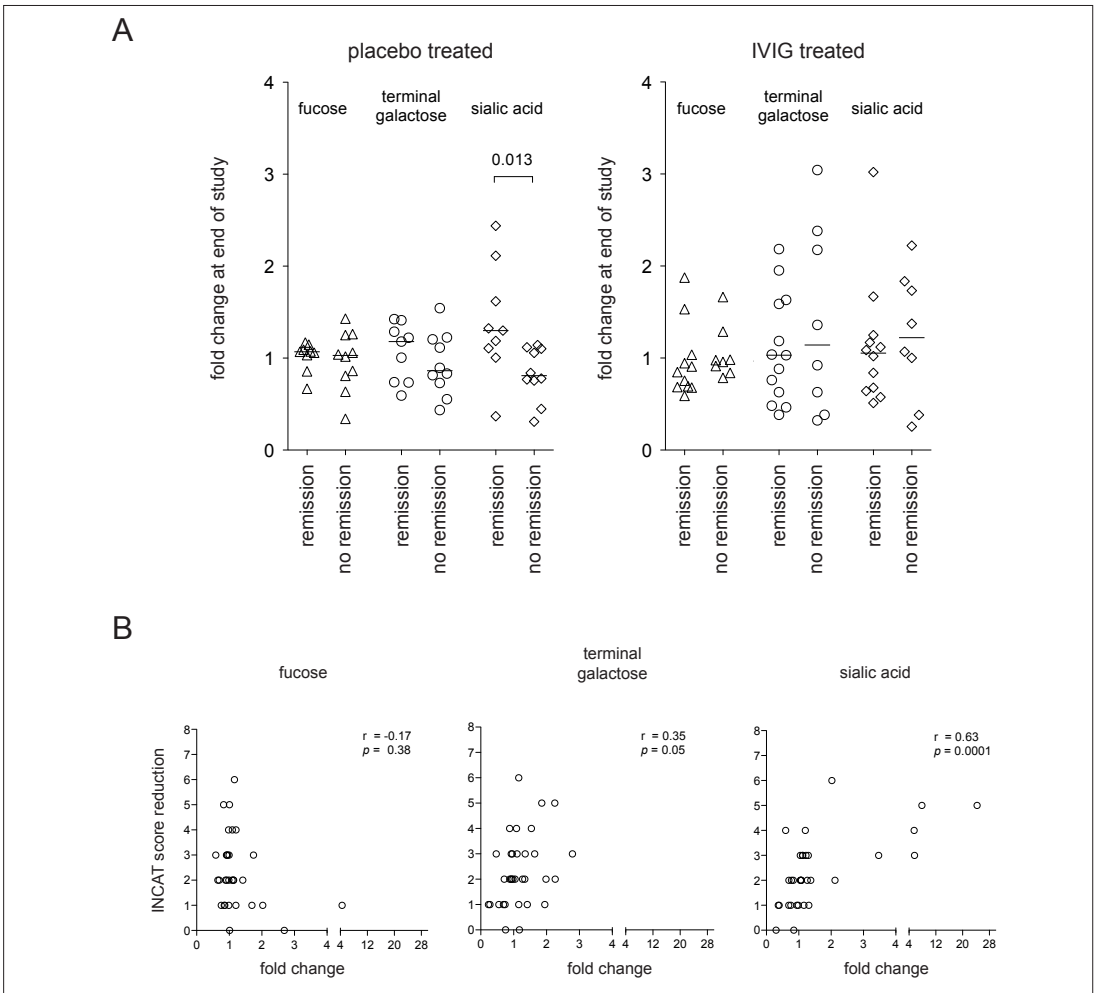

Figure 2.5 (continued on next page)

Figure 2.5 Induction of IgG-Fc sialylation is associated with disease remission in CIDP (continued)
(A) Serum IgG-Fc glycan composition of CIDP patients analyzed by lectin blotting. Relative IgG-Fc glycan abundance of CIDP patients before and after a 24 weeks observation period (1 = no change). Patients undergoing disease remission are compared to those with stable or worsening disease (no remission). Statistics were performed by Mann-Whitney U test. **(B)** IgG-Fc glycan composition analysis of CIDP patients before and 3-5 weeks after receiving the last IVIG injection. Fold changes in glycan composition are compared to disease activity changes reflected by the INCAT overall disability score (maximal score = 10). Statistics were performed by Spearman test.

2.3 Impact of IgG-Fc glycan structure on IgG function

2.3.1 Fc-receptor binding is not affected by IgG-Fc sialylation

In order to investigate the mechanisms by which Fc sialylation may results in remission., we purified de-sialylated (neuraminidase treated) and sialic acid enriched Fc (by SNA-lectin column-affinity) from IVIG. Successful purification was confirmed by lectin blotting (figure 2.6A). PBMC were stained with cell-type specific monoclonal antibodies and incubated with Fc, sialic acid enriched Fc and neuraminidase treated Fc. Additionally, we obtained an homogenously tetra-sialylated glycoform of Rituximab (RTX) prepared by chemoenzymatic glycoengineering of commercial RTX (kindly provided by L. X. Wang and J. Giddens) [239] (figure 2.6B). Tetra-sialylation refers to the prescence of two sialic acids in present on each of the tow IgG-Fc glycans.
No binding differences of Fc and sialic acid enriched Fc to FcγR expressing monocytes and NK cells was found (figure 2.7A). De-sialylated Fc bound slightly better to $CD14^{-}$ monocytes and $CD56^{bright}$ NK cells which both express FcγRIIIA. No binding was detecton to B cells, which only express the low-affinity FcγRIIB (figure 2.7A).
FcγR binding properties of RTX and tetra-sialylated RTX were analysed using CHO cells transfected with one of the human FcγRs (kindly provided by F. Nimmerjahn) [240]. For FcγRIIA and FcγRIIIA both of the two most frequent isoforms were analysed. Similar to sialic acid enriched Fc, no differences in FcγR binding were detected for tetra-sialylated RTX compared to unmodified, non-sialylated RTX (figure 2.7B).

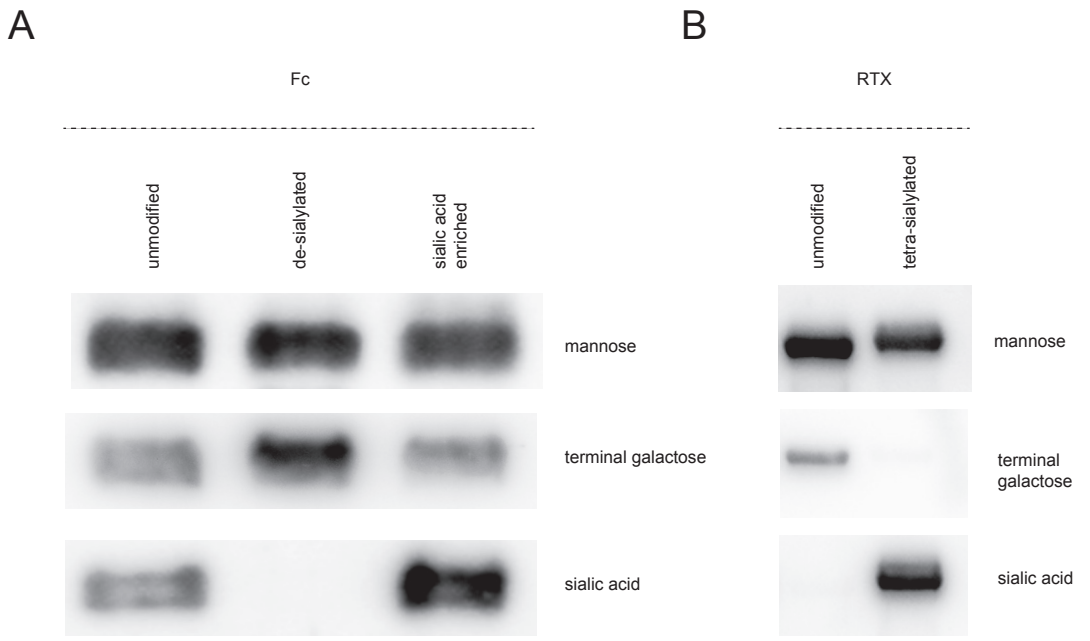

Figure 2.6 Confirmation of polyclonal Fc and RTX glycovariants
(A) Lectin immunoblotting of Fc purified from polyclonal IgG and enriched for sialylated Fc or de-sialylated **(B)** Lectin immunoblotting of RTX glycovariants. (mannose: *Lens culinaris* agglutinin; terminal galactose: *Erythrina cristagalli* lectin; sialic acid: *Sambucus nigra* agglutinin)

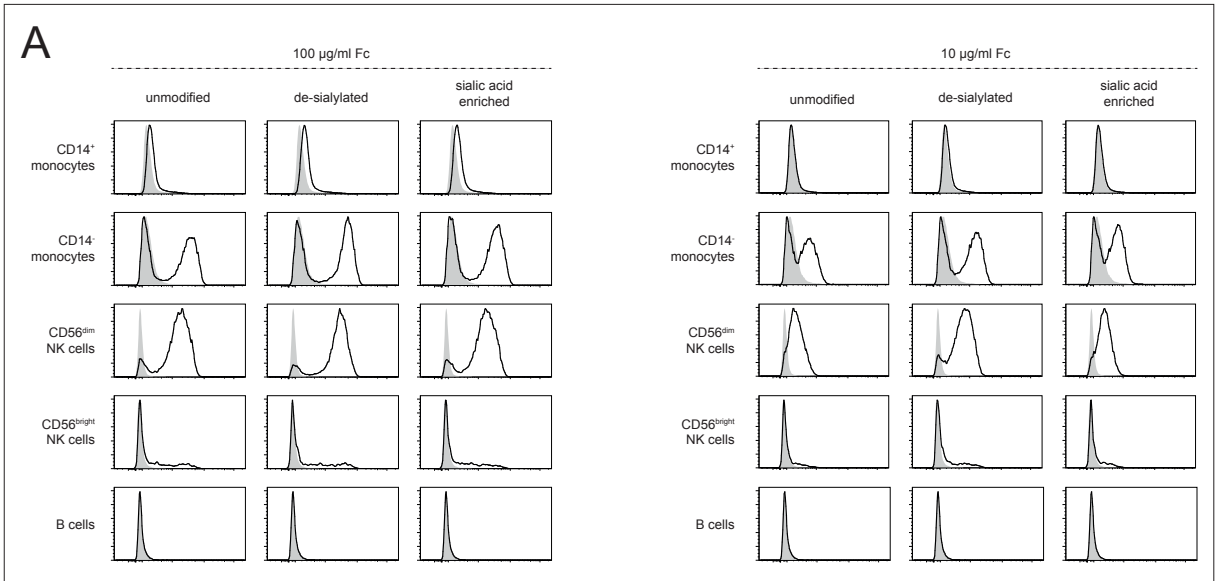

Figure 2.7 (continued on next page)

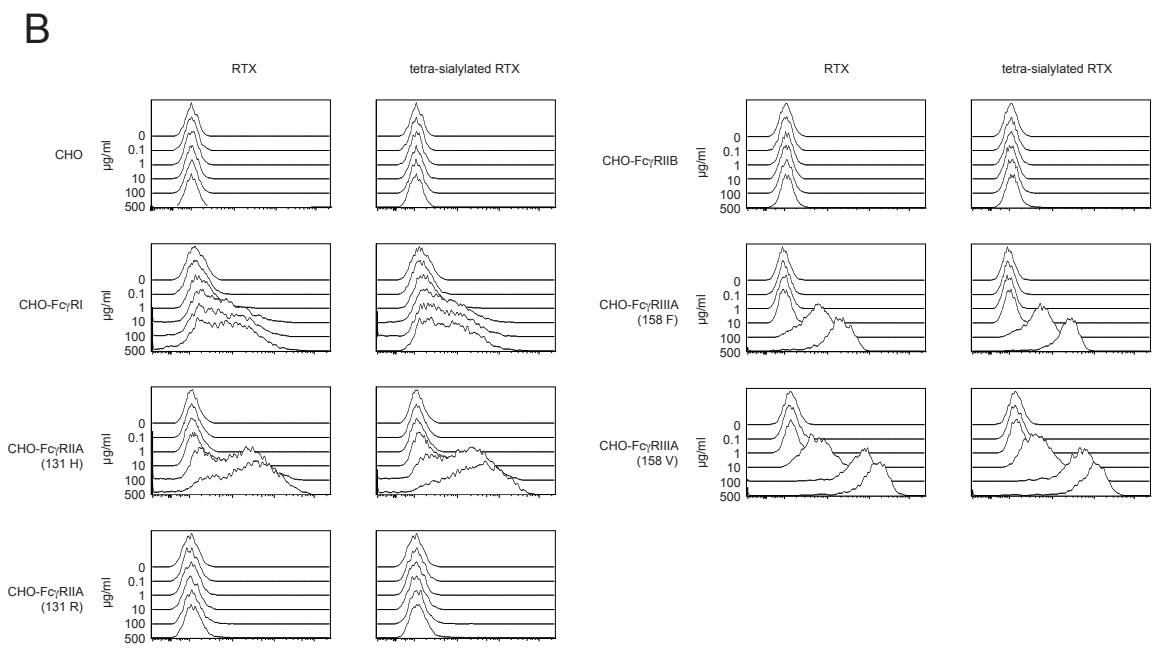

Figure 2.7 Sialic acid does not influence FcγR binding properties (continued)
(A) PBMC of a healthy blood donor were stained with cell-lineage specific fluorescent labelled antibodies and binding of differentially sialylated polyclonal Fc to lymphocyte subsets was analyzed by flow cytometry. **(B)** Binding of RTX and tetra-sialylated RTX to CHO cells either untransfected or transfected with the indicated FcγRs analyzed by flow cytometry.

2.3.2 FcγR mediated target cell lysis is not affected by IgG-Fc sialylation

We employed these two glycoforms, i.e. commercial RTX not carrying sialic acid *vs.* tetra-Fc-sialylated RTX, to determine whether IgG-Fc sialylation impacts the efficacy of CD20-targeted B cell lysis. Incubation of Natural killer (NK) cells with either the unmodified or tetra-Fc-sialylated antibody resulted in efficient lysis of autologous B cells and the depleting efficacy was similar between the two glycoforms (figure 2.8).

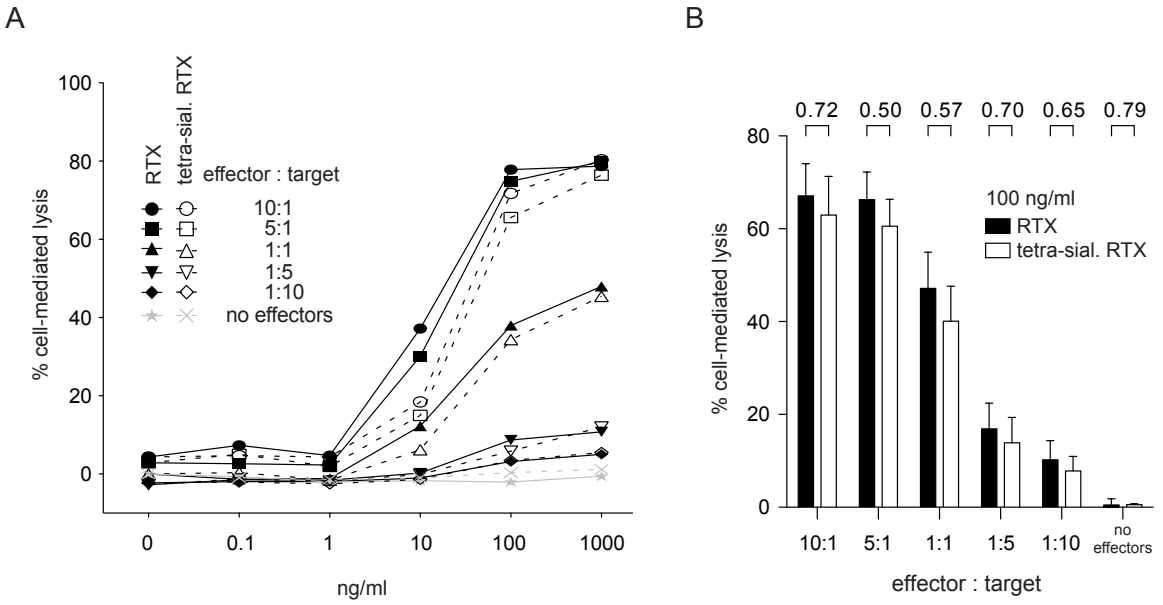

Figure 2.8 ADCC is not affected by Fc sialylation
(A) RTX and tetra-sialylated RTX mediated lysis of B cells (targets) by autologous NK cells (effectors). **(B)** Representative experiment and quantification of 3 independent experiments. Statistics were performed by t-test.

2.3.2 IgG-Fc glycan structure regulates complement-dependent cytotoxicity

2.3.2.1 IgG-Fc tetra-sialylation impairs CDC

Complement-dependent cytotoxicity (CDC) of unmodified RTX and tetra-sialylated RTX was analyzed using CD20 expressing Burkitt lymphoma cell lines Raji or Ramos (figure 2.9A and C, respectively). In contrast to ADCC, tetra-Fc-sialylated RTX was much less efficient than unmodified RTX at inducing CDC of both Raji (figure 2.9B) and Ramos (figure 2.9D) cells.

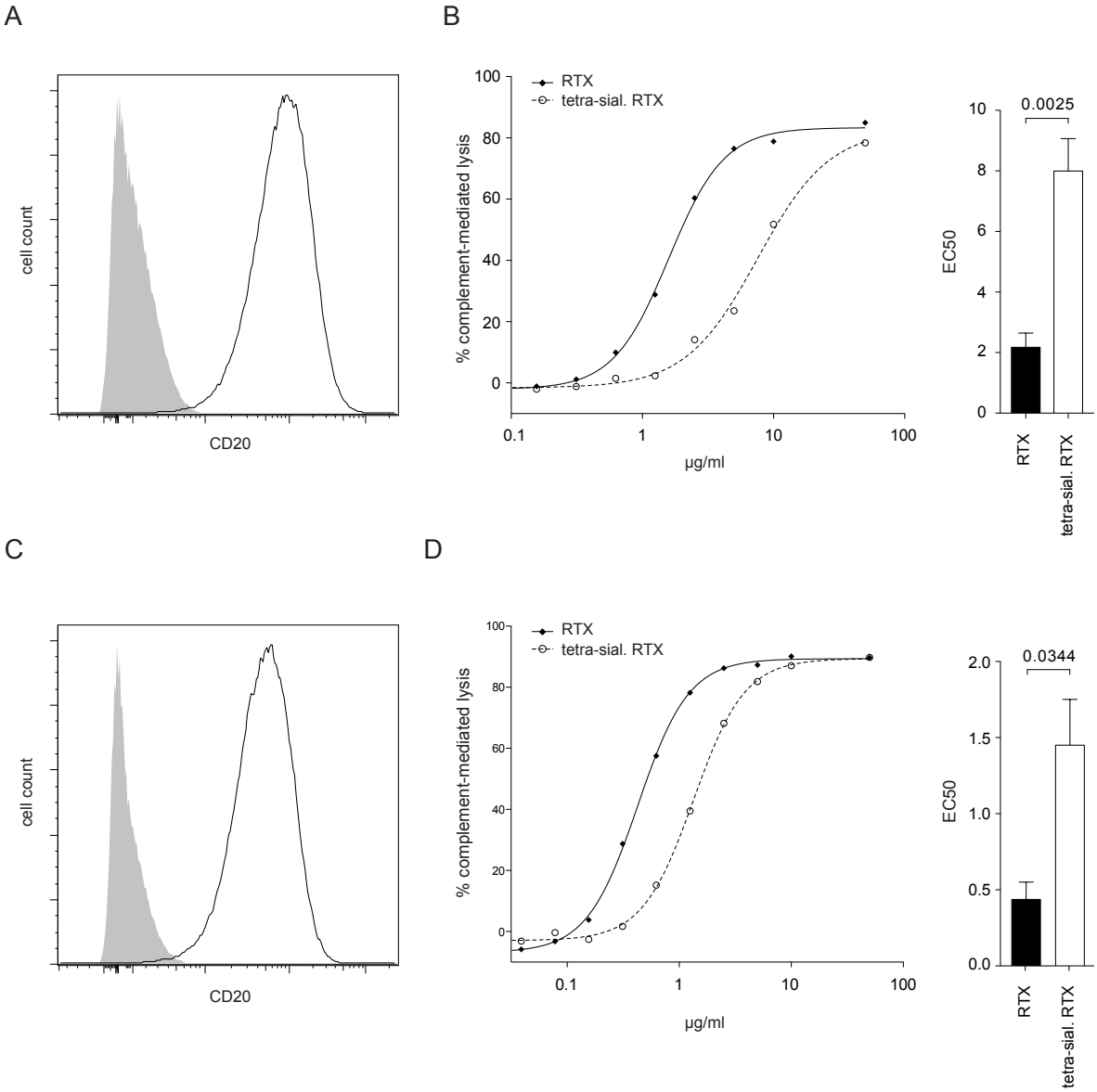

Figure 2.9 IgG-Fc tetra-sialylation impairs CDC
(A) CD20 expression of Raji cells analyzed by flow cytometry. Grey histograms, unstained cells; open histograms, stained cells. **(B)** Complement-mediated lysis of Raji cells. Representative experiment and quantification of EC_{50} of 4 independent experiments. Statistics were performed by t-test. **(C)** CD20 expression of Ramos cells analyzed by flow cytometry. Grey histograms, unstained cells; open histograms, stained cells. **(D)** Complement-mediated lysis of Raji cells. Representative experiment and quantification of EC_{50} of 3 independent experiments. Statistics were performed by t-test.

2.3.2.2 Generation and characterization of RTX and hu8-18C5 glycovariants

To confirm that CDC differences are independent of antibody processing and not restricted to RTX we used β1,4 galactosyltransferase-1 (β1,4GalT) and α2,6-sialyltransferase (ST6Gal1) enzymes in the presence of the corresponding sugar nucleotide substrates for the enrichment of mono- and bi-sialylated antibody species[87, 165, 241]. An SNA lectin-affinity column was used to further enrich enzymatically galactosylated and sialylated antibodies for species containing at least two sialic acids per antibody [242]. RTX and a humanized version of the MOG-reactive 8-18C5 (hu8-18C5) antibody [243] were used. The chosen antibodies did not contain N-glycosylation sites in their $F(ab`)_2$ domain (figure 2.10) allowing us to ensure that any glycan modification is restricted to the IgG-Fc N-glycans.

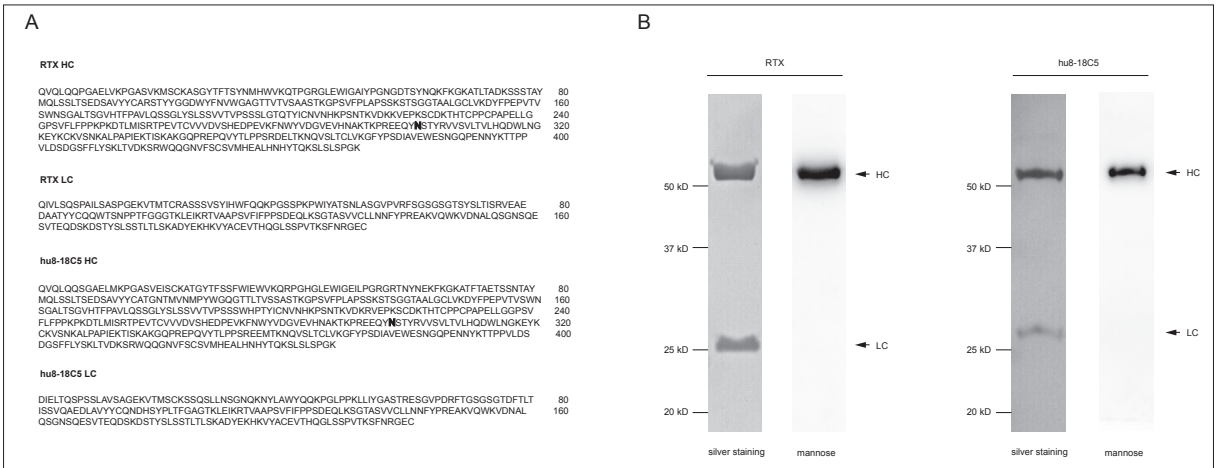

Figure 2.10 RTX and hu8-18C5 N-glycosylation sites.
(A) Amino acid sequence of RTX and hu8-18C5 heavy chain (HC) and light chain (LC) were analyzed for potential N-glycosylation sites. Both antibodies only contain the conserved Fc-N-glycosylation site at asparagine 297 (N297, depicted in bold) and no glycosylation sites in the HC and LC variable regions. N-glycosylation sites (Asn-Xaa-Ser/Thr) were identified using the NetNGlyc 1.0 server from the Technical University of Denmark (DTU). RTX sequences were obtained from www.drugbank.ca (Acc. Nr. DB00073) and hu8-18C5 sequences were translated from the expression plasmids. **(B)** SDS-Polyacrylamide gel electrophoresis of RTX and hu8-18C5. Silver staining (left lane) and immunoblotting (right lane) using the mannose-specific lectin Lens culinaris agglutinin. (HC, heavy chain; LC, light chain)

We generated galactosylated, galactosylated and sialylated as well as de-galactosylated variants of the antibodies. Lectin-blotting was performed to confirm the glycan profile and to determine the approximate relative contribution of the individual glycan species in the final product (figure 2.11).

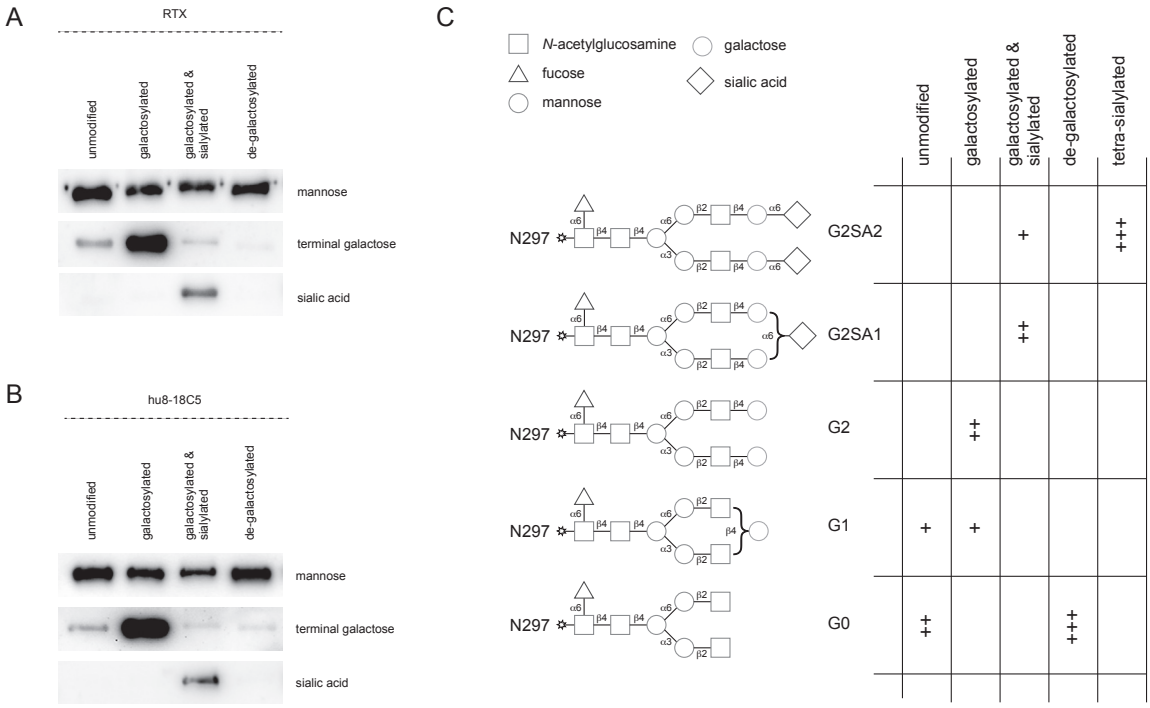

Figure 2.11 Confirmation of antibody glycovariants by lectin immunoblotting
(A) Lectin immunoblotting of RTX glycovariants. **(B)** Lectin immunoblotting of hu8-18C5 glycovariants. **(C)** Relative abundance of individual IgG-Fc glycans in the antibody glycovariants. Terminal galactose refers to an IgG-Fc linked galactose not succeeded by sialic acid.

To confirm the integrity and functionality of the generated antibodies, binding of RTX and hu8-18C5 antibody glycovariants to their cognate antigen was tested. To do so, a human oligodendroglial cell line (MO3.13) transduced to express human full-length MOG cDNA [244] (MO3.13 MOG, figure 2.12A) was used as a target for hu8-18C5 and $CD20^+$ Raji cells for RTX. As shown in figure 2.12B and C, galactosylation and sialylation led to a slightly increased antigen-binding capacity. Contrary, tetra-sialylation of RTX led to decreased antigen binding (figure 2.12B).

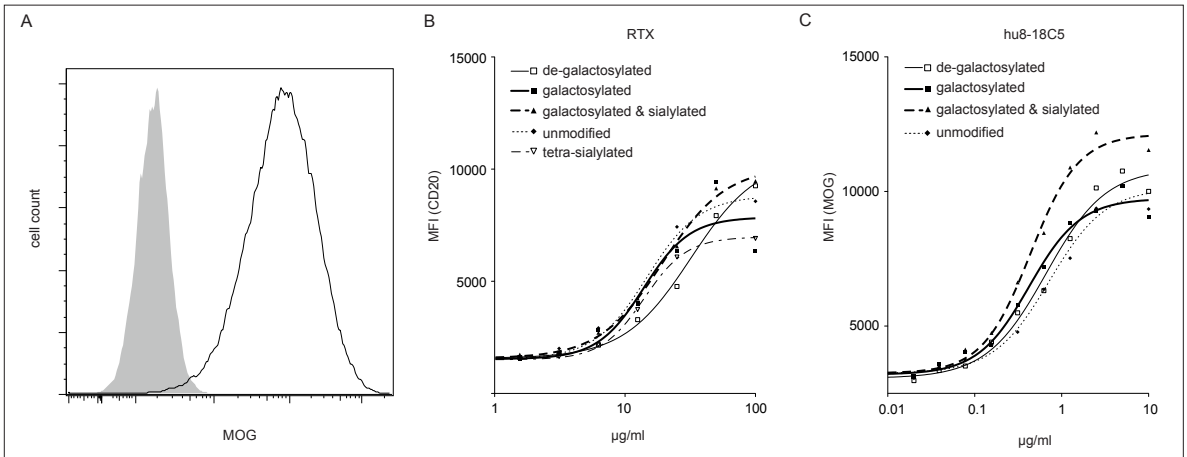

Figure 2.12 MO3.13 MOG cell line antigen expression antigen binding properties of antibody glycovariants (continued on next page)

Figure 2.12 MO3.13 MOG cell line antigen expression antigen binding properties of antibody glycovariants (continued)
(A) MO3.13 cells lentivirally transduced to express human myelin oligodendrocyte glycoprotein (MOG) and FACS-sorted for MOG positive cells were analyzed for MOG expression by flow cytometry. Grey histograms, unstained cells; open histograms, stained cells. $CD20^+$ Raji cells were incubated with RTX or glycovariants of RTX **(B)** or MO3.13 MOG cells with hu8-18C5 (anti-MOG) or glycovariants of hu8-18C5 **(C)** following incubation with a fluorescently labeled anti-Ig antibody and detection of antibody binding by flow cytometry. (MFI, median fluorescence intensity)

2.3.2.3 IgG-Fc sialylation as well as de-galactosylation impairs CDC

CDC was assessed for unmodified RTX using Raji cells as targets and for hu8-18C5 using MO3.13 MOG cells. Enzymatic enrichment of RTX or hu8-18C5 for sialylated glycoforms recapitulated the reduced CDC of tetra-sialylated RTX (figure 2.13A and B). As both sialic-acid enriched RTX variants (tetra-sialylated and galactosylated & sialylated) also have a higher galactose contant than unmodified RTX, we next analyzed the relative influence of galactose and sialic acid on CDC. As shown in figure 2.13C, galactose-enrichment of RTX did not alter CDC compared to the unmodified antibody whereas the addition of sialic acid to the previously galactosylated antibody resulted in reduced CDC and also de-galactosylation of the unmodified RTX compromised CDC to a similar extent. Based on these findings, we set out to further elucidate the underlying mechanism of IgG-Fc glycan mediated CDC regulation by dissecting its influence on the individual steps of the classical complement cascade.

2.3.3 Fc-sialylation inhibits increased C1q binding of Fc-galactosylated IgG

The classical complement pathway is triggered by binding of C1q to the Fc domain in antibody:antigen complexes leading to autoactivation of the C1 complex (comprising C1q, C1r and C1s) and activation of complement by cleavage of C4 and C2. The resulting C4bC2a convertase cleaves C3 causing the covalent coupling of C3b to reactive surfaces such as the cell membrane which culminates in the formation of the membrane attack complex and lysis of the target cell [245]. The binding affinity of C1q for murine IgG was shown to be reduced upon the removal of galactose from the IgG-Fc linked glycan [116]. To investigate the mechanism by which Fc-sialylation impacts complement-mediated cytotoxicity, we tested galactosylated, sialylated, and de-galactosylated Fc glycovariants of RTX and hu8-18C5 for their ability to bind C1q and induce complement activation.

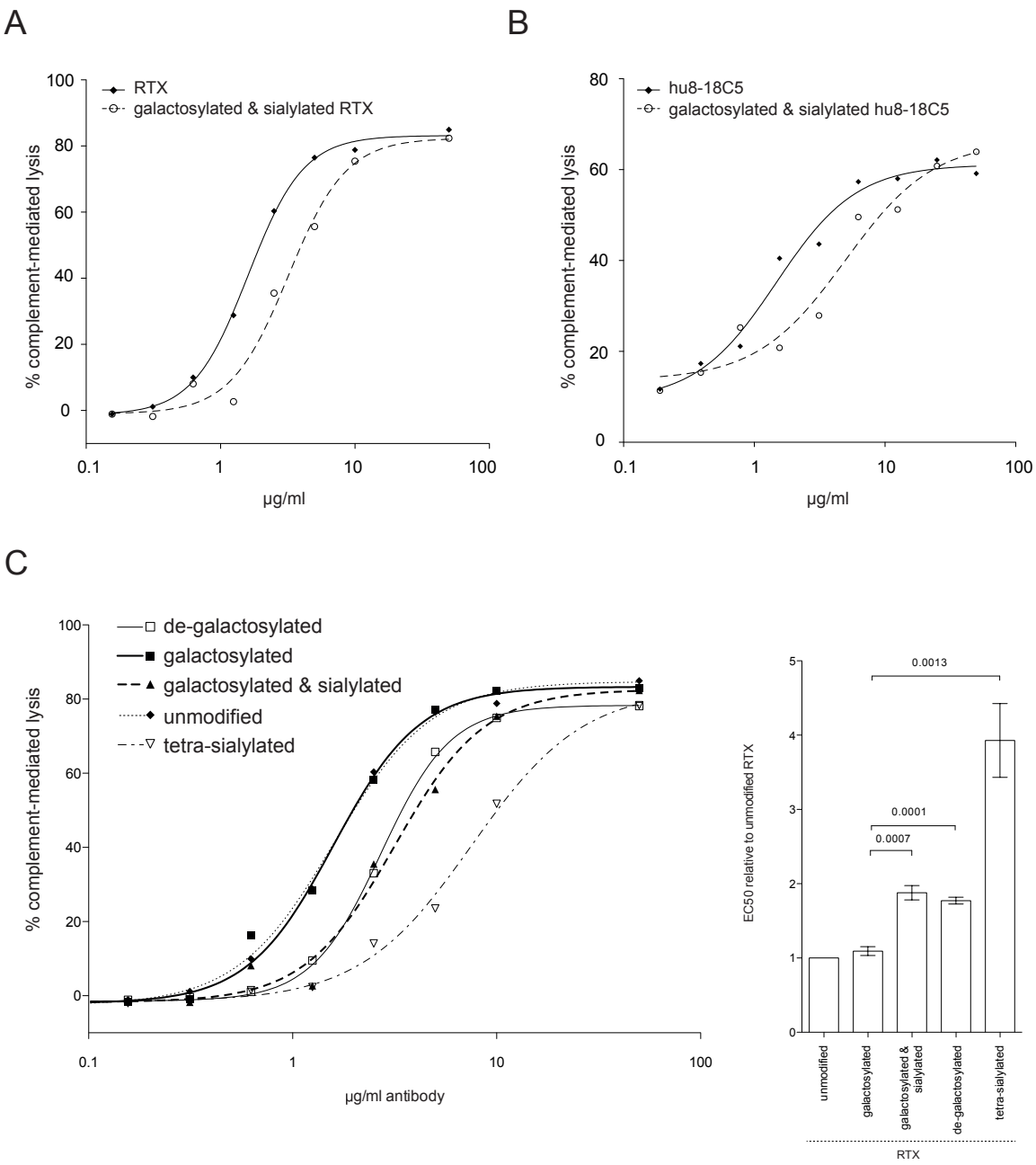

Figure 2.13 IgG-Fc galactose and sialic acid content influence CDC
(A) CDC of Raji cells with RTX or galactosylated and sialylated RTX **(B)** CDC of MO3.13 MOG with hu8-18C5 or galactosylated and sialylated hu8-18C5. **(C)** CDC of Raji cells with RTX glycovariants. Representative experiment (left) and quantification of EC_{50} of 3 independent experiments (right). EC_{50} obtained for unmodified RTX was set to 1 and the relative EC_{50} was calculated. Statistics were performed by t-test.

2.3.3.1 C1q binding to antibody glycovariants

The generated antibody glycovariants of RTX and hu8-18C5 (figure 2.6B and 2.11) were used in combination with the respective target cell lines (Raji and Ramos) for RTX and MO3.13 MOG for hu8-18C5) to analyze cell-surface deposition of C1q. To avoid cell lysis by CDC, C5 depleted serum was used. Incubation of the antibodies with their target cells in the presence of human serum complement led to rapid binding of C1q (figure 2.14A and B). Fc-galactosylation of unmodified antibodies resulted in a markedly increased capacity to bind C1q. Subsequent addition of sialic acid abrogated increased C1q binding of Fc-galactosylated IgG. Fully tetra-Fc-sialylated RTX was largely devoid of C1q binding (figure 2.14A-E). To investigate whether these effects can be transferred to polyclonal IgG, Fc purified from IVIG and enriched for sialylated Fc or de-sialylated, i.e. terminally galactosylated (figure 2.6A) was analyzed for C1q binding in ELISA. Similar to the monoclonal IgGs tested, the presence of more terminal galactosylated (as a result of de-sialylation) resulted in increased C1q binding. Conversely, the enrichment for sialic acid-containing IgG-Fc led to reduced C1q binding (figure 2.14F).

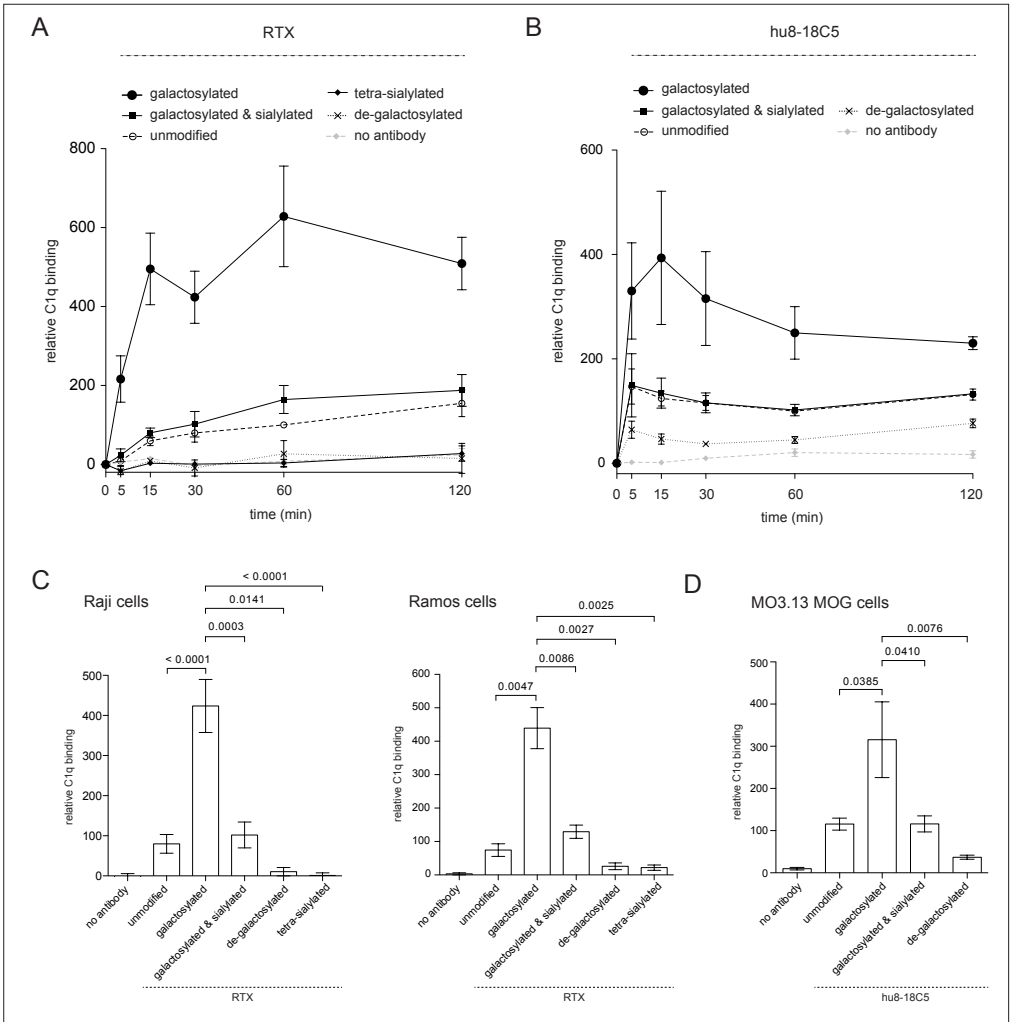

Figure 2.14 (continued on next page)

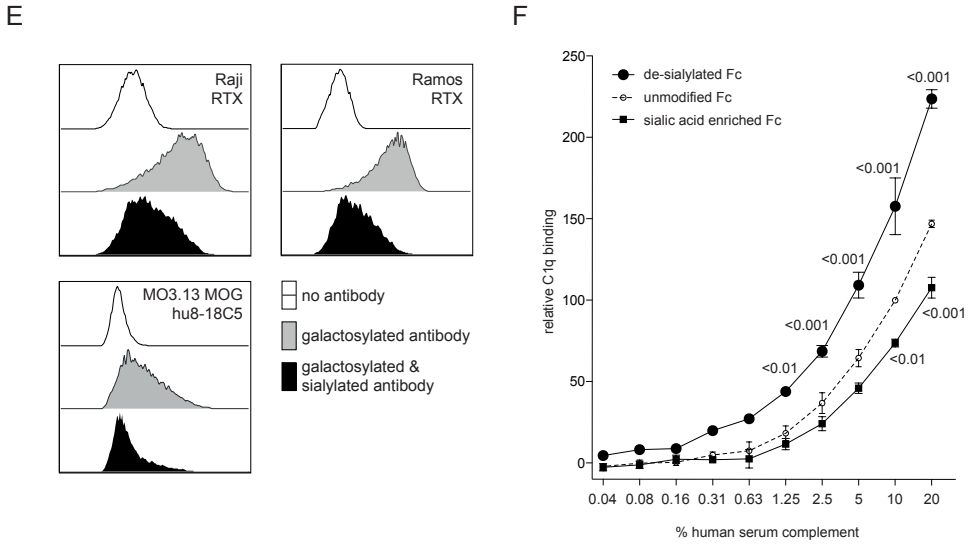

Figure 2.14 C1q binding to IgG Fc glycovariants. (continued)
(A) Time-course of C1q binding to CD20$^+$ Raji cells in the presence or absence of differentially glycosylated RTX. Mean and SEM of at least three independent experiments. Median fluorescence intensity obtained for the unmodified antibody after 60 minutes was set to 100 and the relative signals were calculated. **(B)** Time-course of C1q binding to MO3.13 MOG cells in the presence or absence of differentially glycosylated variants of hu8-18C5 (anti-MOG). Mean and SEM of at least 3 independent experiments. **(C)** Quantification of RTX antibody-glycovariant dependent C1q binding to CD20$^+$ Raji (left) and Ramos (right) cells after 30 minutes incubation. Mean and SEM of at least 3 independent experiments. Statistics were performed by t-test. **(D)** Quantification of hu8-18C5 antibody-glycovariant dependent C1q binding to MO3.13 MOG cells after 30 minutes. Statistics were performed by t-test. **(E)** Representative flow cytometry stainings showing C1q binding to the indicated cell type and antibody after one hour incubation. **(F)** C1q binding to differentially glycosylated Fc measured by ELISA. Mean and SEM of three independent experiments. C1q binding was normalized to unmodified Fc at 10 % serum. Individual curves were compared to Fc using 2-way ANOVA and Bonferroni posttest comparing Fc and de-sialylated Fc (p values above curve) or Fc and sialic acid enriched Fc (p values below curve)

2.3.3.2 IgG-Fc glycosylation influences C3b deposition

Next, we investigated whether the capacity of Fc-sialylation to block C1q binding also translates into decreased downstream activation of complement proteins. As shown in figure 2.15, levels of C3b deposition to the cell surface were also decreased upon antibody sialylation or de-galactosylation. However, the markedly increased levels of C1q binding to galactosylated antibodies did only partially translate into increased C3b deposition.

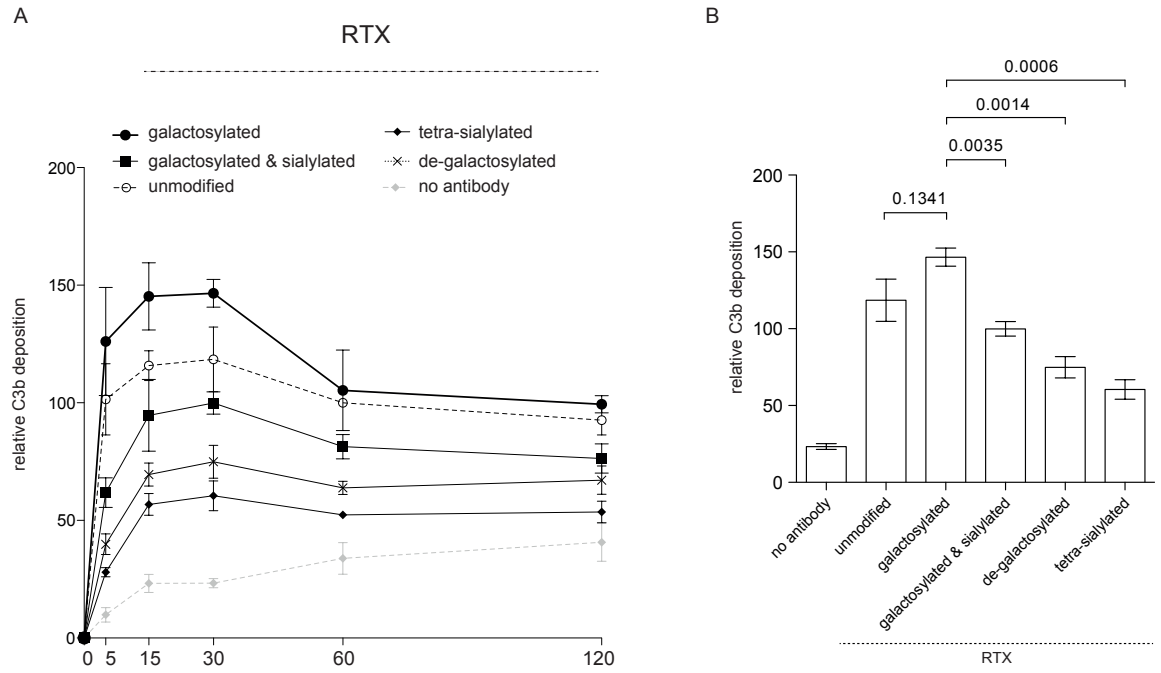

Figure 2.15 IgG-Fc sialylation reduces C3b deposition.
C3b deposition to Raji cells in the presence or absence of 10 µg/ml RTX or glycovariants of RTX analyzed by flow cytometry **(A)** and quantification of C3b deposition after 30 minutes **(B)** Mean and SEM of 3 independent experiments. For inter-assay normalization the median fluorescence intensity signal obtained for the unmodified antibody after 60 min was set to 100 and the relative signal was calculated for all other data points; p values by t test.

These data indicate that Fc-sialylation exerts immunoregulatory functions through inhibition of C1q binding and subsequent initiation of the classical complement pathway, leading to reduced CDC.

2.4 IVIG treatment of T cell mediated autoimmunity

Pooled polyclonal human IgG (referred to as IVIG, intravenous immunoglobulin) was shown to be an efficient treatment of several antibody-mediated autoimmune disease models [139, 152, 236] and its protective effect was mainly attributed to the Fc domain of IgG [133, 158, 161, 165]. Similarly, IVIG was shown to ameliorate T cell mediated autoimmunity [246] but its mechanism of action is incompletely understood [166, 247]. We therefore aimed to investigate the requirement of $F(ab`)_2$ and Fc as well as its mode of action for the protective effect in EAE.

2.4.1 Therapeutic efficacy of IVIG in EAE

First we established which timing and dosage of IVIG is required in order to ameliorate EAE. IVIG was given daily starting one day before CFA + MOG_{35-55} immunization. As shown in figure 2.16A, low-dose IVIG (0.01 g/kg) slightly worsened the disease whereas high dose IVIG (1 g/kg) completely protected animals from disease development. Treatment from one day before CFA + MOG_{35-55} immunization until day 6 led to delayed onset of disease and reduced severity whereas treatment from day 7 increased EAE severity (figure 2.16B). Therefore, IVIG is required at high dose and continuously for its protective effect.

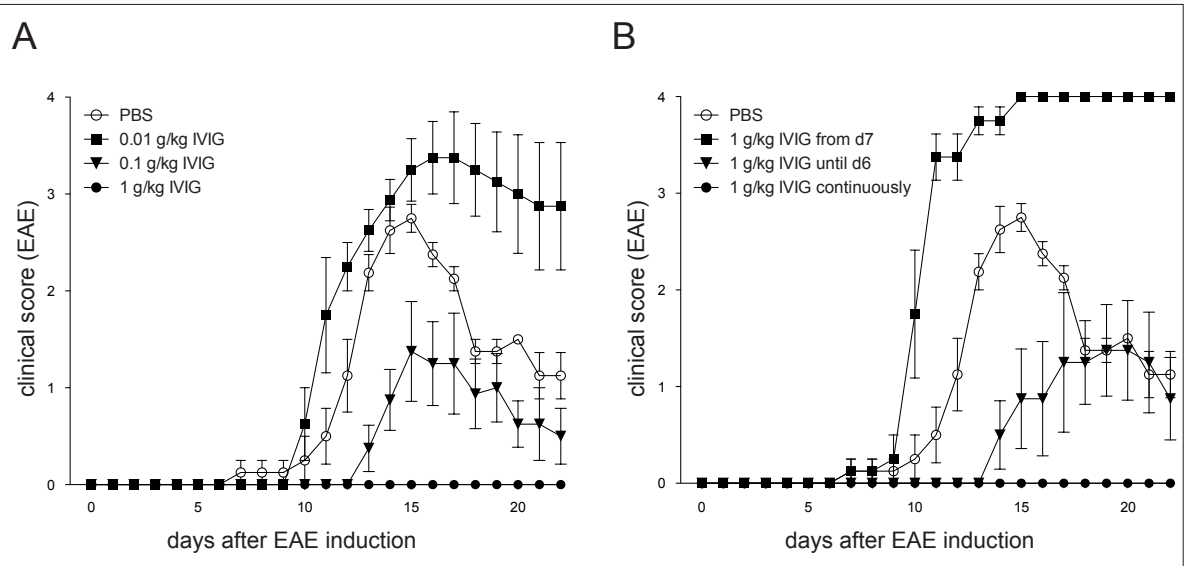

Figure 2.16 Timing and dosage of IVIG treatment
EAE was induced in C57BL/6 mice by immunization with MOG_{35-55} peptide in CFA and mice were treated i.p. with IVIG or PBS starting one day before EAE induction and every day thereafter (or as indicated). **(A)** Titration of IVIG treatment. **(B)** Timing of IVIG treatment. Means and SEM are shown. n = 4 animals per group

2.4.2 FcγRIIB may be dispensable for the protective effect of IVIG

Treatment of autoimmunity with IVIG has been shown to be dependent on FcγRIIB in several animal models [139, 158]. We immunized C57BL/6 mice deficient of FcγRIIB$^{-/-}$ and compared the disease development to their heterozygous littermates (FcγRIIB$^{+/-}$). No difference in the disease course was found (figure 2.17A). Treatment of FcγRIIB$^{-/-}$ animals with IVIG led to a delayed disease onset and reduced severity (figure 2.17B). FcγRIIB may therefore be dispensable for the protective effect of IVIG in EAE.

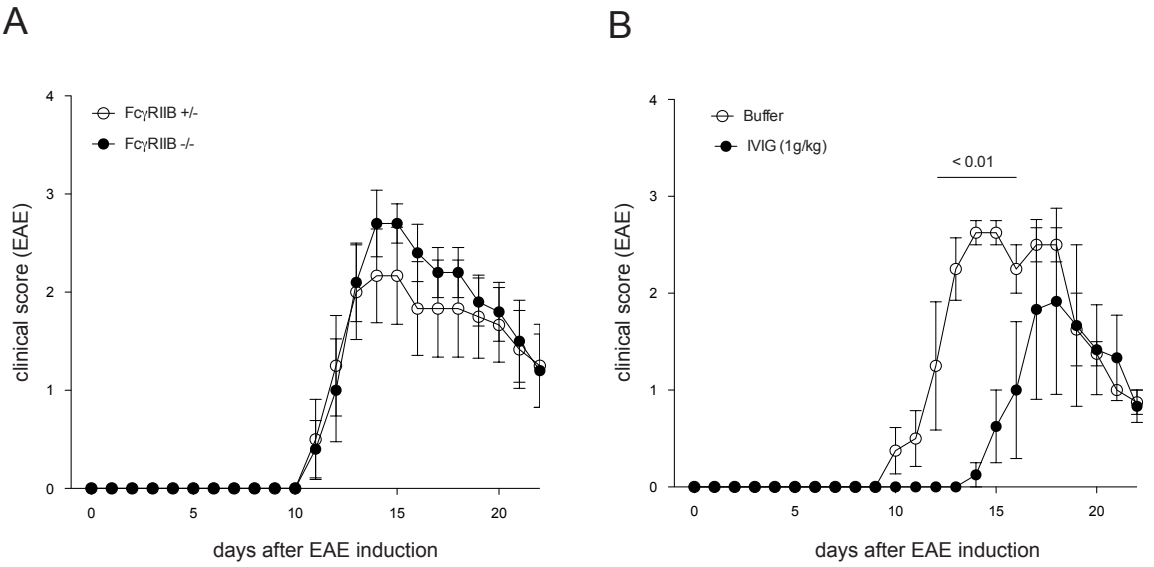

Figure 2.17 EAE disease course and IVIG treatment response in FcγRIIB$^{-/-}$ mice
(A) EAE was induced in C57BL/6 mice deficient for FcγRIIB (FcγRIIB$^{-/-}$) and their heterozygous littermates (FcγRIIB$^{+/-}$) by immunization with MOG_{35-55} peptide in CFA. Means and SEM are shown. n = 5 to 6 animals per group. **(B)** IVIG treatment of FcγRIIB$^{-/-}$ starting one day before EAE induction and every day thereafter. Means and SEM are shown. n = 4 animals per group.

2.4.3 F(ab')$_2$ is sufficient for the protective effect of IVIG

We next addressed which functional domain of IVIG (IgG) is required for protection of EAE. Therefore, the Fc portion of IVIG-derived IgG was removed by cleavage with Ide-S [248] and F(ab')$_2$ was purified by size-exclusion (see figure 4.7).
CFA + MOG_{35-55} immunized mice were treated with equimolar amounts of IVIG (0.5 g/kg), F(ab')$_2$ (0.33 g/kg) or PBS starting one day before immunization. F(ab')$_2$ fragments completely recapitulated the protective effect of IVIG for both disease severity (figure 2.18A) and disease incidence (2.18B).

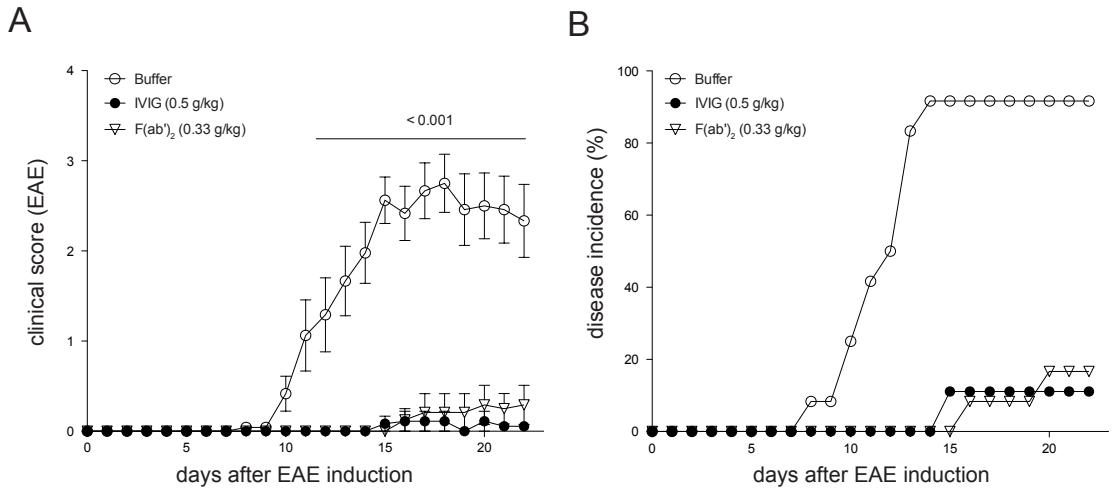

Figure 2.18 F(ab')$_2$ is sufficient for the protective effect of IVIG
EAE was induced in C57BL/6 mice by immunization with MOG$_{35-55}$ peptide in CFA and mice were treated i.p. with Buffer (PBS + 50 mM arginine + 50 mM glutamic acid), IVIG or F(ab')$_2$ starting one day before EAE induction and every day thereafter. Disease severity **(A)** and incidence **(B)** are shown. n = 12 animals per group. Individual curves in (A) were compared to Buffer using 2-way ANOVA and Bonferroni posttest.

2.4.4 IVIG does not ameliorate adoptively transferred EAE

The observation that withdrawal of IVIG at day 6 led to delayed disease onset (figure 2.16B) and previous reports clearly demonstrating an essential role for T cells during the development EAE [219, 249-251] raised the question how T cell responses are shaped by IVIG. To separate T cell priming from the encephalitogenic effector phase, we used adoptive transfer EAE. Spleen and lymph node (LN) cells from CFA + MOG$_{35-55}$ immunized mice carrying the transgenic 2D2 T cell receptor recognizing MOG$_{35-55}$ peptide [252] (2D2 mice) were *in vitro* re-stimulated with IL-23 and MOG$_{35-55}$ peptide and adoptively transferred into naïve B6 wildtype (wt) mice. IVIG treatment (1 g/kg) was started one day before the cell transfer and continued daily throughout the experiment. Both experimental groups developed comparable EAE symptoms (figure 2.19A), suggesting the IVIG treatment cannot inhibit disease development once the encephalitogenic immune response got initiated.

To test if MOG-reactive T cells develop at all in IVIG treated CFA + MOG$_{35-55}$ immunized mice, we purified spleen and LN cells from CFA + MOG$_{35-55}$ immunized mice either untreated (PBS) or treated with IVIG. After *in vitro* re-stimulation with IL-23 and MOG$_{35-55}$ peptide, cells were transferred into naïve mice and EAE disease progression was monitored. No difference was found between the groups (figure 2.19B) suggesting that IVIG treatment does not prevent the development and/or expansion of MOG specific T cells but rather inhibits their encephalitogenic capacity, an observation that has also been previously made in Lewis rats [253].

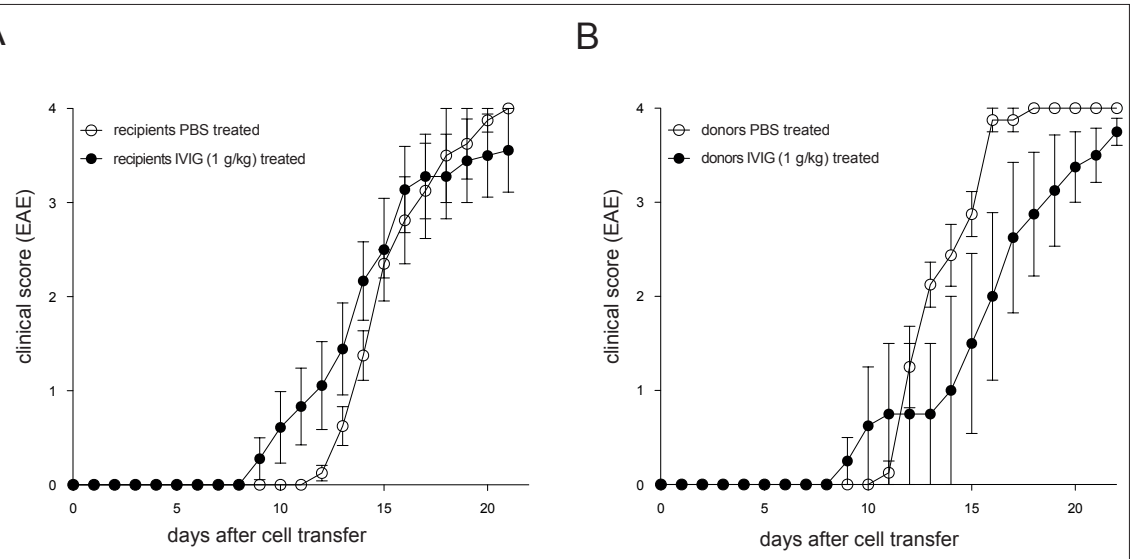

Figure 2.19 IVIG treatment does not ameliorate adoptively transferred EAE
(A) EAE was induced by adoptive transfer of 1×10^7 cells derived from CFA + MOG_{35-55} immunized 2D2 mice 6 days post immunization and *in vitro* re-stimulation with IL-23 and MOG_{35-55} peptide for 2 days into naïve C57BL/6 mice. Mice received daily i.p. injection of IVIG (1 g/kg) or PBS starting one day before immunization. Means and SEM are shown. n = 10 animals per group **(B)** C57BL/6 mice were CFA + MOG_{35-55} immunized immunized and treated with PBS or IVIG (1 g/kg i.p.) treatment starting one day before immunization and daily thereafter. Spleen and LN cells were harvested 6 days post immunization and re-stimulated with IL-23 and MOG_{35-55} for 2 days. From these cultures 1×10^7 cells were injected i.p. in naïve C57BL/6 mice and disease progression was monitored. Means and SEM are shown. n = 4 animals per group.

2.4.5 Modulation of leukocytes by EAE induction and F(ab')$_2$ treatment

To get an insight into how F(ab')$_2$ can prevent the development of EAE, we purified spleen and draining lymph nodes (dLNs) 9 days after immunization with CFA + MOG_{35-55} or CFA + PBS. Comparison of the two groups was used to see if the overall activation of the immune system by the adjuvant (CFA) is altered or only a specific response towards the encephalitogenic peptide (MOG_{35-55}). Mice received daily i.p. injections with PBS or 0.33 mg/kg F(ab')$_2$ starting one day before immunization and every day thereafter. Compared to naïve mice, CFA + PBS or CFA + MOG_{35-55} immunization resulted in increased splenic cellularity in both PBS and F(ab')$_2$ treated animals (figure 2.20B). The cellularity of dLNs was less altered and no difference was found between F(ab')$_2$ or PBS treated animals. We next analyzed the frequency and absolute numbers of CD4 and CD8 T cells by flow cytometry (figure 2.20A and C). F(ab')$_2$ treatment led to a reduction in frequency and absolute CD4 and CD8 T cell numbers in the spleen of CFA + MOG_{35-55} immunized animals whereas dLNs showed the opposite trend. Changes in CFA + PBS immunized animals largely phenocopied CFA + MOG_{35-55} immunized animals.

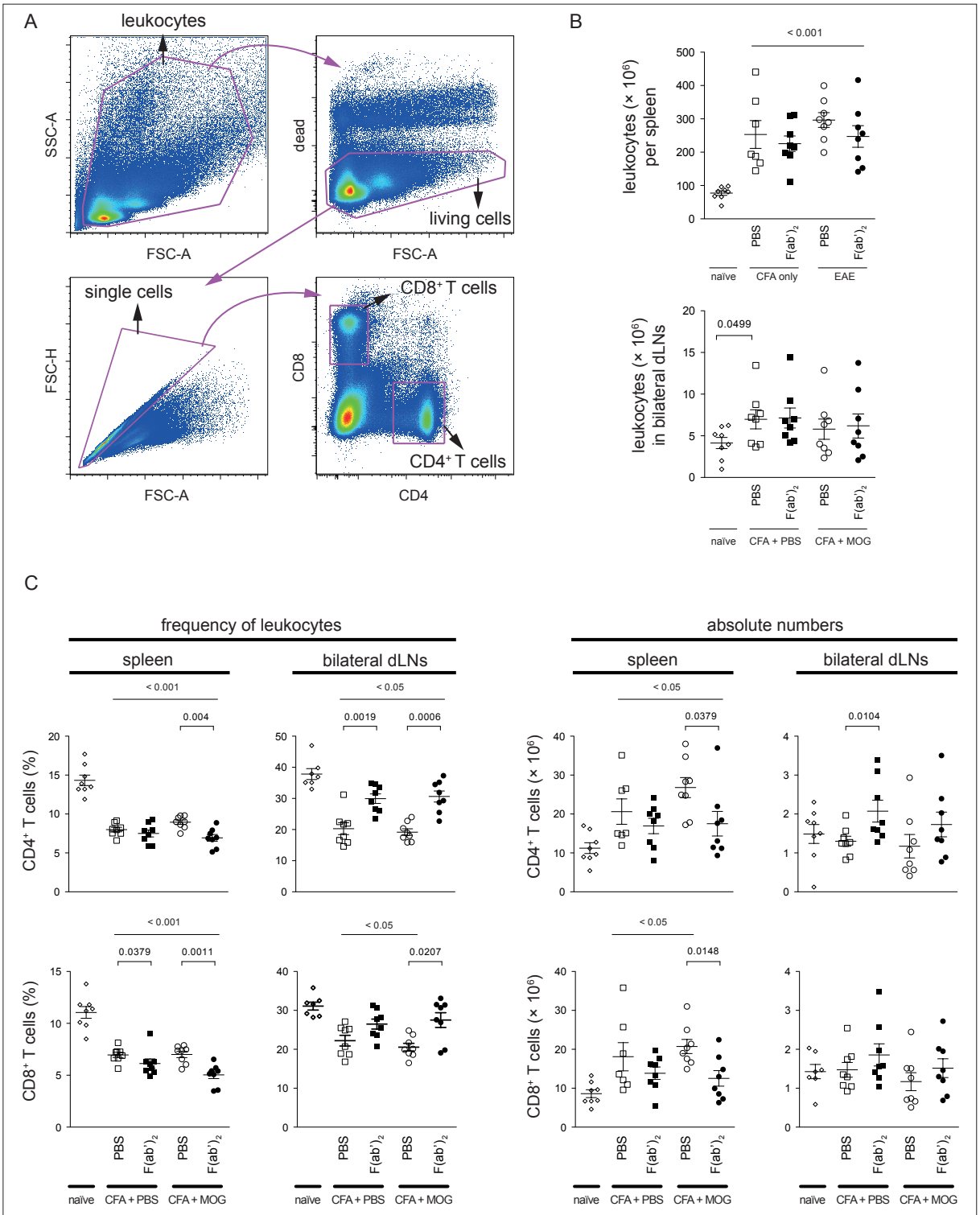

Figure 2.20 Leukocyte and T cell frequencies and total cell numbers following CFA + PBS or CFA + MOG_{35-55} immunization and $F(ab')_2$ treatment.

Mice were immunized subcutaneously with CFA and PBS (squares) or CFA and MOG_{35-55} peptide (circles) and injected subcutaneously with PBS (open symbols) or $F(ab')_2$ (closed symbols). Naïve mice (open diamonds) remained untouched. Spleens and dLNs were isolated on day 9 after immunization. **(A)** Representative sequential flow cytometry gating strategy to identify living, singular leukocytes as used for all subsequent analysis of leukocyte subsets. Anti-CD4 and anti-CD8 staining was used to identify conventional T cell subsets **(B)**. Total number of purified leukocytes in spleens and dLNs measured by CASY cell counter. **(C)** Frequency and total numbers of $CD4^+$ and $CD8^+$ T cells in spleen and dLNs. (continued on next page)

Results of two independent experiments with 7 to 8 animals per group are shown. Statistics by Mann Whitney U test. p value above non-capped lines represents comparison of the subjacent groups to naïve mice. p values for the comparison of CFA + PBS and CFA + MOG_{35-55} immunized animals are not shown. Only p values reaching significance (< 0.05) are shown. dLNs, draining lymph nodes; CFA, complete Freund's adjuvant; MOG, myeloid oligodendrocyte glycoprotein; PBS, phosphate buffered saline; SSC-a, side scatter-area; FSC-A, FCS-area; FSC-H, FSC-height.

2.4.5.1 Modulation of CD4 T cells by EAE induction and $F(ab')_2$ treatment

MHC-II restricted CD4 T cells are sufficient to adoptively transfer EAE disease to naïve mice indicating a predominant role of this T cell subset for disease development [219, 254]. We therefore analyzed the overall distribution of $CD4^+$ T cell subsets (figure 2.21) and their cytokine secretion profile (figure 2.22). Regulatory T cells (Tregs) were identified by the expression of the transcription factor FoxP3. $F(ab')_2$ treatment led to increased frequency of Tregs in spleen and reduced frequency in dLNs. However, absolute numbers remained largely unchanged in all experimental groups. Compared to naïve mice, the $CD4^+$ T cell composition of immunized animals showed increased frequencies of central and effector memory T cells and reduced frequencies of naïve T cells. In particular, effector memory T cells were increased in absolute numbers in both spleen and dLNs. $F(ab')_2$ treatment reduced the expansion of naïve, central memory and effector memory $CD4^+$ T cells in the spleen of CFA + MOG_{35-55} immunized animals. CFA + PBS immunized mice showed less expansion and no significant reduction upon $F(ab')_2$ treatment. To further analyze the functional profile of $CD4^+$ T cells, purified cells from spleen and dLNs were *in vitro* re-stimulated with PMA and ionomycin to induce cytokine production following intracellular cytokine staining for IFN-γ, GM-CSF and IL-17 (figure 2.22 A). CFA + PBS and CFA + MOG_{35-55} immunized animals resembled each other in most parameters analyzed with the exception that CFA + MOG_{35-55} immunized animals showed reduced frequency and absolute numbers of cytokine-producing $CD4^+$ T cells in the dLNs. $F(ab')_2$ treatment reduced the frequency of cells producing IFN-γ, GM-CSF or IL-17 in spleen and dLNs and the absolute numbers of CFA + MOG_{35-55} immunized animals in the spleen and CFA + PBS animals in the dLNs.

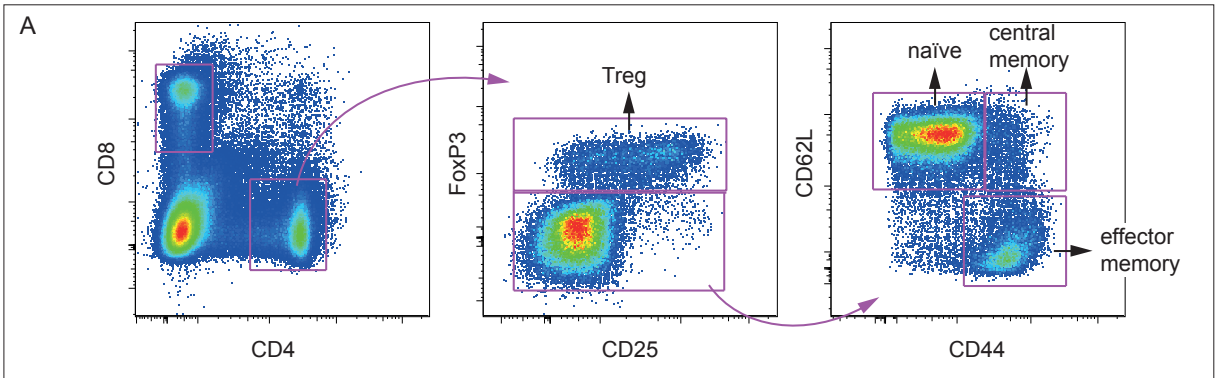

Figure 2.21 (continued on nest page)

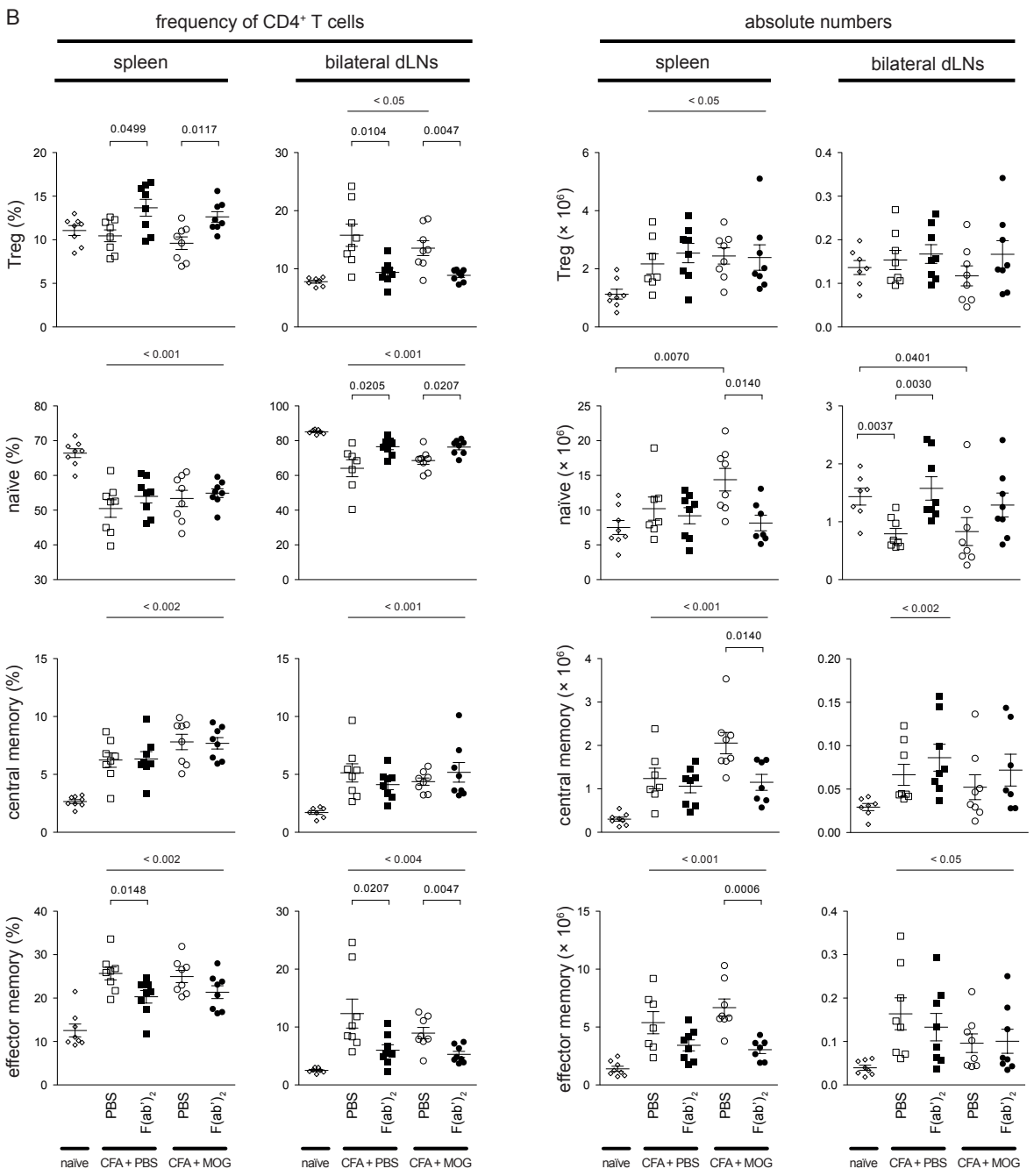

Figure 2.21: Distribution of CD4 T cell subsets following CFA + PBS or CFA + MOG_{35-55} immunization and $F(ab')_2$ treatment.

Mice were immunized subcutaneously with CFA and PBS (squares) or CFA and MOG_{35-55} peptide (circles) and injected subcutaneously with PBS (open symbols) or $F(ab')_2$ (closed symbols). Naïve mice (open diamonds) remained untouched. Spleens and dLNs were isolated on day 9 after immunization. **(A)** Exemplary sequential flow cytometry gating strategy. Living, singular leukocytes were gated as described in figure 2.20. Intracellular staining for the transcription factor FoxP3 was used to identify Tregs. Non-Tregs were analyzed for CD62L and CD44 to distinguish naïve, central and effector memory T cells. **(B)** Frequency of the individual subset among $CD4^+$ T cells (left two columns) and their total numbers (right two columns) in spleen and dLNs. Results of two independent experiments with 7 to 8 animals per group are shown. Statistics by Mann Whitney U test. p value above non-capped lines represents comparison of the subjacent groups to naïve mice. p values for the comparison of CFA + PBS and CFA + MOG_{35-55} immunized animals are not shown. Only p values reaching significance (< 0.05) are shown. dLNs, draining lymph nodes; CFA, complete Freund's adjuvant; MOG, myeloid oligodendrocyte glycoprotein; PBS, phosphate buffered saline; Treg, regulatory T cells.

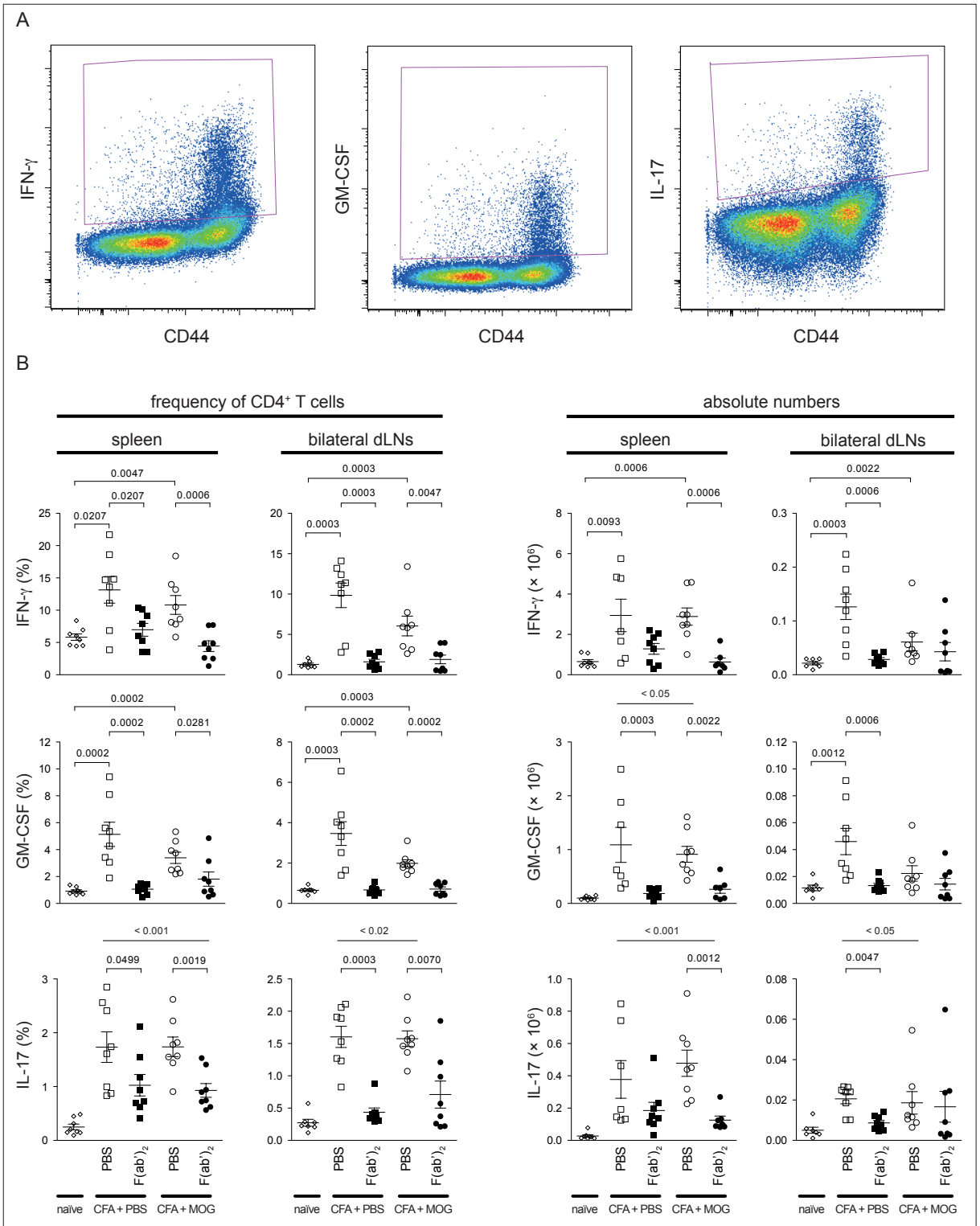

Figure 2.22: Cytokine profile of CD4 T cells in mice after CFA + PBS or CFA + MOG_{35-55} immunization and $F(ab')_2$ treatment.

Mice were immunized subcutaneously with CFA and PBS (squares) or CFA and MOG_{35-55} peptide (circles) and injected subcutaneously with PBS (open symbols) or $F(ab')_2$ (closed symbols). Naïve mice (open diamonds) remained untouched. Spleens and dLNs were isolated on day 9 after immunization. Cells were re-stimulated for 4 hours with PMA and ionomycin in the presence of Brefeldin A to block cytokine secretion. Intracellular staining with fluorescently labeled monoclonal antibodies was used to detect cytokine production. **(A)** CD4 T cells were identified by flow cytometry as described in figure 2.20. Exemplary cytokine stainings are shown in comparison to CD44 cell-surface expression, which identifies activated T cells. **(B)** Frequency of cytokine producing cells among CD4⁺ T cells (left two columns) and total numbers (right two columns) in spleen and dLNs. (continued on next page)

Results of two independent experiments with 7 to 8 animals per group are shown. Statistics by Mann Whitney U test. p value above non-capped lines represents comparison of the subjacent groups to naïve mice. p values for the comparison of CFA + PBS and CFA + MOG_{35-55} immunized animals are not shown. Only p values reaching significance (< 0.05) are shown. dLNs, draining lymph nodes; CFA, complete Freund's adjuvant; MOG, myeloid oligodendrocyte glycoprotein; PBS, phosphate buffered saline.

2.4.5.2 Modulation of B cells and myeloid cells by EAE induction and F(ab')$_2$ treatment

Reduced expansion of CD4 T cells as well as their functional capacity upon F(ab')$_2$ treatment could be due to a direct effect on T cells or by modulation of the underlying responses of innate immune cells. We therefore analyzed the frequencies, absolute numbers and activation state of innate immune cells and B cells by flow cytometry (figure 2.23 – 2.25). Leukocyte subsets were identified as indicated in figure 2.20. B cells were identified by co-expression of CD19 and MHC-II. Dendritic cells (DCs) co-express high levels of MHC-II and CD11c and were further subdivided in $CD8^+$ and $CD8^-$ DCs. Neutrophils are co-expressing Ly6G and Ly6C. Monocytes stain highly positive for Ly6C and co-express CD11b.

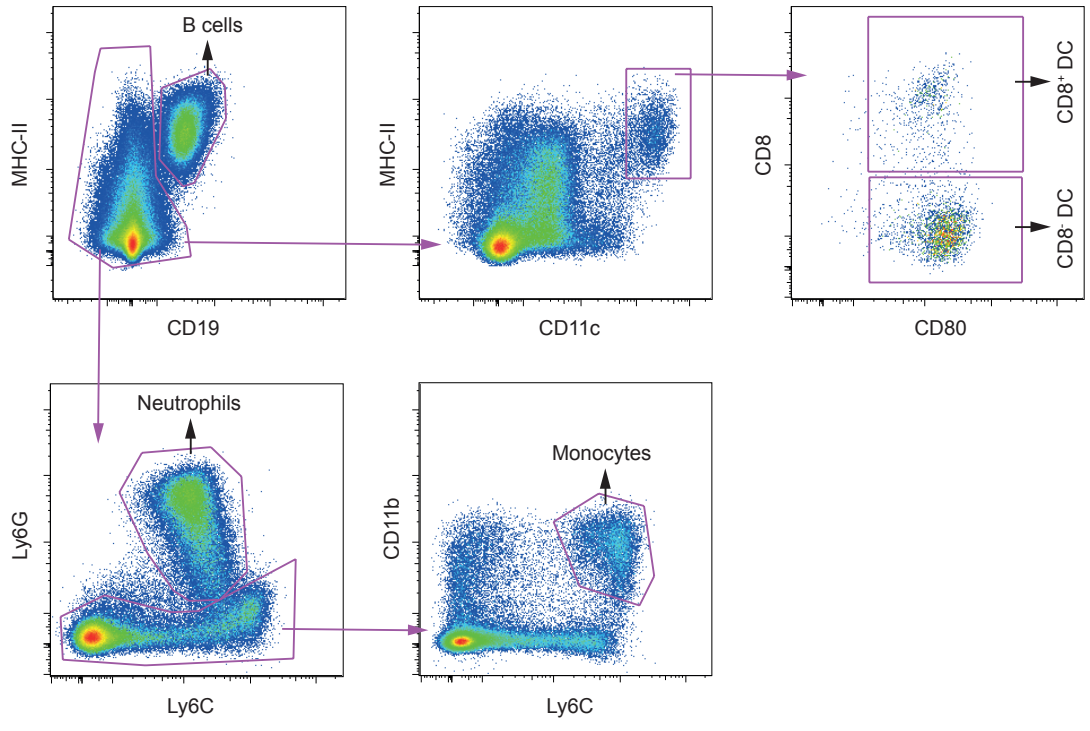

Figure 2.23: Identification of B cells and myeloid cell subsets by flow cytometry
Sequential flow cytometry gating to identify B cells and myeloid cell subsets in spleen and lymph nodes. Living, single leukocytes were identified as shown in figure 2.20. B cells were identified by co-expressing CD19 and MHC-II. DCs were identified by their high expression of both CD11c and MHC-II. CD8 was used to discriminate the two functional subsets of DCs. Neutrophils were identified as being positive for Ly6G and Ly6C. Finally, monocytes were identified by electronic gating on non-B cells and non-neutrophils and their co-expression Ly6C and CD11b.

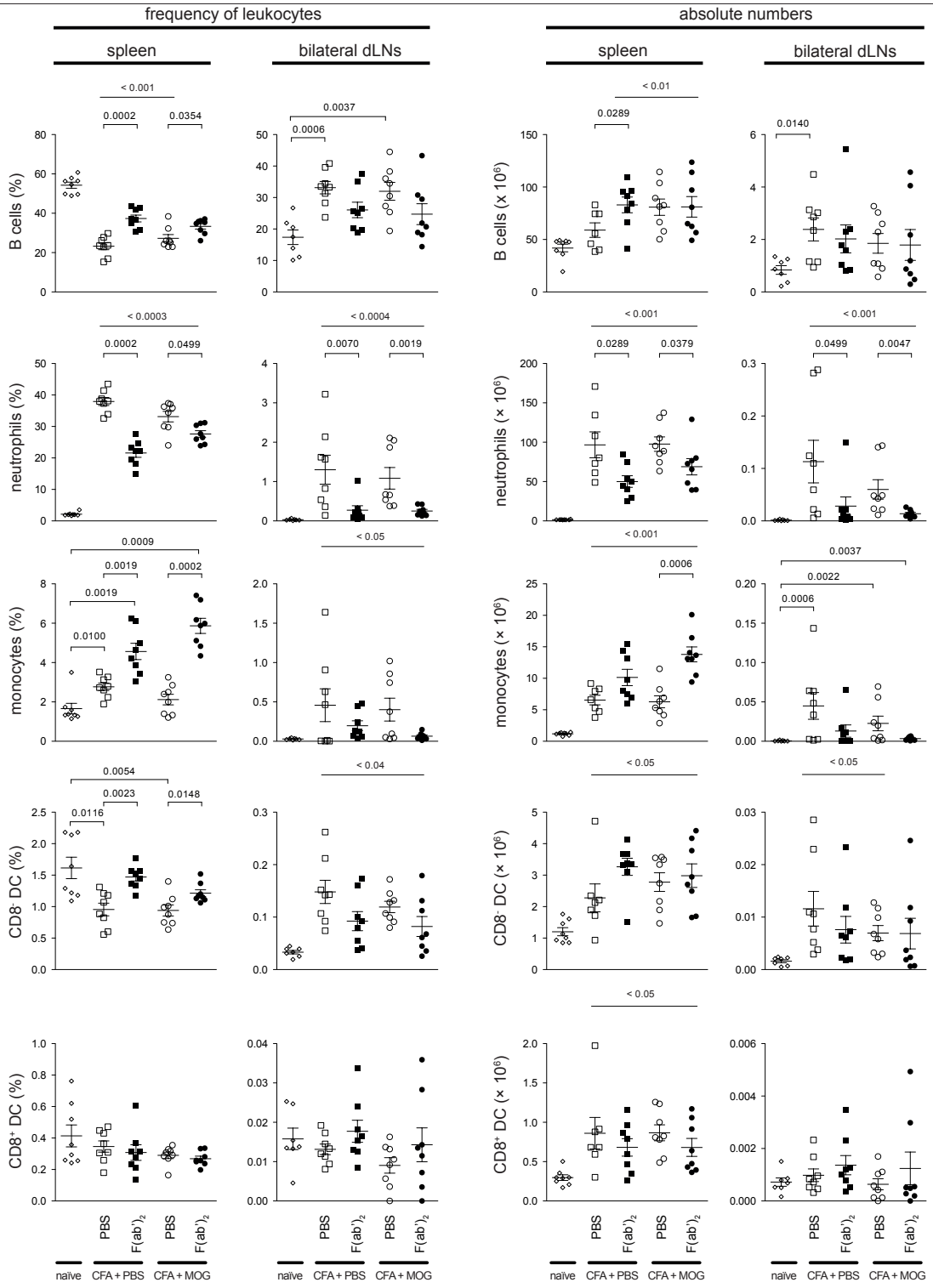

Figure 2.24: Frequency and absolute numbers of myeloid cells and B cells in mice following CFA + PBS or CFA + MOG_{35-55} immunization and $F(ab')_2$ treatment.

Mice were immunized and treated as described in Figure 2.22**.** Subsets were identified by flow cytometry as described in figure 2.23. Frequency (left two columns) and total numbers (right two columns) of B cells, neutrophils, monocytes as well as $CD8^-$ and $CD8^+$ DCs are shown.

Results of two independent experiments with 7 to 8 animals per group are shown. Statistics by Mann Whitney U test. p values above non-capped lines represents comparison of the subjacent groups to naïve mice. p values for the comparison of CFA + PBS and CFA + MOG_{35-55} immunized animals are not shown. Only p values reaching significance (< 0.05) are shown. dLNs, draining lymph nodes; CFA, complete Freund's adjuvant; MOG, myeloid oligodendrocyte glycoprotein; PBS, phosphate buffered saline; DCs, dendritic cells.

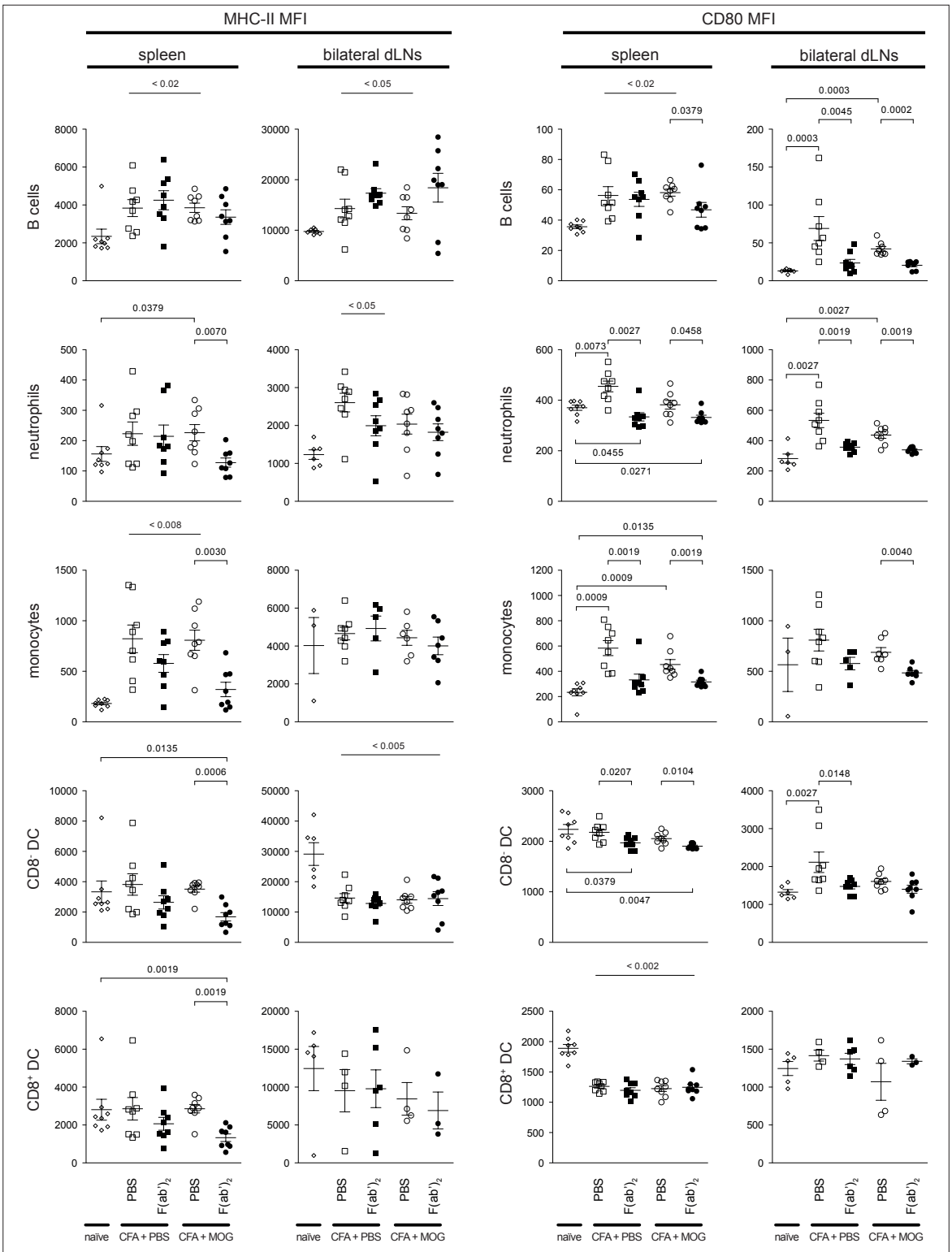

Figure 2.25: Expression levels of MHC-II and CD80 on myeloid cells and B cells in mice following CFA + PBS or CFA + MOG_{35-55} immunization and $F(ab')_2$ treatment.
Mice were immunized and treated as described in Figure 2.22. Subsets were identified by flow cytometry as described in figure 2.23. MFI of MHC-II and CD80 on B cells, neutrophils, monocytes as well as CD8 positive and negative DCs are shown. (continued on next page)

Results of two independent experiments with 7 to 8 animals per group are shown. Mice were excluded if less than 10 signals (cells) were present in the final gate (this was the case for some neutrophil-, monocyte- and DC gates in dLNs of few mice). Statistics by Mann Whitney U test. p values above non-capped lines represents comparison of the subjacent groups to naïve mice. p values for the comparison of CFA + PBS and CFA + MOG_{35-55} immunized animals are not shown. Only p values reaching significance (< 0.05) are shown. dLNs, draining lymph nodes; CFA, complete Freund's adjuvant; MOG, myeloid oligodendrocyte glycoprotein; PBS, phosphate buffered saline; DC, dendritic cell; MFI, median fluorescence intensity.

Similar to what was found for T cells, the frequency, absolute numbers and activation state of B cells and myeloid cells in CFA + PBS and CFA + MOG_{35-55} immunized animals largely resembled each other in most parameters analyzed (figure 2.24 and 2.25). In the spleen, a pronounced increase in neutrophils and monocytes results in reduced frequencies of B cells and $CD8^-$ DCs. However if total numbers are analyzed, all subsets increase upon immunization. dLNs of immunized animals contained increased frequencies and total numbers of monocytes, neutrophils and $CD8^-$ DCs. B cells numbers also tend to be elevated. The most prominent effect of $F(ab')_2$ is a reduction of neutrophils in spleen and dLNs and an increase of monocytes in the spleen.

Next, cell surface expression of MHC-II and the co-stimulatory molecule CD80 (also known as B7-1) were analyzed (figure 2.25). Again, both molecules were regulated similarly in CFA + PBS and CFA + MOG_{35-55} immunized animals. Immunization led to increased expression of MHC-II on B cells, neutrophils and monocytes in the spleen and on B cells and neutrophils in dLNs. In contrast, the MHC-II expression level on DC in the spleen remained largely unchanged and was markedly reduced on $CD8^-$ DC in dLNs. $F(ab')_2$ treatment reduced MHC-II expression on neutrophils, monocytes and both subsets of dendritic cells in the spleen of CFA + MOG_{35-55} immunized animals. On DCs, MHC-II was reduced below the levels found on naïve mice. In contrast, MHC-II expression in dLNs was hardly effected by $F(ab')_2$ treatment. Immunization resulted in increased expression of CD80 on B cells, neutrophils (CFA + PBS group only) and monocytes in the spleen and on B cells and neutrophils in dLNs. Immunization hardly affected the expression of CD80 on $CD8^-$ DCs (with the exception of increased expression in dLNs of CFA + PBS immunized mice) and $CD8^+$ DCs from dLNs. In contrast, spleen-derived $CD8^+$ DCs reduced the expression of CD80 upon immunization. $F(ab')_2$ treatment reduced CD80 expression on B cells (CFA + MOG_{35-55} group only), neutrophils, monocytes and $CD8^-$ DCs of the spleen. CD80 expression on neutrophils and $CD8^-$ DCs was even below the level of naïve mice. In dLNs, $F(ab')_2$ treatment led to reduced CD80 expression on B cells, neutrophils, monocytes (CFA + MOG_{35-55} group only) and $CD8^-$ DCs (CFA + PBS group only).

Collectively, these data indicate that $F(ab')_2$ treatment prevents the development of encephalitogenic T cells by reducing the overall inflammatory state. This is indicated by reduced neutrophilia and reduced expression of MHC-II and CD80 on professional and non-professional antigen presenting cells.

3. Discussion

This study aimed to investigate the mechanisms responsible for the regulation of IgG-mediated anti-inflammatory properties in humans and mice. We found that clinical disease remission in patients with chronic inflammatory demyelinating polyneuropathy (CIDP), an autoimmune disease of the peripheral nervous system during which humoral immune responses are central in mediating tissue damage, is associated with deregulated expression of activating and inhibitory FcγRs and with changes in the IgG-Fc glycan profile. IVIG treatment partially restored FcγR expression and disease remission correlated with increased IgG-Fc sialylation. We demonstrate that Fc sialylation impairs IgG's capability to activate the complement system resulting in reduced complement-mediated cytotoxicity. Finally, studies in EAE revealed that IVIG can also induce $F(ab')_2$-mediated anti-inflammatory pathways indicating that more than one mechanism may be responsible for its therapeutic efficacy during autoimmunity.

Balanced signaling through activating and inhibitory FcγRs regulates innate and adaptive immune responses [94, 255] and impairment of the FcγR regulatory system is associated with an increased susceptibility to develop autoimmune pathologies [97, 256-259]. Whereas deficiency in activating Fc receptors renders mice resistant to autoimmunity in several disease models [256, 260, 261], mice lacking FcγRIIB show an autoimmune-prone phenotype [97, 258, 259]. The latter appears to be partly dependent on the genetic background of the mice [257]. In addition, analysis of genetic polymorphisms partially confirms the relevance of FcγRs in human autoimmunity: polymorphisms leading to higher-affinity variants of activating FcγRIIA (FcγRIIA 131H) [262, 263] have been associated with systemic lupus erythematosus (SLE) and the high-affinity variant of FcγRIIIA (FcγRIIIA 158V) with SLE [264] and rheumatoid arthritis (RA) [265]. The available data for FcγRIIB are still contradictory. A loss of function mutation of FcγRIIB (FcγRIIB 232T) [266] has been associated with SLE in some patient cohorts [267, 268] but not in others [269, 270]. In addition, a promotor region associated with increased expression of FcγRIIB was also found to be associated with SLE [271].

We found that patients with CIDP have increased expression levels of activating FcγRI and FcγRIIA on blood monocytes but decreased expression of FcγRIIB on blood monocytes and naïve and memory B cells. Reduced FcγRIIB expression in CIDP has been previously reported [157] and could be potentially explained by functionally relevant single-nucleotide polymorphisms (SNPs) in the FcγRIIB promoter [271, 272] which are associated with autoimmune phenotypes and have been found to be associated with CIDP [157]. A recent study in humanized mice showed that alleles encoding functionally impaired FcγRIIB variants lead to higher frequencies

of plasmacytoid B cells, increased serum antibody levels and generation of autoantibodies, confirming the importance of FcγRIIB for humoral immune tolerance in the human immune system [273]. FcγRIIB regulates B cell activation and homeostasis [100, 274] and the balance between FcγRIIA and FcγRIIB was shown to set the threshold for the activation of monocyte-derived DCs [94]. Increased monocyte expression of the activating FcγRI was identified as a potential biomarker for disease activity in patients with SLE and RA in whom monocyte expression levels of FcγRI are significantly higher in active compared to inactive disease [275]. Our data indicate that deregulated monocyte expression of FcγRI is not confined to patients with SLE and RA. FcγRI expression is induced by interferon-α (IFN-α), among other cytokines, and increased FcγRI levels on monocytes derived from SLE patients were attributed to higher IFN-α production in these patients [275]. A role for IFN-α in the pathogenesis of CIDP is less well established, although some studies report increased levels of type I IFN signaling in CIDP patients [276] or development of CIDP associated with IFN-α therapy [277-283]. Activation of FcγRI on monocytes triggers differentiation into immature dendritic cells that induce autoreactive T cell responses and has therefore been implicated to mediate tissue injury in antibody-mediated autoimmune diseases [284]. FcγRI-mediated activation and differentiation of myeloid cells might also contribute to peripheral nerve damage in CIDP, where myeloid cells are believed to be the main local effector cells [235].
The analysis of concomitant expression of activating and inhibitory FcγRs indicates that the FcγR regulatory system rather than expression levels of a single receptor is disturbed in patients with CIDP. Altogether, these data suggest that deregulated expression of activating versus inhibitory FcγRs might lower the activation threshold for myeloid cells and B cells [94, 285], thereby contributing to the susceptibility to develop CIDP [286].

Since the discovery of the anti-inflammatory properties of pooled high-dose gammaglobulins in Idiopathic thrombocytopenic purpura (ITP) [140, 141], IVIG has been approved for several autoimmune diseases including ITP, Kawasaki's disease, CIDP and multifocal motor neuropathy (MMN) [142]. Clinical efficacy in ITP [155] and studies in animal models [133, 158, 159, 165] suggest that IgG-Fc mediates the anti-inflammatory actions of IVIG. Several [139, 158] but not all [287-289] animal models of autoimmunity also found that signaling via the inhibitory FcγRIIB is required for IVIG to protect from the development of autoimmunity. Additionally, in murine models of ITP, RA and nephrotoxic nephritis IVIG administration results in an up-regulation of FcγRIIB surface expression on effector macrophages or enhanced recruitment of FcγRIIB positive myeloid cells to the site of inflammation [158, 236]. Our data suggest that restoration of deregulated activating *versus* inhibitory FcγR expression might contribute to the clinical efficacy of IVIG in CIDP patients. IVIG treatment in CIDP patients requires repeated infusions in order to maintain a clinical benefit [192]. Notably, upregulation of the inhibitory

FcγRIIB on B cells and downmodulation of the activating FcγRI on $CD14^{low}CD16^{+}$ inflammatory monocytes was stronger after 2 weeks as compared to 4-8 weeks in most patients investigated suggesting that a single treatment course of IVIG does not lead to sustained restoration of FcγR expression levels in patients with CIDP.

There are several limitations to our study. First, due to the relatively small number of patients and the high response rate to IVIG therapy, patients were not stratified for disease severity and treatment response. Second, we did not monitor FcγR levels beyond 8 weeks following therapy. As mentioned above, repeated infusions of IVIG are generally necessary to maintain a clinical benefit [192, 290] and it is tempting to speculate that FcγR expression levels might return to pre-treatment levels beyond an observation period of 8 weeks. Third, low cell frequencies precluded the analysis of potentially important cell subsets such as DCs and neutrophils. Nevertheless, our findings should provide an incentive to conduct larger prospective investigations to examine FcγR expression in leukocyte subsets of patients with CIDP to evaluate the applicability of FcγR expression as a biomarker for disease progression and treatment response.

Our data support the notion that modulating FcγR expression represents an attractive target for immune modulation. Numerous studies suggest that attempts should be made to develop therapeutics, such as antibodies which specifically block activating FcγRs, and test their clinical efficacy for the treatment autoimmune disease [291-293].

In addition to the requirement of IgG-Fc and FcγRIIB for the clinical efficacy of IVIG in several autoimmune disease models [139, 158], a small quantity of sialic acid containing IgG-Fc was found to mediate protection in a mouse model of arthritis [133, 165]. Subsequent studies implicated a protective mechanism involving the inhibitory Fc receptor (FcγRIIB) and the C-type lectin SIGNR1 (CD209b) or its human ortholog DC-SIGN (CD209) [161, 294]. Signaling downstream of DC-SIGN was found to induce IL-33 which in turn induces IL-4 in basophils leading to the upregulation of FcγRIIB on macrophages [161]. Although the relevance of DC-SIGN (or SIGNR1) for the initiation of a sialic-acid specific response is supported by several studies [139, 161, 165, 294], it remains unclear whether direct binding of Fc-linked sialic acid to these receptors [136] is the initial step as no binding of IgG-Fc (independent of its glycosylation) to DC-SIGN was detected by others [138]. Also, conflicting data exist about the absolute requirement of sialic acid [166, 167, 295]. However, these studies rose the question to which extent IgG-Fc sialylation is regulated in health and disease and which consequences it has for antibody functionality.

We found that patients with CIDP show higher levels of IgG-Fc N-glycans lacking terminal

galactose and sialic acid residues as compared to demographically matched healthy individuals. Furthermore, increased levels of Fc-sialylation in CIDP sera were associated with clinical disease remission in both placebo- and IVIG-treated patients. IgG-Fc sialylation led to reduced CDC, providing a functional rationale for the observed disease-related changes.

IgG-Fc galactose content has long been known to be affected by various pathologic conditions. Early observations indicating that the amount of galactosylated IgG is negatively correlated with RA and primary osteoarthritis [78] were later confirmed for other autoimmune diseases such as Crohn`s disease, SLE and Ankylosing spondylitis [127, 128]. Also, loss of galactose on anti-citrullinated protein antibodies precedes the development of RA [296] and the extent of pregnancy-induced spontaneous remission of RA correlates with an increase of IgG galactosylation [297, 298]. In healthy individuals, the amount of circulating IgG-G0 antibodies increases with age [299] and decreases during pregnancy followed by an increase to pre-pregnancy levels post partum [298]. Additionally, correlation of increased IgG-G0 with infections such as HIV-1 [129, 130], infectious endocarditis [128], and hepatitis-C infection accompanied by fibrosis and cirrhosis [131] suggests regulation of IgG-Fc galactosylation during an ongoing immune response. While the aforementioned studies narrowed the focus on the presence or absence of galactose, not the lack of galactose residues themselves but rather the concomitant absence of terminal sialic acid may be responsible for the enhanced inflammatory activity exerted by aglycosylated glycoforms. Supporting this argumentation, increased IgG-Fc sialylation was found to be positively correlated with disease remission of RA [298], Wegener`s granulomatosis [300] and CIDP (this study and [301]). Our data suggest that IVIG treatment and spontaneous disease remission is associated with an increase of patient-derived IgG-Fc sialylated antibodies. In CIDP, the clinical efficacy of plasma exchange therapy and C3d deposition in patient biopsies on Schwann cells and compact myelin indicates that the complement system may play an important role for mediating peripheral nerve damage [181, 203]. These data suggest that increased IgG-Fc sialylation of pathologic autoantibodies could reduce their potency to activate the complement system resulting in reduced immune-mediated tissue damage and clinical disease remission.

Both Fc-receptor dependent (ADCC) and complement dependent (CDC) cytotoxic properties of antibodies have been shown to require the presence of the IgG-Fc glycan [114, 302]. Consequentially, it is not surprising that also the composition of the glycan impacts antibody functionality. From the three variable glycans fucose, galactose and sialic acid, absence of fucose has been shown to significantly enhance ADCC [92]. Human sialylated antibodies show a reduced binding to murine FcγRs [133] and were reported to convey reduced ADCC [134]. We could not find changes in human FcγR binding properties for both sialic acid enriched Fc

or tetra-sialylated Rituximab, a humanized IgG1 antibody. In accordance, also ADCC was not affected. Previous studies [134] did not distinguish between Fc and Fab sialylation, which may provide an explanation for the discrepancy as Fab glycosylation can influence antigen binding properties [72] which may influence ADCC independent of the Fc glycan structure. Antibodies lacking galactose have been shown to depend on Fc-receptors for their *in vivo* functionality [116] and increased pathogenicity of agalactosylated antibodies was found for murine IgG1 but not IgG2a autoantibodies indicating subclass-specific effects of galactosylation [303]. Initial studies indicated that lack of galactose allows binding of mannose-binding lectin (MBL), the initiator of the lectin pathway of the complement system [115]. However, MBL polymorphisms were not found to be associated with RA [304] or pregnancy-induced remission [305] and animal studies could also not find a role of MBL and complement for the functionality of agalactosylated antibodies *in vivo* [116, 303]. In accordance with previous data [116], we show that aside of the increased affinity for MBL, removal of galactose markedly reduces the affinity for C1q. De-galactosylated and sialylated antibodies displayed a similar reduction in C1q binding indicating that not only the presence of galactose but its location as a terminal sugar on the glycan is essential for increased binding. This is in sharp contrast to what was found for FcγRIIB binding of IgG1-Fc, which was not influenced by the presence or absence of terminal galactose [84] indicating that the structural binding requirements for FcγRs and C1q are different. Of note, data acquired in murine models have to be interpreted with caution concerning their transferability to humans as binding of C1q to human IgG1 was shown to have distinct requirements from its murine ortholog IgG2b [306]. For human IgG1, four spatially close sites on the surface of the antibody, D270, K322, P329, and P331, were shown to constitute the C1q binding epicenter [306]. However, most of the aforementioned sites are conserved in human IgG isotypes that are deficient in C1q binding and it has therefore been suggested that the composition of the N-glycan and the hinge region of the antibody might be critical for the antibodies' conformation and its ability to bind C1q [83, 306]. Chrystal structures of differentially glycosylated Fc permit at least two possible explanations how the IgG-Fc glycan structure may influence Fc structure and function. First, removal of terminal galactose [85] or addition of sialic acid on top of galactose [137] both were reported to favor a so-called "closed confirmation" (minimal C2-C2 domain distance) in contrast to an "open confirmation" (maximal C2-C2 domain distance) as found for fully galactosylated antibodies [85]. Second, tetra-sialylated antibodies were reported to exhibit increased conformational flexibility [137, 307]. Both a "closed confirmation" and a less-well defined structure may disfavor C1q binding. Crystal structures of the C1q globular head and galactosylated, de-galactosylated and tetra-sialylated IgG would be required in order to clarify how the glycan structure influences C1q binding. An indication for the relevance of C1q in human autoimmune diseases is given by the finding that polymorphisms of C1q leading to increased C1q serum levels are associated with the risk to develop RA [308] and classical

complement pathway activity correlates with disease activity in multifocal motor neuropathy [309]. An important consideration for antibody-mediated autoimmunity is that complement activation does not only result in cytotoxicity but generates potent inflammatory mediators. Amongst them, proteolytic activation of the complement proteins C3 and C5 results in the anaphylatoxins C3a and C5a which were implicated in a long list of pathologic conditions including RA and SLE [310]. Anaphylatoxins are potent regulators of innate and adaptive immune responses by acting on a wide range of cells and tissues via the interaction with their G-protein coupled receptors [311]. For example C3a and C5a are involved in T cell activation and differentiation [312-314] DC homing [315] and vascular permeability [316]. Complement activation also promotes the initiation of an adaptive immune response by opsonization of cells and pathogens. For example, C1q can be directly recognized by C1q receptors (CD35, CR1 and CD93, C1qRp) and complement-activation associated C3 cleavage products (iC3b) can be recognized by CD11b/CD18 (CR3) amongst others [317, 318]. These receptors are expressed on various cell types including DCs and monocytes/macrophages [318-321] where they contribute to the phagocytosis of opsonized cells or bacteria and play an essential role for the removal of apoptotic cells [318, 320, 322]. Increased IgG sialylation may therefore also influence the extent of antigen presentation to B and T cells and their subsequent development in antibody-secreting plasma cells or effector T cells. It is also worth mentioning that the presence of galactose on the IgG-Fc glycan may mediate complement-inhibitory effects by a mechanism involving Dectin-1 and FcγRIIB dependent inhibition of C5a receptor signaling [132], highlighting the complexity of complement-regulatory mechanisms influenced by the IgG-Fc glycan. It would be interesting to investigate if the presence of sialic acid in addition to galactose still allows this signaling pathway to take place. This would result in sialylated antibodies having both low intrinsic CDC activity and at the same time reduce pro-inflammatory signaling by C5a.

In CIDP, autoantibodies, complement, T cells, and myeloid cells are currently thought to be involved in mediating peripheral nerve demyelination [181]. In such a scenario an unknown trigger would initiate the development of peripheral nerve specific autoantibodies leading to nerve destruction by the complement system and myeloid cells. The inflammatory milieu would then facilitate autoantigen presentation by DCs/myeloid cells supporting the development of further pathologic autoantibodies and potentially also autoantigen-specific T cells. De-regulated FcγR expression and IgG-Fc glycosylation could therefore predispose for the development of autoimmunity but also amplify and sustain the disease. The identified FcγR-independent mechanism by which Fc-sialylated glycovariants limit pro-inflammatory IgG effector function might complement immunomodulatory effects of IVIG associated with upregulation of the inhibitory FcγRIIB [139, 157, 158, 161] and supports the development of strategies that target increased Fc-sialylation for the treatment of autoimmune diseases [323].

The anti-inflammatory properties of IVIG have been extensively studied in murine models of antibody-mediated autoimmunity most of which indicated that the Fc part of IgG conveys the immunosuppressive properties [139, 158, 165]. IVIG has been previously reported to also reduce disease severity of EAE, an animal model for T cell mediated autoimmune neuroinflammation [253, 324, 325]. We aimed to investigate the structural requirements of IgG to exert its protective function. EAE is induced by subcutaneous immunization with MOG_{35-55} peptide emulsified in CFA, resulting in a strong inflammatory response and the generation of autoantigen-specific $CD4^+$ T cells. Confirming published data [246], IVIG was found to be required continuously and at high dose in order to protect from EAE development. The most frequently reported requirement for IVIG`s protective action in murine models of autoimmunity is the presence of the inhibitory FcγR, FcγRIIB [139, 158]. Activating and inhibitory FcγRs have been implicated in regulating EAE development [326], further supporting a role for FcγRIIB. However, we were not able to reproduce previous data showing an increased susceptibility of FcγRIIB knockout mice [326]. In addition, IVIG treatment was still able to reduce disease severity in the absence of FcγRIIB although to a lesser extent as seen in B6 wt mice. This may be due to FcγRIIB flanking regions, which are insufficiently backcrossed and harbor autoimmune susceptibility genes [327]. Increased inflammation may hamper the efficacy of IVIG and require even higher dosage for complete protection. In line with that, the dependency on FcγRIIB can be overcome by increasing IVIG dose to 2.5 g/kg in experimental ITP [287]. These findings suggested that a novel, FcγRIIB-independent mechanism is responsible for IVIG mediated protection in EAE. To further test this hypothesis, digestion of IVIG with Ide-S, an enzyme that specifically removes the Fc part of IgG was used to generate $F(ab')_2$ fragments. We found that $F(ab')_2$ fragments were as protective as IVIG. This is particularly surprising as the *in vivo* half-life of $F(ab')_2$ can be expected to be lower than that of IgG because murine FcRn binds to human IgG [328] which significantly increases its half-life [329]. It can therefore be assumed that the total dose of IVIG (IgG) in circulation is accumulating more than $F(ab')_2$.

If IVIG treatment was stopped, the first EAE symptoms developed around 6 days later. A combination of several factors could account for this observation. First, the circulating antibody concentration could remain at sufficiently high levels for several days and remain protective. Second, it may simply take several days until newly starting demyelination progressed to cause paralysis. Third, T cells may be primed only after interruption of IVIG treatment and require several days to mount a full-blown adaptive immune response. Because EAE is an established model of T cell mediated autoimmunity, the latter was investigated by adoptively transferring splenocytes from CFA + MOG_{35-55} immunized mice either treated or not treated with IVIG into naïve recipients. Before transfer, cells were re-stimulated with MOG_{35-55} peptide and IL-23 to promote their inflammatory properties [330, 331]. Both mice treated and not treated with IVIG

were able to transfer the disease to naïve mice suggesting that autoantigen-specific T cells are generated under both conditions. To investigate if IVIG can inhibit primed, MOG specific T cells, we adoptively transferred *in vitro* re-stimulated splenocytes from MOG-specific TCR-transgenic mice [252] into naïve recipients and treated with IVIG. Again, treatment was not protective indicating that once T cells have been primed, IVIG cannot protect from disease development.

A polyclonal antibody preparation like IVIG contains an almost unlimited number of binding partners, which could be relevant for the protective mechanism. One simple explanation would be that $F(ab')_2$ fragments prevent adjuvant (CFA) mediated inflammation. Supporting this hypothesis, IVIG was found to contain antibodies recognizing the active component of CFA, *Mycobacterium tuberculosis* [332]. In addition, recognition of soluble mediators or cell surface molecules can be envisaged to provide an important contribution. Comparison of naïve, CFA + PBS and CFA + MOG_{35-55} immunized animals showed that the main effect seen upon immunization is mediated by the adjuvant as both groups behaved very similar in all parameters analyzed. Also, irrespective of $F(ab')_2$ treatment, both CFA + PBS or CFA + MOG_{35-55} immunized animals developed comparable splenomegaly. To get an insight, we performed in-depth leukocyte profiling following CFA + MOG_{35-55} immunization and $F(ab')_2$ treatment. It has recently been shown that both IVIG and $F(ab')_2$ can reduce the number of cytokine-producing T cells in EAE [333]. The proposed mechanism involved an expansion of Tregs cells and prevention of T cell egress from lymph nodes. We could confirm largely reduced frequencies and total numbers of IFN-γ, IL-17 or GM-CSF producing $CD4^+$ T cells in the spleen. However, although the frequency of Tregs cells was increased in the spleen, it was reduced in dLNs and remained unchanged in both compartments if total cell numbers were taken into account. Increased numbers of effector T cells in immunized, PBS treated animals were rather responsible for the relatively increased frequency of Tregs in $F(ab')_2$ treated animals. This argues against an active, $F(ab')_2$ mediated expansion of Tregs. We hypothesized that alterations in cells of the innate immune system underlie the variations seen in $CD4^+$ T cell activation. The most striking observation in $F(ab')_2$ treated mice was a marked reduction of neutrophil expansion in spleen and dLNs. Neutrophils have been shown to play an important role during EAE disease initiation and serve as a source of pro-inflammatory cytokines in the circulation and during neuroinflammation in the CNS [334]. Importantly, neutrophil depletion can prevent EAE disease despite MOG-specific T cell priming takes place [334]. IVIG was shown to contain SIGLEC-9 specific autoantibodies which can induce apoptosis in human neutrophils [168, 335]. It is tempting to speculate that $F(ab')_2$ can similarly induce cell death of murine neutrophils [336], thereby limiting the availability of pro-inflammatory constituents that mediate DC/APC maturation for subsequent T cell activation [334]. Direct inhibition of

inflammatory mediators is another potential mechanism of IVIG efficacy [148-150].

More work is needed to define the mechanism responsible for reduced EAE pathology in $F(ab')_2$ treated animals. So far, our data suggest that less activation of innate immune cells underlies reduced T cell activation. Whether $F(ab')_2$ leads to apoptosis of neutrophils, blocks the action of inflammatory mediators, inhibits leukocyte migration or employs yet another mechanism for its therapeutic efficacy will be the matter of future investigations.

Concluding remarks

More than 30 years after the first use of IVIG for the treatment of autoimmunity, the number of pathological conditions found to be treatable with this agent steadily increases. The success of IVIG urgently demands for a better understanding of the underlying mechanisms of action. However, over 13 000 scientific publications later, our picture is still incomplete. Because a high dose of IVIG is required for its efficacy, it is conceivable that a rare constituent is the active component. As such, sialylated Fc is an attractive target considering its anti-inflammatory properties in several animal models. Efforts are currently being made to implement it for clinical use [241, 247]. Alternatively, immunomodulation may be mediated by one or several rare antibody specificities. However, the most consistent finding in IVIG research seems to be that different human autoimmune diseases or animal models lead to different results concerning both structural requirements of IVIG (IgG, Fab, Fc, Fc-glycan) and the relevance of specific host factors (e.g. FcγRIIB, DC-SIGN). Although unsatisfactory at first sight, this could actually reflect IVIG's capability to modulate disease activity in a multitude of different autoimmune disease conditions. Therefore, it seems unlikely that IVIG can be replaced with a single drug which could recapitulate all aspect of its clinical efficacy. The success of Fc fragments in ITP unequivocally demonstrated the dispensability of Fab polyclonality. Still, this does not exclude a potential involvement in other diseases. In line with that, we could show that T cell mediated autoimmunity in mice can be successfully prevented by $F(ab')_2$ fragments. Additionally, we describe that IgG-Fc sialylation is associated with autoimmune-disease remission and results in reduced complement activation. Based on this, a novel treatment approach could be envisaged in which IgG-Fc sialylation is actively stimulated in patients affected by antibody-mediated autoimmune disease [323].

IgG is long known for its pro-inflammatory effector functions essential for the defense of our body. Considered paradoxical in the beginning, it became obvious that IgG is also a modulator of the immune system contributing to the maintenance of immune tolerance and homeostasis.

4. Human subjects and Methods

4.1 FcγR expression analysis in human PBMC

4.1.1 Human subjects

Patients with CIDP (n = 24) and healthy controls matched by age and gender (n = 19) were recruited between 2010 and 2013 at the Department of Neurology, University of Marburg, Germany (table 4.1). All patients fulfilled the EFNS/PNS diagnostic criteria for CIDP. They were prospectively followed during IVIG therapy (2 g/kg over 5 days) using the modified Rankin disability scale to monitor clinical treatment response [157, 238]. Improvement in the modified Ranking scale within 4 weeks after IVIG treatment was defined as a positive treatment response. Patients did not receive IVIG therapy or immunosuppressive treatment including corticosteroids before study entry. PBMC samples were collected at each visit and obtained before, 2 weeks and 4-8 weeks following treatment with IVIG. The University's IRB approved the study according to the Declaration of Helsinki, GCP and German law (IRB file reference: 46/00).

Demographic an clinical characteristics of CIDP patients and their controls

	CIDP n=24	Controls n=19
Age	59.0 ± 9.4	58.7 ± 9.1
(Years ± SD; range)	(36 ↔ 72)	(34 ↔ 74)
Duration of symptoms	0.5 ± 0.4	N/A
(Years ± SD; range)	(0.1 ↔ 2.0)	
Male to female ratio	3	5
Fulfilling modified AAN criteria, n; %	24; 100	N/A
Fulfilling EFNS/PNS criteria, n; %	24; 100	N/A
Clinical course		N/A
RR[1)], n; %	8; 33.3	-
PP[2)], n; %	14; 58.3	-
Monophasic[3)], n; %	2; 8.3	-
CIDP subtype[4)]		N/A
CIDP-I, n; %	16; 66.7	-
CIDP-MGUS, n; %	2; 8.3	-
DADS-I, n; %	2; 8.3	-
MADSAM, n; %	4; 16.6	-
Treatment response[5)], n; %	21; 87.5	N/A

[1)] RR – relapsing-remitting
[2)] PP – primary progressive
[3)] but no Guillain-Barré syndrome
[4)] MGUS – monoclonal gammopathy of uncertain significance; DADS – Distal acquired demyelinating sensory polyneuropathy; MADSAM – Multifocal acquired demyelinating sensory-motor polyneuropathy
[5)] defined as ≥ 1point decrease in the modified Rankin' scale

Table 4.1 Demographic and clinical characteristics of CIDP patients and their controls

4.1.2 Flow cytometry analysis of human PBMC

Fluorochrome labeled antibodies were purchased from Biolegend (CD3-PE-Cy5 (clone HIT3a), HLA-DR-Pacific Blue (L243), CD19-AlexaFluor700 (HIB19), CD64-APC-Cy7 (10.1)), BD Pharmingen (CD11c-PE-Cy7 (B-Ly6), CD27-PE (M-T271)), Stem Cell Technologies (CD32A-FITC (IV.3)) eBioscience (CD16-e-fluor605 (eBioCB16), CD123-PerCPCy5.5 (6H6)), Invitrogen (CD14-QDot655 (TüK4), CD56-PE-Texas-Red (MEM-188)). Miltenyi (BDCA-1-PE (AD5-14H12), BDCA-3-PE (AD5-(8E7)) The CD32B (FcγRIIB) specific monoclonal antibody clone 2B6 was in-house purified and coupled to Alexa Fluor 647. Dead cells were excluded using Fixable Aqua Dead Cell Stain Kit (Invitrogen). Cells were suspended in PBS + 0.01 % sodium azide (FACS buffer) containing the fluorochrome-labeled antibodies and incubated for 30 minutes on ice. Cells were washed, suspended in FACS buffer and acquired using BD LSR Fortessa cell analyzer (table 4.2). All analysis was performed with FlowJo 9 (Tree Star).

Optical configuration of BD SLR Fortessa

Laser	Mirror	Filter	Intended dye(s)
Violet (405 nm)	735LP	800/50	Qdot800, BV785
	685LP	710/50	Qdot705, BV711
	640LP	670/30	Qdot 655, eFluor 650nc, BV650
	600LP	610/20	Qdot605, eFluor 605nc, BV605
	505LP	525/50	AmCyan, Aqua L/D stain, Pacific Orange, BV510
		450/50	Pacific Blue, V450, BV421, Cell Trace Violet
Blue (488 nm)	635LP	690/50	PerCP, PerCP-Cy5.5
	505LP	525/50	FITC, Alexa 488, GFP
		488/10	SSC
Yellow/Green (561 nm)	750LP	780/60	PE-Cy7
	685LP	710/50	PE-Cy5.5
	635LP	670/30	PE-Cy5, 7aad
	600LP	610/20	PE-Texas Red, mCherry
		582/15	PE, DsRED, PKH26
Red (640 nm)	750LP	780/60	APC-Cy7, APC-H7, APC-Alexa750, Near IR-L/D stain
	685LP	730/45	AlexaFluor 700
		670/30	APC, Alexa 647, TO-PRO-3

Optical configuration of BD FACS Canto-II

Laser	Mirror	Filter	Intended dye(s)
Violet (405 nm)	502LP	510/50	AmCyan, Aqua L/D stain
		450/50	Pacific Blue, V450, BV421, Cell Trace Violet
Blue (488 nm)	735LP	780/60	PE-Cy7
	655LP	670LP	PerCP, PerCP-Cy5.5, 7aad
	556LP	585/42	PE, DsRED, PKH26
	502LP	530/30	FITC, Alexa 488, GFP
		488/10	SSC
Red (640 nm)	735LP	780/60	APC-Cy7, APC-H7, APC-Alexa750, Near IR-L/D stain
	685LP	660/20	APC, Alexa 647, TO-PRO-3

Table 4.2 Optical configuration of flow cytometers

4.1.2.1 Identification of naïve and memory B cells

B cells were identified using the B cell specific molecule CD19 and removal of contaminating cells by gating out cells expressing CD14, CD16, CD64, CD3 and CD56, which are all known to be absent on B cells. Subsequently, naïve and memory B cells were identified based on the expression of CD27, which is a memory B cell specific cell surfase protein(figure 4.1) [337].

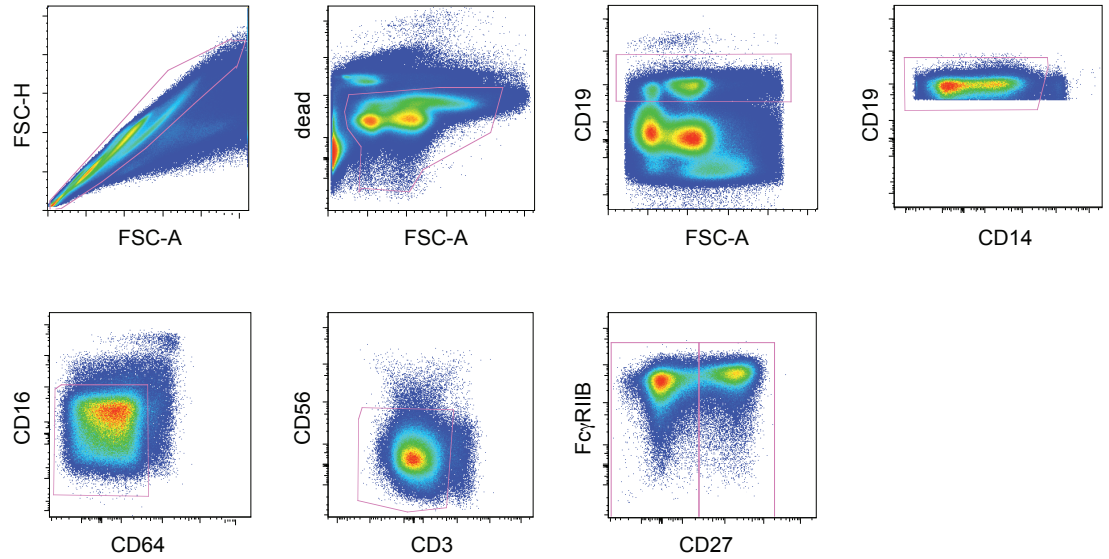

Figure 4.1 B cell gating strategy.
PBMC were stained with fluorescently labelled antibodies followed and analysed by flow cytometry. An exemplary gating is shown starting. Gates are indicated in magenta. B cells were identified by sequentially gating on single, living, CD19 positive and CD14 as well as CD16, CD64, CD56 and CD3 negative cells. Finally, naïve and memory B cells were identified using CD27 staining.

4.1.2.2 Identification of monocytes and monocyte subsets

Monocytes were identified as being CD11c and MHC class II (MHC-II) positive and CD19 negative and functionally distinct monocyte subsets were distinguished based on their expression of CD14 and CD16 (figure 4.2) [338, 339].

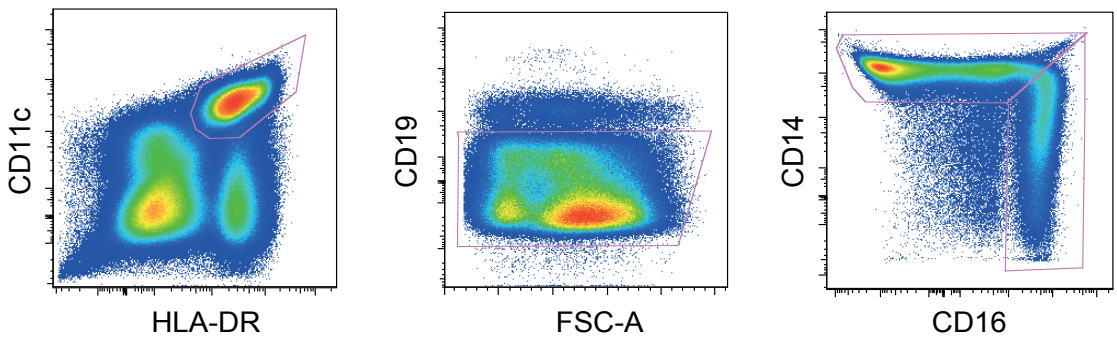

Figure 4.2 Monocyte cell gating strategy.
Single, living cells were gated as shown in figure 4.1. Monocytes were identified by their co-expression of CD11c and MHC-II while being negative for CD19. Finally, monocyte subsets were identified by their CD14 and CD16 expression pattern.

4.2 IgG-Fc glycosylation analysis

4.2.1 Human subjects

Samples and clinical data were collected during a randomized placebo-controlled trial (ICE trial) testing the efficacy of intravenous injection of 10 % caprylate-chromatography purified immune globulin (IGIV-C, Gamunex; referred to as IVIG) in patients with CIDP [192]. Patients received either IVIG (2 g/kg body weight initially, 1 g/kg body weight every 3 weeks thereafter) or 0.1% albumin (placebo) were followed over 24 weeks [192]. Post-treatment samples were taken 2 weeks after the last infusion. Disease remission was defined as improvement in the adjusted INCAT score after 24 weeks and was observed in 32 of 59 (54%) patients treated with IVIG and 12 of 58 (21%) patients who received placebo [192]. The predicted rate of improvement during treatment with placebo in the ICE trial was 15% [192] based on previous data obtained in randomized controlled treatment trials in CIDP patients.

An additional cohort of patients was recruited between 2010 and 2013 at the Department of Neurology, University of Marburg, Germany (table 4.3). All patients fulfilled the EFNS/PNS diagnostic criteria for CIDP. Patients received IVIG (2 g/kg body weight initially and 1 g/kg body weight for maintenance therapy) for at least 2 months. Post-treatment samples were taken 3 - 5 weeks following the last infusion of IVIG (mean ± SD: 4 ± 0.6). Similar to the ICE trial [192], a clinical response to IVIG was defined as improvement in the adjusted INCAT score and observed in 31/33 (94 %) patients. The University's IRB approved the study according to the Declaration of Helsinki, GCP and German law (IRB file reference: 46/00).

Number of patients	33	
Age at study entry (Median; range)	62; 32 - 79	
Duration of symptoms (years)	< 1 - 15	
Male to female ratio	22:11	
Fulfilling modified AAN criteria	94%	
Fulfilling EFNS/PNS criteria	100%	
Clinical course	number of patients	% of patients
Relapsing-remitting	5	15.1
Primary progressive	26	78.8
Monophasic	2	6.1
CIDP subtype		
CIDP	25	75.8
CIDP-MGUS	0	0
DADS	3	9.1
MADSAM	5	15.2
Treatment response	31	94

Table 4.3 Demographic and clinical characteristics of "Marburg cohort " CIDP patients

4.2.2 Reagents

RPMI-1640, DMEM, Penicillin-Streptomycin (P/S), pooled human serum, TO-PRO-3 Stain, LIVE/DEAD Fixable Near-IR Dead Cell Stain Kit, LIVE/DEAD Fixable Aqua Dead Cell Stain Kit, 1-StepTM Ultra TMB-ELISA Substrate Solution and CAPTURESELECT IgG-C_H1 PRO Affinity Matrix were purchased from Life Technologies (Zug, Switzerland). Fetal calf serum (FCS) was purchased from BIOCHROM AG. (Berlin, Germany). Recombinant human IL-2 was purchased from PeproTech EC Ltd. (London, UK). PKH26 Red Fluorescent Cell Linker Kit and was purchased from SIGMA-ALDRICH (Buchs, Switzerland). Ficoll- Paque was purchased from GE Healthcare. Accutase was purchased from Stemcell Technologies (Grenoble, France). MACS NK Cell Isolation Kit-II (negative selection) and B Cell Isolation Kit (CD19 positive selection) were purchased from Miltenyi Biotech (Bergisch Gladbach, Germany). Human serum complement and C5 depleted human serum were purchased from TECOmedical Group (Sissach, Switzerland). EZ- Link NHS-PEG12-Biotin was purchased from Thermo Scientific (Rockford, USA). Papain and Nutridoma-SP were purchased from Roche (Basel, Switzerland). HiLoad 16/60 Superdex 200 column, HiTrap Protein G HP Columns, StrepTrap HP Columns, HisTrap HP columns and Protein G Sepharose 4 Fast Flow were purchased from GE Healthcare (Glattbrugg, Switzerland). Ceramic Fluoroapatite (CFT-II, 40 μM) was purchased from Bio-Rad (Hercules, CA, USA). Biotinylated lectins (*Lens culinaris* agglutinin (LCA), *Sambucus nigra* agglutinin (SNA), *Erythrina cristagalli* lectin (ECL) and *Aleuria aurantia* lectin (AAL) and SNA-Agarose were purchased from Vector Laboratories (Burlingame, USA). Neuraminidase was purchased from New England Biolabs (Ontario, Canada). UDP-Galactose, CMP-Sialic Acid, β1,4-Galactosidase and Amicon Ultra centrifugal filters were purchased from Merck Millipore (Billerica, USA). StarGate cloning and expression system was purchased from IBA (Göttingen, Germany).

4.2.3 Antibodies and streptavidin

RTX (MabThera) was purchased from Roche (Basel, Switzerland). Monoclonal mouse anti-human C1q as well as biotinylated anti-human C1q and anti-human-C3c were purchased from TECOmedical Group. Anti-human IgG-Fc-HRP was purchased from Sigma-Aldrich (Buchs, Switzerland). Anti-CD20- PE-Cy7 was purchased from eBioscience (San Diego, USA). Polyclonal rabbit anti- Mouse IgG (H+L)-A488 was purchased from Life Technologies (Zug, Switzerland). Streptavidin-FITC and Streptavidin-PE were purchased from Biolegend (San Diego, USA).

4.2.4 Serum IgG quantification

Serum samples were taken before the initiation of the study (baseline) and 24 weeks (ICE trial) or < 7 weeks (Marburg cohort) thereafter, stored at -80 ºC. Total serum IgG levels were determined using a commercially available human IgG ELISA (Immundiagnostik, Bensheim, Germany) according to the manufacturer's instructions.

4.2.5 2-AB labeled glycosylation analysis (2-AB HPLC-FL)

Papain digestion and Protein-G sepharose was used to purify IgG-Fc (done as for lectin blotting, see 4.2.6). For release of N-Glycans, 110 µg protein samples were dried and suspended at 100 °C for 10 min in 20 mM HEPES buffer pH 8.2 containing 1 % SDS. SDS was blocked by NP-40 and N-glycans were released by PNGaseF and separated from glycopeptides using a Sep-Pak C18 cartridge. The carbohydrates contained in the flow-trough were applied to a porous graphitized carbon (PGC). Under aqueous conditions, oligosaccharides bind to the PGC cartridge, while salts and buffers pass through. Glycans were eluted by 15-100 % Acetonitrile and used for 2-AB tagging and HPLC-FL analysis. For labeling with 2-Aminobenzamide (2-AB) 100 µl of the cyanoborohydride mixture (prepared by adding 6.5 mg of sodium cyanoborohydride in 200 µl of a 35:65 glacial acetic acid: DMSO mixture) were added to 6 mg of 2-AB reagent, vortexed and sonicated to mix thoroughly. 10 µl of 2-AB reagent were added to each sample and incubated at 65 °C for 2.5 hours. After 2-AB labeling the samples were purified by passing through a Glycoclean S-cartridge (Prozyme) and dried in a speed vac. Analysis of 2-AB labeled glycans was performed by HPLC-fluorescence detection (HPLC-FL) using a Dionex DX-600 HPLC System. Therefore, 2-AB labeled glycans were dissolved in water and separated on a Dionex analytical column (Carbo Pac PA 100, 2 × 250 mm) using 100 mM NaOH (0 - 20 min) and 100 mM NaOH with 250 mM NaOAc (20 - 80 min) gradients. Glycan release, labeling and HPLC-FL was done by Biswa Pronab Choudhury and collegues at Glycobiology Core Resources in La Jolla, California.

4.2.6 Fc purification from serum and sample preparation for lectin blotting

Serum was obtained by centrifugation of complete heparinized blood at 5 000 x g for 2 minutes and stored at –20 C°. 15 µl serum was diluted to 30 µl with PBS. 30 µl 2-fold concentrated papain reaction buffer (0.04 M EDTA + 0.04 M L-Cystein in PBS, pH adjusted to 6.5 with 2 M NaOH). 3 µl papain were added and samples were incubated for 1 h at 25 °C while rotating at 600 rpm. To stop the reaction, 50 µl 10 x protease inhibitor (Roche "Complete") were added. 20 µl Protein G sepharose slurry was washed 3 times with 1 ml PBS (centrifuged

at 1500 g for precipitation of beads). 400 µl PBS were added to the papain-treated-serum-PBS-protease-inhibitor-mix and transferred on the washed beads. To allow binding, samples were incubated over night at 4 °C. For elution, 90 µl 0.1 M glycin at pH 2.7 was added and samples were incubated for 3 minutes at 95 °C while rotating at 1000 rpm. Subsequently, samples were immediately centrifuged for 5 minutes at 1500 x g at 4 °C. The supernatant was transferred to a new tube containing 10 µl Tris buffer at pH 8.8 to neutralize the pH to 7.4. At that stage, samples were either stored at −20 °C or immediately used for lectin blotting.

4.2.7 Lectin blotting and analysis

Fc-linked glycans were analyzed by lectin blotting using biotinylated lectins as previously described [133, 165] (LCA, SNA, ECL, AAL). In brief, 12.5 µl purified serum-derived Fc (see chapter 4.2.6) was mixed with 37.5 µl PBS and 15 µl 5 × Laemmli buffer (1.5 g SDS, 3.75 ml 1 M Tris pH6.8, 0.015 g bromphenol blue, 1.16 g DTT, 7.5 ml (9.5 g) glycerol; 15 ml with ddH_2O) and incubated for 3 minutes at 95 °C. After centrifugation at 16 000 × g, 13 µl (for ECL, SNA and AAL) or 7 µl (for LCA) were loaded on a 10 % Polyacrylamide gel. The protein was transferred to a nitrocellulose membrane in a semi-dry blotter for 1 hour at 12 V. Membranes were blocked for 1 hour with western blocking reagent (Roche) diluted to 1 × in TBS. Lectins were diluted 1:1000 in TBS + 0.1 mM $CaCl_2$, $MgCl_2$ and $MnCl_2$
and incubated for 1 hour in the dark. After washing 6 times with TBS + 0.1 % Tween20, lectin binding was detected using HRP-labeled streptavidin (MABtech) and quantified by chemiluminescence using SuperSignal West Pico Chemiluminescent substrate (Pierce) and digital detection of the chemiluminescence signal with Fusion FX Spectra (Vilber Lourmat). Analysis was performed using Image J (NIH). Signal intensities for each glycan (fucose, terminal galactose, and sialic acid) were normalized to the signal obtained for the core glycan (mannose) and are expressed as glycan contents relative to a reference serum (signal intensity was set to 1).

4.2.7.1 Specific and quantitative detection of individual IgG-Fc glycan residues by lectin-blotting

Human IgG-Fc obtained by papain digestion and protein-G affinity purification analyzed by lectin-blotting using *Lens culinaris* agglutinin (LCA) recognizing mannose [340], *Erythrina cristagalli* lectin (ECL) recognizing terminal galactose [341], *Sambucus nigra* agglutinin (SNA) recognizing sialic acid [342, 343] and *Aleuria aurantia* lectin (AAL) recognizing fucose [340]. Removal of the IgG-Fc glycan by PNGase-F treatment was used to confirm glycan-dependent recognition of IgG-Fc by the lectins. As shown if figure 4.3A, PNGase-F treatment leads to a

molecular weight shift due to the loss of the glycan and the shifted lane is no longer recognized by lectins, confirming their specificity. Neuraminidase treatment specifically removes sialic acid leading to a loss of SNA recognition as well as an increase of ECL signal due to the presence of more terminal galactose upon sialic acid removal (figure 4.3A). Because the IgG-Fc content of different serum samples varies, we needed to identify the linear range of the lectin signal. All lectin signals were linear over the entire relevant range (figure 4.3B).

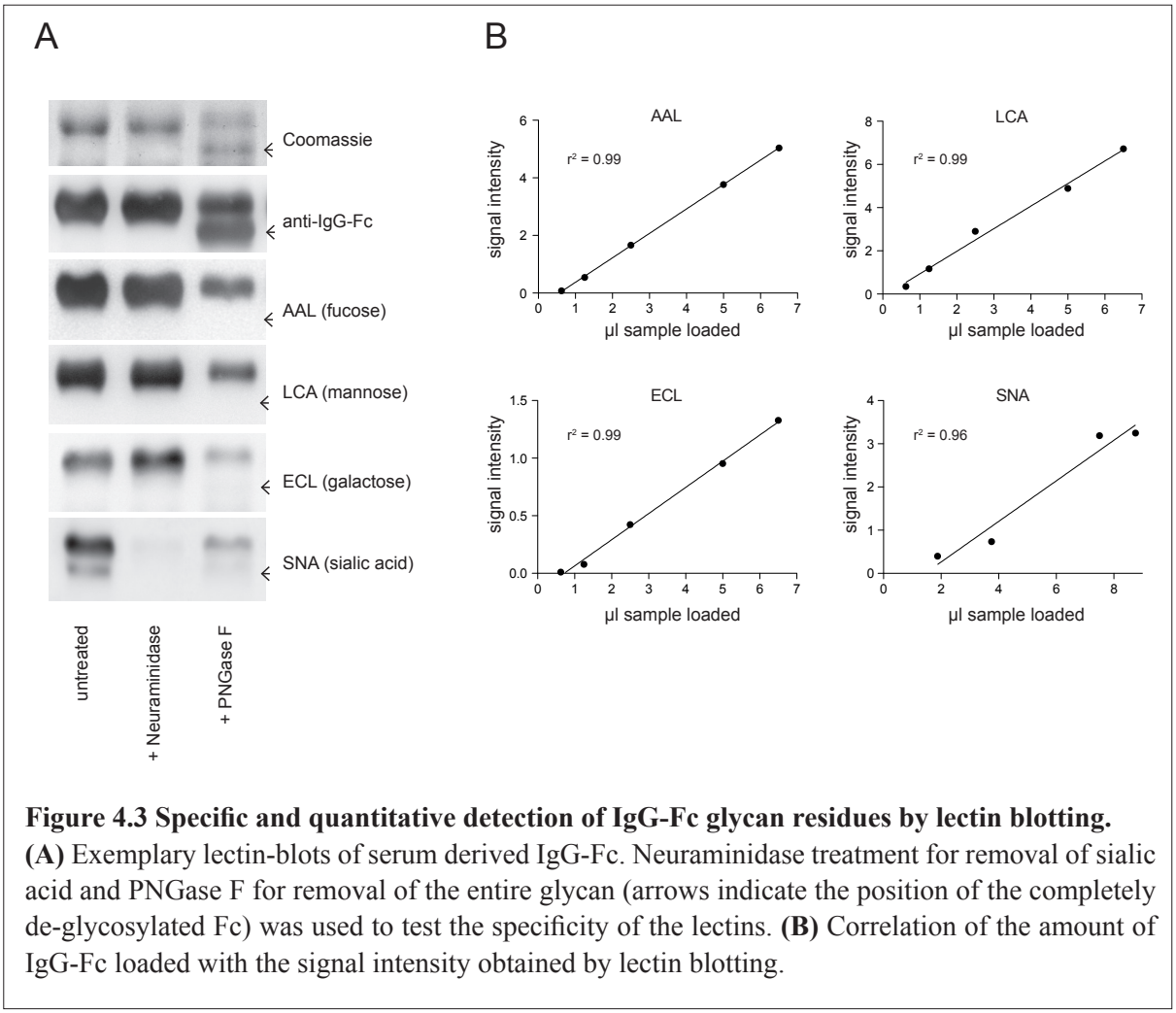

Figure 4.3 Specific and quantitative detection of IgG-Fc glycan residues by lectin blotting. **(A)** Exemplary lectin-blots of serum derived IgG-Fc. Neuraminidase treatment for removal of sialic acid and PNGase F for removal of the entire glycan (arrows indicate the position of the completely de-glycosylated Fc) was used to test the specificity of the lectins. **(B)** Correlation of the amount of IgG-Fc loaded with the signal intensity obtained by lectin blotting.

4.2.8 Purification of Fc, de-sialylated Fc and sialic acid enriched Fc from polyclonal IgG

Intravenous Immunoglobulin (Pivigen, CSL Behring AG, Bern, Switzerland) was used as source of human IgG. 550 mg IgG was incubated in 0.02 M EDTA, 0.02 M L-cysteine in PBS at pH 6.5 with 0.8 mg papain for 2 hours at 25 °C. Uncut IgG and papain were separated by size exclusion with a HiLoad 16/60 Superdex 200 column and GE Aekta purifier. The fraction containing the Fc and Fab fragments was concentrated using Amicon Ultra 15 ml centrifugal filters with a molecular weight cut-off of 10 kDa and dialyzed to 5 mM Na-phosphate buffer pH 7.1. Fab and Fc were separated using a self-packed 50 ml Ceramic Fluoroapatite column (CFT Type II, 40 µm) and Äkta purifier (GE Healthcare) [344]. Therefore, 50 mg Fab/Fc protein

(1 mg per ml CFT material) at a concentration of 5 mg/ml were applied to the column using 5 mM Na-phosphate buffer pH 7.1 as running buffer. At this phosphate concentration, bot Fc and Fab bind to the column. Fc was eluted with 30 mM Na-phosphate buffer pH7.1 (by mixing 10 % 250 mM Na-phosphate buffer to the 5 mM Na-phosphate buffer). After an increase to 42.5 mM Na-phosphate buffer to remove the remaining Fc, Fab was eluted with 155 mM Na-phosphate buffer at pH 7.1 (by mixing 60 % 250 mM Na-phosphate buffer to the 5 mM Na-phosphate buffer). The column was cleared with 250 mM Na-phosphate buffer at pH 7.1 (figure 4.4).
For purification of sialic acid enriched Fc, Fc was dialyzed to TBS and $CaCl_2$ was added to a final concentration of 0.1 M. Sialic acid enriched Fc was purified from 40 mg Fc by binding to 4 ml SNA-Agarose and elution with 0.5 M lactose in TBS as previously described [165]. For neuraminidase treatment, Fc was dialyzed to 50 mM sodium citrate pH 6 and incubated with one unit neuraminidase per µg Fc for 48 hours at 37 °C. Neuraminidase was removed using Protein-G sepharose. For further purification, Fc, de-sialylated Fc and sialic acid enriched Fc were cleared from residual Fab using a Captureselect IgG-C_H1 pro affinity matrix and re-applied to a HiLoad 16/60 Superdex 200 column.

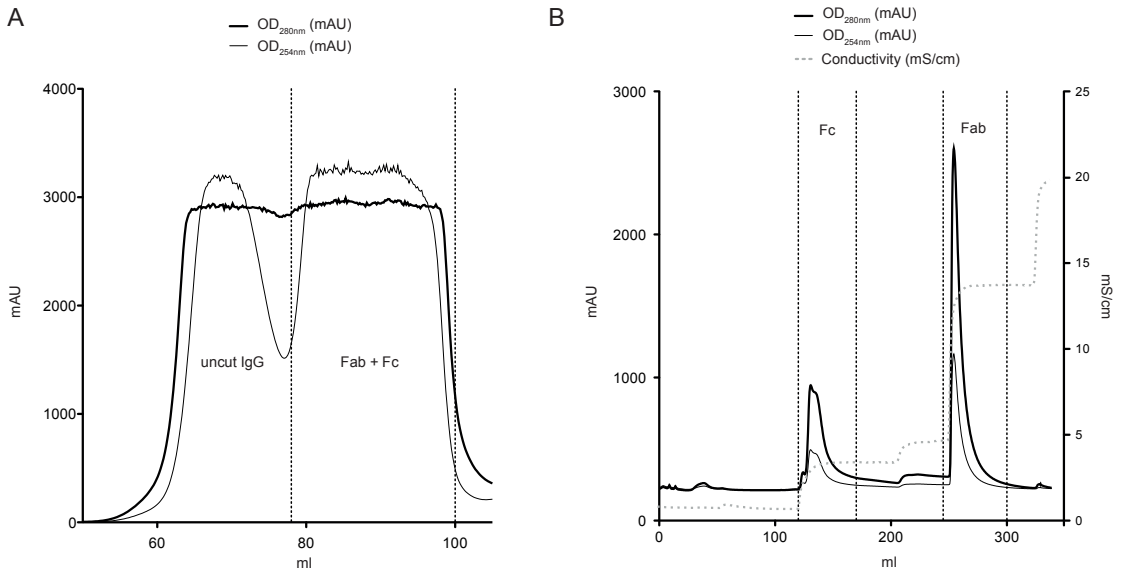

4.4 Purification of Fab and Fc from IVIG
(A) Size-exclusion chromatography profile of papain digested IVIG. The collected fraction corresponding to Fab and Fc is indicated with dotted lines. **(B)** CFT-II column chromatography profile. The collected fractions containing Fab and Fc are indicated with dotted lines. The buffer conductivity is shown as a dotted grey line.

4.2.9 Purification of hu8-18C5 antibody

The hu8-18C5 antibody has been generated by cloning of the 8-18C5 hybridoma-derived *Igh* and *Igk* variable-region sequences into human IgG1 heavy-chain and kappa light chain expression vectors as previously described (21). hu8-18C5 was purified by co-transfecting

the calcium phosphate precipitated expression vectors in HKB-11 cells [345]. After 12 hours the medium was exchanged to DMEM containing P/S (50 U/ml) and 1 % Nutridoma-SP. The culture supernatant was harvested four days later and antibodies were purified using HiTrap Protein G HP columns according to the manufacturer's instructions using GE Aekta prime plus.

4.2.10 Purification of recombinant glycosyltransferases

For the purification of human sialylatransferase, a plasmid containing the cDNA of human ST6Gal-I was purchased from Sino Biological Inc. and the extracellular domain (AA 27 - 406) was cloned into the pCSG-IBA-144 expression vector using the StarGate cloning system according to the manufacturer's instructions. This yields plasmids encoding for proteins containing an N-terminal Twin-Strep-tag and a C-terminal Hexahistidine-tag (figure 4.5A). HEK293T cells were cultured under standard cell-culture conditions in DMEM containing 10 % FCS and P/S (50 U/ml) and transfected with calcium-phosphate precipitated plasmids encoding ST6Gal-I. After 12 hours, the medium was replaced with fresh DMEM containing 10 % FCS and P/S (50 U/ml) and cells were cultured for another 3 days. The cell supernatant was harvested and proteins were purified by immobilized metal ion affinity chromatography (HisTrap HP columns) and subsequently Strep-Tactin affinity chromatography (Strep-Trap HP columns) according to the manufacturer's instructions using GE Aekta prime plus.
For the purification of bovine β1-4Gal-T (GenBank ref.: BC120415.1), the cDNA coding for amino acids 115 to 402 was synthesized by GeneArt (Life Technologies) (figure 4.5B) [346]. Re-cloning, expression and purification was done as described for ST6Gal-I.

A

Amino acid sequence of the expressed human ST6GAL-I protein construct

MASAWSHPQFEKGGGSGGGSGGSAWSHPQFEKSGM**KEKKKGSYYDSFKL**
QTKEFQVLKSLGKLAMGSDSQSVSSSSTQDPHRGRQTLGSLRGLAKAKP
EASFQVWNKDSSSKNLIPRLQKIWKNYLSMNKYKVSYKGPGPGIKFSAE
ALRCHLRDHVNVSMVEVTDFPFNTSEWEGYLPKESIRTKAGPWGRCAV
VSSAGSLKSSQLGREIDDHDAVLRFNGAPTANFQQDVGTKTTIRLMNSQL
VTTEKRFLKDSLYNEGILIVWDPSVYHSDIPKWYQNPDYNFFNNYKTYRK
LHPNQPFYILKPQMPWELWDILQEISPEEIQPNPPSSGMLGIIIMMTLCDQ
VDIYEFLPSKRKTDVCYYYQKFFDSACTMGAYHPLLYEKNLVKHLNQGT
DEDIYLLGKATLPGFRTIHCGSAHHHHHH

B

Amino acid sequence of expressed bovine β1-4Gal-T protein construct

MASAWSHPQFEKGGGSGGGSGGSAWSHPQFEKSGM**GSNLTSAPVPSTTTRS**
LTACPEESPLLVGPMLIEFNIPVDLKLVEQQNPKVKLGGRYTPMDCISPH
KVAIIIPFRNRQEHLKYWLYYLHPILQRQQLDYGIYVINQAGESMFNRAK
LLNVGFKEALKDYDYNCFVFSDVDLIPMNDHNTYRCFSQPRHISVAMDK
FGFSLPYVQYFGGVSALSKQQFLSINGFPNNYWGWGGEDDDIYNRLAFR
GMSVSRPNAVIGKCRMIRHSRDKKNEPNPQRFDRIAHTKETMLSDGLNS
LTYMVLEVQRYPLYTKITVDIGTPSGSAHHHHHH

Figure 4.5 (continued on next page)

Figure 4.5 Amino acid sequence of expressed ST6Gal-I and β1-4Gal-T protein constructs (continued)
The extracellular domains of human ST6GAL-1 **(A)** and bovine β1-4Gal-T **(B)** were cloned into separate pCSG-IBA144 vectors. *In silico* sequence translation of the resultant open reading frame shows the N-terminal Twin-Strep-II tag followed by the respective extracellular domain (depicted in bold) and a C-terminal hexa-HIS tag.

4.2.11 Generation of antibody glycovariants

Tetra-sialylated RTX was generated by chemoenzymatic glycoengineering as previously described [239] with adequate modifications. Briefly, commercial rituximab (8 mg) was incubated with EndoS WT (25 μg) at 37 °C for 1 hour and the completion of deglycosylation was confirmed by LC-MS analysis. The deglycosylated antibody was purified using a HiTrap protein A column and the eluted fractions were concentrated and buffer exchanged into 1 x PBS pH 7.4. The purified Fuc-α1,6-GlcNAc-rituximab (7 mg) and sialylated complex type oxazoline (3.5 mg) were incubated with EndoS D233Q (175 μg) at 37 °C in 100 mM Tris pH 7.4 (500 μL total volume). The reaction progress was monitored using LC-MS analysis and complete transfer was achieved in 1.5 hours. The tetra-sialylated rituximab was purified using a Hitrap protein A column and was concentrated and buffer exchanged into 1x PBS pH 7.4. LC-MS: heavy chain of rituximab with sialylated complex type glycan, M = 51412 Da; found (m/z), 51412 (deconvolution data). Enzymatic galactosylation and sialylation were performed as previously described [87, 165]. For galactosylation, antibodies were buffer-exchanged to 0.2 mM MES pH 6.5 and incubated for 24 hours at 37 °C in the presence of 5 μg β1-4 Gal-T per mg antibody, 10 mM UDP-galactose and 20 mM $MnCl_2$. Non-galactosylated antibodies ("unmodified") were treated the same way but without addition of UDP-galactose and β1-4 Gal-T. After buffer exchange to 25 mM MOPS 100 mM KCl (pH 7.2) galactosylated antibodies were sialylated by addition of 50 μg ST6Gal-I per mg antibody and CMP-sialic acid at a final concentration of 1.5 mM. The reaction was incubated for 24 hours at 37 °C. Non-sialylated antibodies ("unmodified" and "galactosylated") were treated the same way but without the addition of CMP-sialic acid and ST6Gal-I. All antibodies were buffer-exchanged to TBS. To enrich for antibodies containing sialic acid, *sambucus nigra* agglutinin (SNA) lectin affinity chromatography was performed as previously described [165]. For de-galactosylation, RTX or hu8-18C5 was dialyzed to 50 mM sodium phosphate pH 6.0 and incubated 6 hours at room temperature and 1 hour at 37 °C in the presence of 30 mU β1,4-galactosidase per mg antibody. Finally, all antibodies were purified using protein-G sepharose 4 fast flow according to the manufacturer`s instruction, dialyzed to PBS and sterilized by 0.2 μM filtration.

SDS-Polyacrylamide gel electrophoresis (SDS-PAGE) and silver staining were performed to test antibody integrity and purity and lectin-blotting was used to confirm glycan modifications.

4.2.12 FcγR binding assay

RTX and tetra-sialylated RTX were biotinylated using EZ-Link NHS-PEG12-Biotin according to the manufacturer's recommendations. 1×10^5 CHO cells stably expressing none or one of the human FcγRs [240] were incubated for 30 minutes on ice in the presence of RTX or tetra-sialylated RTX. Cells were washed twice with PBS and incubated for 30 min with streptavidin-FITC for detection of binding and LIVE/DEAD Fixable Near-IR Dead Cell Stain Kit for dead cell exclusion. After washing twice with PBS, cells were acquired using BD FACS Canto- II (see table 4.2 for optical configuration) and analyzed with FlowJo (Tree Star).

4.2.13 Antibody-dependent cell-mediated cytotoxicity (ADCC) assay

ADCC assay was performed as previously described [347]. Human peripheral blood mononuclear cells (PBMC) were isolated from buffy-coats using Ficoll gradient centrifugation. NK cells were negatively selected using MACS NK cell isolation kit and B cells were positively selected using MACS CD19 positive selection kit. Both cells were cultured over night in RPMI supplemented with P/S (50 U/ml) and 5 % heat-inactivated pooled human serum in 24-well plates at 5×10^6 cells per well. NK cell medium was additionally supplemented with 100 IU IL-2. On the next day, B cells were stained with PKH26 according to the manufacturer's recommendation. 1×10^4 B cells were incubated in the presence of autologous NK cells (1×10^3 to 1×10^5) and RTX (0.1 µg/ml to 1 ng/ml) in RPMI supplemented with P/S (50 U/ml), 5 % heat-inactivated pooled human serum and 100 IU IL-2 in 96-well round-bottom plates for 18 hours in a humidified incubator at 37 °C and 5 %. For cell death assessment TO-PRO-3 stain was added to a final concentration of 200 nM and cells were acquired using BD FACS Canto-II (see table 4.2 for optical configuration) and analyzed with FlowJo (Tree Star).

4.2.14 Complement-dependent cytotoxicity (CDC) assay

Raji or Ramos cells were used to assess RTX (anti-CD20)-mediated CDC. Therefore, 7×10^4 cells were placed in a humidified incubator at 37 °C and 5 % CO_2 in RPMI-1640 containing P/S (50 U/ml) in 96-well V-bottom plates in the presence or absence of RTX (MabThera, Roche) or glycovariants of it. After 30 minutes human serum complement was added to a final concentration of 5 % and the incubation was continued for 12 hours. For hu8-18C5- mediated CDC 2×10^4 MO3.13 MOG cells were seeded in 96-well flat-bottom plates in DMEM +

10 % FCS. On the next day the medium was removed and DMEM containing 15 % serum complement with or without hu8-18C5 or a glycovariant of it following incubation for 4 hours in a humidified incubator at 37 °C and 5 % CO_2. For cell death assessment TO-PRO-3 stain was added to a final concentration of 200 nM and cells were analyzed using BD FACS Canto-II (see table 4.2 for optical configuration) and analyzed with FlowJo (Tree Star).

4.2.15 C1q binding assay

For C1q binding to Raji or Ramos cells, 2×10^5 cells were seeded in RPMI-1640 containing 1 % C5-depleted human serum in the presence of 10 µg/ml RTX or RTX glycovariants for 5, 15, 30, 60 or 120 minutes in a humidified incubator at 37 °C and 5 % CO_2. For C1q binding to MO3.13 MOG cells, cells were detached using accutase and 1×10^5 cells were seeded in DMEM containing 1 % C5-depleted serum in the presence of 2.5 µg hu8-18C5 or hu8-18C5 glycovariants for 5, 15, 30, 60 or 120 minutes in a humidified incubator at 37 °C and 5 % CO_2. C1q binding was detected by staining on ice with biotinylated anti-C1q for 1 hour. Cells were washed twice with PBS and incubated on ice with streptavidin-PE and LIVE/DEAD Fixable Aqua Dead Cell Stain Kit for 25 minutes. After washing twice with PBS samples were acquired using BD FACS Canto-II (see table 4.2 for optical configuration) and analyzed with FlowJo (Tree Star).

4.2.16 C3b deposition assay

2×10^5 Raji cells were seeded in RPMI-1640 containing 1 % C5-depleted serum in the presence of 10 µg/ml RTX or RTX glycovariants for 5, 15, 30, 60 or 120 minutes in a humidified incubator at 37 °C and 5 % CO_2. For C3 deposition assessment cells were stained with biotinylated anti-C3c for 1 hour on ice. Cells were washed twice with PBS and incubated on ice with streptavidin-PE and LIVE/DEAD Fixable Aqua Dead Cell Stain Kit for 25 minutes. After washing twice with PBS samples were acquired using BD FACS Canto-II (see table 4.2 for optical configuration) and analyzed with FlowJo (Tree Star).

4.2.17 C1q binding ELISA

Microtiter plates (Nunc Maxisorp) were coated over night at 4 °C with 0.5 µg Fc, de-sialylated Fc or sialic acid enriched Fc in coating buffer (0.05 M sodium carbonate buffer, pH 9). Binding efficiency to the plate was examined using anti-human IgG-Fc- HRP as the probe. Wells were washed and incubated with human serum complement diluted in PBS containing 0.05 % Tween20 (PBS-T) and 1 % BSA for 2 hours at room temperature. After washing with PBS-T

wells were incubated for 1 hour with biotinylated anti-C1q, washed with PBS-T and incubated for 1 hour with streptavidin- HRP. HRP activity was quantified using incubation TMB-ELISA substrate and colorimetric detection at 450 nm.

4.3 Analysis of IVIG and F(ab')$_2$ in EAE

4.3.1 Purification of Ide-S

A plasmid containing the cDNA of Ide-S (NCBI Reference Sequence: NP_269065.1) was synthesized and cloned into the pMA-T vector invitrogen and subcloned in a modified pET28a (GE Healthcare) vector containing an n-terminal deka-HIS tag and a PreScission protease cutting site (Ge Healthcare, PreScission protease cutting for HIS tag removal was done). MC1060/pWTZ594 e.coli were used for cloning and plasmid amplificatin. The final plasmid was transferred into BL21 E.coli (NEB) for protein expression. Bacteria were grown to and OD_{600nm} of 0.3-0.4 and expression was induced by addition of 0.1 mM IPTG for 3 hours at 37 °C. The bacteria pellet was resuspended in PBS containing DNAse (20 µg/ml final, Sigma) and 1.6 mM PMSF. Bacteria were lysed by sonication and Ide-S was purified by immobilized metal ion affinity chromatography (HisTrap HP columns, GE healthcare) using Äkta prime plus (GE healthcare). Successful purification was monitored by SDS-PAGE and coomassie staining. Finally, the protein was extensively dialyzed to PBS, sterile filtered through a 0.2 µM filter, supplemented with 20 % glycerol and protein concentration was adjusted to 1 mg/ml before snap-freezing in liquid nitrogen and storage at −80 °C.

MHHHHHHHHHHLEVLFQGPS**ADSFSANQEIRYSEVTPYHVTSVWTKGVTP PANFTQGEDVFHAPYVANQGWYDITKTFNGKDDLLCGAATAGNMLHW WFDQNKDQIKRYLEEHPEKQKINFNGEQMFDVKEAIDTKNHQLDSKLFE YFKEKAFPYLSTKHLGVFPDHVIDMFINGYRLSLTNHGPTPVKEGSKDPR GGIFDAVFTRGDQSKLLTSRHDFKEKNLKEISDLIKKELTEGKALGLSHT YANVRINHVINLWGADFDSNGNLKAIYVTDSDSNASIGMKKYFVGVNSAG KVAISAKEIKEDNIGAQVLGLFTLSTGQDSWNQTN**

Figure 4.6: Ide-S amino acid sequence
Ide-S was cloned into the pET28 nHIS vector. The *in silico* translation of the resultant protein is shonw. Amino acids corresponding to the Ide-S are depicted in bold.

4.3.2 Purification of F(ab')$_2$ from IVIG

For F(ab')$_2$ purification from IVIG, 2 mg Ide-S were incubated with 3 ml (300 mg) IVIG at room temperature for at least 8 hours (or over night). F(ab')$_2$ was separated from uncut IgG and monomeric Fc using a HiLoad 26/60 Superdex 75 prep grade column (GE Healthcare) and Äkta Purifier with PBS as running buffer. The F(ab')$_2$ containing fraction was concentrated by ammonium-sulfate precipitation. Therefore, F(ab')$_2$ in PBS was mixed with twice the volume of saturated ammonium sulfate solution and incubated or 1 hour at room temperature. After centrifugation for 30 minutes at 3 000 × g, the supernatant was removed and the precipitate resuspended in PBS. F(ab')$_2$ was extensively dialyzed to PBS and applied to a self-packed protein A sepharose (GE-Healthcare) column by gravity flow to remove remaining full-length IgG. The column flow-through, containing the F(ab')$_2$, was concentrated using Amicon Ultra 15 ml centrifugal filters with a molecular weight cut-off of 10 kDa according to the manufacturers instructions to reach a final concentration of 35 to 45 mg/ml. Succesful purification of F(ab')$_2$ was confirmed by SDS-PAGE and coomassie staining (figure 4.7B). Finally, the solution was sterile filtered through a 0.2 µM filter and stored at 4 °C until use.

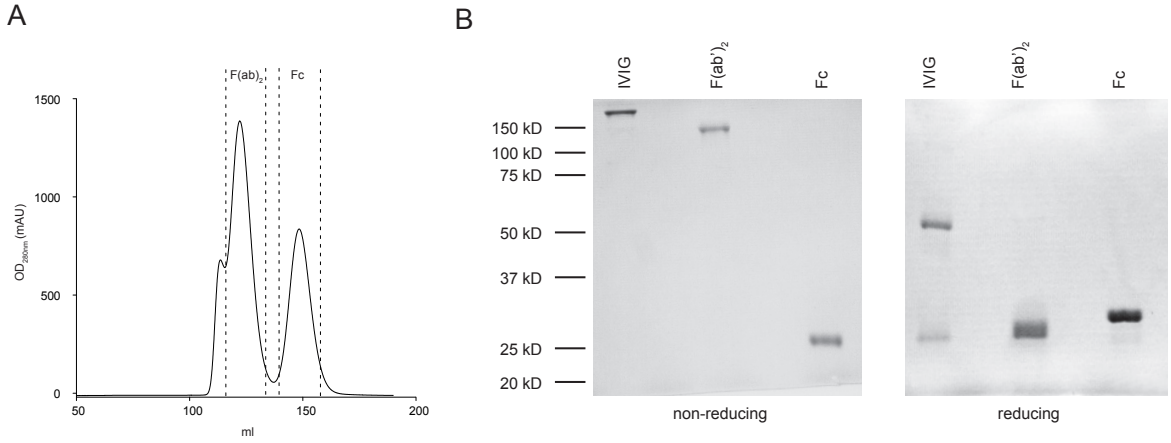

4.7 F(ab')$_2$ purification
(A) Size-exclusion chromatography profile of Ide-S digested IVIG. The peaks corresponding to F(ab')$_2$ and Fc are indicated. **(B)** Coomassie stained non-reducing (left) or reducing (right) SDS-PAGE showing IVIG and purified F(ab')$_2$ and Fc.

4.3.3 Purification and biotinylation of anti-mouse FcγRIIB antibody (K9.361)

An antibody specifically recognizing FcγRIIB was purified from K9.361 hybridoma [348] (kindly provided by Ulrich Hammerling) supernatant. To do so, hybridoma cells were cultured in CELLine culture flasks (BD Bioscience) in PFHM-II medium (Gibco, Life Technologies) according to the manufacturers instructions. The antibody-containing cell suspension was harvested after 2 weeks and centrifuged three times at 4000 × g to remove cells and debris. After filtration through a 0.4 µM filter, antibodies were precipitated by dropwise addition of saturated ammonium-sulfate at a temperature of 4 °C. After incubation for 1 hour, the suspenson was centrifuged at 4000 × g and the pellet was resuspended in 25 ml PBS. After a second precipitation step, the antibody was resuspended in 2.5 ml PBS and de-salted using a de-salting column (PD-10 column, GE Healthcare) according to the manufacturers instructions. The purified antibody was dialyzed to PBS, sterile-filtered through a 0.2 µM filter and stored at 4 °C. For biotinylation, a 20-fold molar excess of EZ-Link NHS-PEG12-Biotin (Life Technologies) was added for 4 hours at room temperature followed by dialysis to PBS.

4.3.4 Genotyping of FcγRIIB$^{-/-}$ mice

The genotype of FcγRIIB$^{-/-}$ mice (kindly provided by Jeffrey V. Ravetch) was confirmed by flow cytometry analysis of blood collected from the animal's tail vain. To do so, red blood cells were lysed using RBC lysis buffer (Biolegend) and the cells were stained with anti-CD19-Pacific blue (clone 6D5, Biolegend) and in-house purified and biotinylated anti-FcγRIIB [348] (clone K9.361). Cells were incubated for 20 minutes at 4 °C and washed once with PBS. For detection of K9.361 binding, cells were stained with Streptavidin-FITC (Biolegend). After washing with PBS, cells were acquired using BD FACS Canto-II (see table 4.2 for optical configuration) and analyzed with FlowJo (Tree Star).
Heterozygous animals were obtained by crossing FcγRIIB$^{-/-}$ mice with B6 wildtype mice.

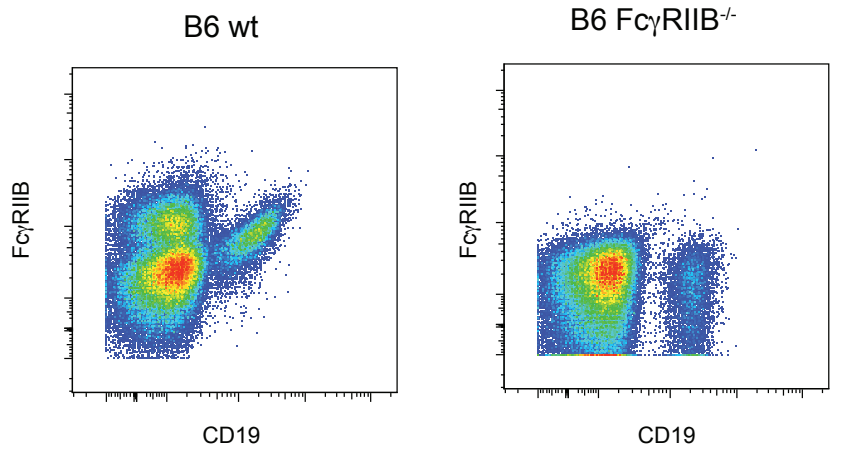

Figure 4.8 Exemplary flow cytometry analysis for FcγRIIB genotyping
Blood from B6 wt or FcgRIIB$^{-/-}$ mice was stained with anti-CD19 and anti-FcγRIIB and analyzed by flow cytometry.

4.3.5 EAE induction and monitoring of disease

EAE was induced induced C57BL/6 (B6) mice as previously described [349] with minor adaptations. MOG_{35-55} peptide (MEVGWYRSPFS-RVVHLYRNGK; GenScript) was dissolved in PBS to reach a final concentration of 5 mg/ml. 30 ml CFA (Adjuvant complete H37 Ra, Difco Laboratories, Detroit, USA) was supplemented with 100 mg dried inactivated *mycobacterium tuberculosis* (M. Tuberculosis Des. H37 Ra, Difco Laboratories, Detroit, USA). On the day of immunization, 20 µl (100 µg) peptide solution was supplemented with 80 µl PBS and emulsified in 100 µl supplemented CFA (values are given for one mouse; 20 % excess should be prepared) by vigorously mixing the solution via transfer in between two syringes connected to each other with a Luer-Lock connector for 15 minutes. 6 to 8 weeks old female B6 mice, 2D2 TCR transgenic mice or FcγRIIB$^{-/-}$ mice were used for immunization. Therefore, mice were anesthetized with isoflurane and 100 µl emulsion was injected into the left and right lateral abdomen using a 24 G x 1'' needle. In addition, mice received i.p. injection of 200 ng pertussis toxin (pertussis toxin in Glycerol, List Biological Laboratories) on the day of immunization and two days thereafter. Mice were monitored daily for general health and disease progression. The following scoring system was applied:

0 - no detectable signs of EAE; 0.5 - Distal limp tail; 1.0 - Complete limp tail; 1.5 - limp tail and hind limb weakness; 2.0 - unilateral partial hind limb paralysis; 2.5 - bilateral partial hind limb paralysis; 3.0 - complete bilateral hind limb paralysis; 3.5 - complete bilateral hind limb paralysis and partial forelimb paralysis; 4.0 - moribund; 5.0 – dead

Mice were euthanized by CO_2 inhalation if a disease score of 3 was maintained for more than 7 days, a disease score of 3.5 was maintained for more than 3 days or disease score of 4 was reached.

4.3.6 Passive induction of EAE by adoptive cell transfer

Donor mice (B6 or 2D2 TCR transgenic) were actively immunized as described above. On day 7 post immunization, spleen and draining lymph nodes were harvested and leukocytes purified (see below). Cells were restimulated *in vitro* by cultivation for 2 days at a density of 1 x 10^7 cells/ml at 37 °C and 5 % CO_2 in 12 cm cell-culture dishes (Greiner) in RPMI 1640 medium (10 ml per dish) supplemented with P/S, 10 ng/ml recombinant IL-23 (eBioscience) and 20 µg/ml MOG_{35-55}. Recipient mice were sublethally irradiated ad 550 rad one day before i.p. injection of 1 x 10^7 restimulated cells. Disease progression was monitored as described above.

4.3.7 Lymphocyte isolation from spleen and lymph nodes

Mice were euthanized by CO_2 inhalation. Spleen and inguinal lymph nodes were removed and mechanically disrupted using scissors. If myeloid cell isolation was aimed, disrupted tissues were incubated at 37 °C in 3 ml PBS containing 0.4 mg/ml Collagenase D (Roche) and 0.1 mg/ml DNase (Sigma) for 30 minutes. The reaction was stopped by adding EDTA to a final concentration of 10 mM. Thereafter, a syringe plunger was used to further disrupt the tissue by filtering through a 70 µm mesh. Cells were washed once with PBS. Red blood cells (RBC) were lysed using RBC lysis buffer (Biolegend) according to the manufacturers instructions. Casy counter (Innovatis) was used to determine cell numbers.

4.3.8 Flow cytometry analysis of murine splenocytes and LN cells

For the analysis of cell surface antigens, 2 x 10^7 cells were resuspended in 25 µl PBS and an equal volume of two-fold concentrated antibody solution was added. After incubation on ice for 30 minutes, cells were washed twice with 200 µl PBS before acquisition. For intracellular cytokine staining, 2 x 10^7 cells were incubated per well of a 96-well V bottom plate in 100 µl RPMI-1640 containing 10 % FCS, 50 ng/ml PMA, 500 ng/ml Ionomycin and 10 µg/ml Brefeldin A (Sigma) for 4 hours at 37 °C and 5 % CO_2 in a humidified incubator. For intracellular detection of cytokines and transcription factors, FoxP3 transcription factor staining buffer set (eBioscience) was used according to the manufacturers instructions. Fluorochrome labeled antibodies were purchased from Biologend (anti-CD8a-FITC or -BV785 (clone 53-6.7), anti-CD11b-APC-Cy7 (clone M1/70), anti-CD11c-PE-Cy7 (clone N418), anti-CD25-BV605 (clone PC61), anti-CD44-Pacific Blue (clone IM7), anti-CD80-PE (clone 16-10A1), anti-IL-17a-PE-Cy7 (clone TC11-18H10), anti-IFN-γ-FITC (clone XMG1.2), anti-Ly6C-PerCp-Cy5.5 (clone HK1.4), anti-Ly6G-APC (clone 1A8) and anti-MHC-II-Pacific Blue (I-A/I-E, clone M5/114.15.2)) and eBioscience (anti-CD19-Alexa-Fluor700 (clone eBio1D3 (1D3), anti-FoxP3-PerCp-Cy5.5

(clone FJK-16s) and anti-GM-CSF-PE (clone MP1-22E9)) and BD Pharmingen (anti-CD4-APC (clone RM4-5) and anti-CD62L-PE-CF594 (clone MEL-14)). Fixable L/D staining kits (aqua/amcyan and near-IR) were purchased from Invitrogen. Samples were acquired using BD LSR Fortessa (see table 4.2 for optical configuration).

5. References

1. Janeway, C.A., et al., *Immunobiology, The immune system in health and disease, 5th edition*. 5 ed. 2001: Garland Science.
2. Litman, G.W., M.K. Anderson, and J.P. Rast, *Evolution of antigen binding receptors.* Annu Rev Immunol, 1999. **17**: p. 109-47.
3. Abbas, A.K., A.H. Lichtman, and S. Pillai, *Cellular and molecular immunology, 6th edition*. 6 ed. 2007: Saunders Elsevier.
4. Matsushita, T., et al., *Regulatory B cells inhibit EAE initiation in mice while other B cells promote disease progression.* J Clin Invest, 2008. **118**(10): p. 3420-30.
5. Llewelyn, M.B., R.E. Hawkins, and S.J. Russell, *Discovery of antibodies.* BMJ, 1992. **305**(6864): p. 1269-72.
6. Turk, J.L., *Paul Ehrlich--the dawn of immunology.* J R Soc Med, 1994. **87**(6): p. 314-5.
7. Bosch, F. and L. Rosich, *The contributions of Paul Ehrlich to pharmacology: a tribute on the occasion of the centenary of his Nobel Prize.* Pharmacology, 2008. **82**(3): p. 171-9.
8. Winau, F., O. Westphal, and R. Winau, *Paul Ehrlich--in search of the magic bullet.* Microbes Infect, 2004. **6**(8): p. 786-9.
9. Van Epps, H.L., *How Heidelberger and Avery sweetened immunology.* J Exp Med, 2005. **202**(10): p. 1306.
10. Van Epps, H.L., *Michael Heidelberger and the demystification of antibodies.* J Exp Med, 2006. **203**(1): p. 5.
11. Kabat, E.A., *The Molecular Weight of Antibodies.* J Exp Med, 1939. **69**(1): p. 103-18.
12. Stokes, J., E.P. Maris, and S.S. Gellis, *Chemical, Clinical, and Immunological Studies on the Products of Human Plasma Fractionation. Xi. The Use of Concentrated Normal Human Serum Gamma Globulin (Human Immune Serum Globulin) in the Prophylaxis and Treatment of Measles.* J Clin Invest, 1944. **23**(4): p. 531-40.
13. Janeway, C.A., *Use of Concentrated Human Serum gamma-Globulin in the Prevention and Attenuation of Measles.* Bull N Y Acad Med, 1945. **21**(4): p. 202-22.
14. Fagraeus, A., *Plasma cellular reaction and its relation to the formation of antibodies in vitro.* Nature, 1947. **159**(4041): p. 499.
15. Porter, R.R., *The hydrolysis of rabbit y-globulin and antibodies with crystalline papain.* Biochem J, 1959. **73**: p. 119-26.
16. Edelman, G.M. and M.D. Poulik, *Studies on structural units of the gamma-globulins.* J Exp Med, 1961. **113**: p. 861-84.
17. Edelman, G.M., et al., *Structural differences among antibodies of different specificities.* Proc Natl Acad Sci U S A, 1961. **47**: p. 1751-8.
18. Ribatti, D., *Edelman's view on the discovery of antibodies.* Immunol Lett, 2015. **164**(2): p. 72-5.
19. Burnet, M., *The Clonal Selection Theory of Acquired Immunity*. 1959, Cambridge University Press: Cambridge, UK.
20. Burnet, M., *Auto-immune disease. I. Modern immunological concepts.* Br Med J, 1959. **2**(5153): p. 645-50.
21. Kohler, G. and C. Milstein, *Continuous cultures of fused cells secreting antibody of predefined specificity.* Nature, 1975. **256**(5517): p. 495-7.
22. Nadler, L.M., et al., *Serotherapy of a patient with a monoclonal antibody directed against a human lymphoma-associated antigen.* Cancer Res, 1980. **40**(9): p. 3147-54.

23. Sgro, C., *Side-effects of a monoclonal antibody, muromonab CD3/orthoclone OKT3: bibliographic review.* Toxicology, 1995. **105**(1): p. 23-9.
24. Abramowicz, D., A. Crusiaux, and M. Goldman, *Anaphylactic shock after retreatment with OKT3 monoclonal antibody.* N Engl J Med, 1992. **327**(10): p. 736.
25. Goldstein, G., et al., *OKT3 monoclonal antibody plasma levels during therapy and the subsequent development of host antibodies to OKT3.* Transplantation, 1986. **42**(5): p. 507-11.
26. Riechmann, L., et al., *Reshaping human antibodies for therapy.* Nature, 1988. **332**(6162): p. 323-7.
27. Osbourn, J., L. Jermutus, and A. Duncan, *Current methods for the generation of human antibodies for the treatment of autoimmune diseases.* Drug Discov Today, 2003. **8**(18): p. 845-51.
28. Strebhardt, K. and A. Ullrich, *Paul Ehrlich's magic bullet concept: 100 years of progress.* Nat Rev Cancer, 2008. **8**(6): p. 473-80.
29. Anderson, N.L. and N.G. Anderson, *The human plasma proteome: history, character, and diagnostic prospects.* Mol Cell Proteomics, 2002. **1**(11): p. 845-67.
30. Kaveri, S.V., G.J. Silverman, and J. Bayry, *Natural IgM in immune equilibrium and harnessing their therapeutic potential.* J Immunol, 2012. **188**(3): p. 939-45.
31. Vidarsson, G., G. Dekkers, and T. Rispens, *IgG subclasses and allotypes: from structure to effector functions.* Front Immunol, 2014. **5**: p. 520.
32. Williams, A.F. and A.N. Barclay, *The immunoglobulin superfamily--domains for cell surface recognition.* Annu Rev Immunol, 1988. **6**: p. 381-405.
33. Arnold, J.N., et al., *The impact of glycosylation on the biological function and structure of human immunoglobulins.* Annu Rev Immunol, 2007. **25**: p. 21-50.
34. Alberts, B., et al., *Molecular Biology of the Cell, Sixth Edition.* Molecular Biology of the Cell, Sixth Edition, 2015: p. 1-1342.
35. Dreyer, W.J. and J.C. Bennett, *The molecular basis of antibody formation: a paradox.* Proc Natl Acad Sci U S A, 1965. **54**(3): p. 864-9.
36. Brack, C., et al., *A complete immunoglobulin gene is created by somatic recombination.* Cell, 1978. **15**(1): p. 1-14.
37. Weigert, M., et al., *Rearrangement of genetic information may produce immunoglobulin diversity.* Nature, 1978. **276**(5690): p. 785-90.
38. Lam, K.P., R. Kuhn, and K. Rajewsky, *In vivo ablation of surface immunoglobulin on mature B cells by inducible gene targeting results in rapid cell death.* Cell, 1997. **90**(6): p. 1073-83.
39. Kraus, M., et al., *Survival of resting mature B lymphocytes depends on BCR signaling via the Igalpha/beta heterodimer.* Cell, 2004. **117**(6): p. 787-800.
40. Su, T.T. and D.J. Rawlings, *Transitional B lymphocyte subsets operate as distinct checkpoints in murine splenic B cell development.* J Immunol, 2002. **168**(5): p. 2101-10.
41. Allman, D.M., S.E. Ferguson, and M.P. Cancro, *Peripheral B cell maturation. I. Immature peripheral B cells in adults are heat-stable antigenhi and exhibit unique signaling characteristics.* J Immunol, 1992. **149**(8): p. 2533-40.
42. Allman, D.M., et al., *Peripheral B cell maturation. II. Heat-stable antigen(hi) splenic B cells are an immature developmental intermediate in the production of long-lived marrow-derived B cells.* J Immunol, 1993. **151**(9): p. 4431-44.
43. Berkowska, M.A., et al., *Checkpoints of B cell differentiation: visualizing Ig-centric processes.* Ann N Y Acad Sci, 2011. **1246**: p. 11-25.
44. McHeyzer-Williams, M., et al., *Molecular programming of B cell memory.* Nat Rev Immunol, 2012. **12**(1): p. 24-34.

45. Boes, M., *Role of natural and immune IgM antibodies in immune responses.* Mol Immunol, 2000. **37**(18): p. 1141-9.
46. Chen, Y., et al., *IgM antibodies to apoptosis-associated determinants recruit C1q and enhance dendritic cell phagocytosis of apoptotic cells.* J Immunol, 2009. **182**(10): p. 6031-43.
47. Kerr, M.A., *The structure and function of human IgA.* Biochem J, 1990. **271**(2): p. 285-96.
48. Mostov, K.E. and D.L. Deitcher, *Polymeric immunoglobulin receptor expressed in MDCK cells transcytoses IgA.* Cell, 1986. **46**(4): p. 613-21.
49. Natvig, I.B., et al., *Mechanism for enhanced external transfer of dimeric IgA over pentameric IgM: studies of diffusion, binding to the human polymeric Ig receptor, and epithelial transcytosis.* J Immunol, 1997. **159**(9): p. 4330-40.
50. Chintalacharuvu, K.R. and S.L. Morrison, *Production and characterization of recombinant IgA.* Immunotechnology, 1999. **4**(3-4): p. 165-74.
51. Roos, A., et al., *Human IgA activates the complement system via the mannan-binding lectin pathway.* J Immunol, 2001. **167**(5): p. 2861-8.
52. Macpherson, A.J. and T. Uhr, *Induction of protective IgA by intestinal dendritic cells carrying commensal bacteria.* Science, 2004. **303**(5664): p. 1662-5.
53. Cerutti, A., *The regulation of IgA class switching.* Nat Rev Immunol, 2008. **8**(6): p. 421-34.
54. Kett, K., et al., *Different subclass distribution of IgA-producing cells in human lymphoid organs and various secretory tissues.* J Immunol, 1986. **136**(10): p. 3631-5.
55. Ogra, P.L., G.A. Losonsky, and M. Fishaut, *Colostrum-derived immunity and maternal-neonatal interaction.* Ann N Y Acad Sci, 1983. **409**: p. 82-95.
56. Wu, L.C. and A.A. Zarrin, *The production and regulation of IgE by the immune system.* Nat Rev Immunol, 2014. **14**(4): p. 247-59.
57. Kraft, S. and J.P. Kinet, *New developments in FcepsilonRI regulation, function and inhibition.* Nat Rev Immunol, 2007. **7**(5): p. 365-78.
58. Wedemeyer, J., M. Tsai, and S.J. Galli, *Roles of mast cells and basophils in innate and acquired immunity.* Curr Opin Immunol, 2000. **12**(6): p. 624-31.
59. Chen, K., et al., *Immunoglobulin D enhances immune surveillance by activating antimicrobial, proinflammatory and B cell-stimulating programs in basophils.* Nat Immunol, 2009. **10**(8): p. 889-98.
60. Jefferis, R. and D.S. Kumararatne, *Selective IgG subclass deficiency: quantification and clinical relevance.* Clin Exp Immunol, 1990. **81**(3): p. 357-67.
61. Wiersma, E.J. and M.J. Shulman, *Assembly of IgM. Role of disulfide bonding and noncovalent interactions.* J Immunol, 1995. **154**(10): p. 5265-72.
62. Davis, A.C., et al., *Intermolecular disulfide bonding in IgM: effects of replacing cysteine residues in the mu heavy chain.* EMBO J, 1989. **8**(9): p. 2519-26.
63. Helm, B.A., et al., *The nature and importance of the inter-epsilon chain disulfide bonds in human IgE.* Eur J Immunol, 1991. **21**(6): p. 1543-8.
64. Woof, J.M. and M.W. Russell, *Structure and function relationships in IgA.* Mucosal Immunol, 2011. **4**(6): p. 590-7.
65. Shakib, F. and D.R. Stanworth, *Human IgG subclasses in health and disease. (A review). Part I.* Ric Clin Lab, 1980. **10**(3): p. 463-79.
66. Jackson, K.J., Y. Wang, and A.M. Collins, *Human immunoglobulin classes and subclasses show variability in VDJ gene mutation levels.* Immunol Cell Biol, 2014. **92**(8): p. 729-33.
67. Roux, K.H., L. Strelets, and T.E. Michaelsen, *Flexibility of human IgG subclasses.* J

Immunol, 1997. **159**(7): p. 3372-82.
68. Wong, C.H., *Protein glycosylation: new challenges and opportunities.* J Org Chem, 2005. **70**(11): p. 4219-25.
69. Mimura, Y., et al., *Contrasting glycosylation profiles between Fab and Fc of a human IgG protein studied by electrospray ionization mass spectrometry.* J Immunol Methods, 2007. **326**(1-2): p. 116-26.
70. Anumula, K.R., *Quantitative glycan profiling of normal human plasma derived immunoglobulin and its fragments Fab and Fc.* J Immunol Methods, 2012. **382**(1-2): p. 167-76.
71. Holland, M., et al., *Differential glycosylation of polyclonal IgG, IgG-Fc and IgG-Fab isolated from the sera of patients with ANCA-associated systemic vasculitis.* Biochim Biophys Acta, 2006. **1760**(4): p. 669-77.
72. Sabouri, Z., et al., *Redemption of autoantibodies on anergic B cells by variable-region glycosylation and mutation away from self-reactivity.* Proc Natl Acad Sci U S A, 2014. **111**(25): p. E2567-75.
73. Valliere-Douglass, J.F., et al., *Asparagine-linked oligosaccharides present on a non-consensus amino acid sequence in the CH1 domain of human antibodies.* J Biol Chem, 2009. **284**(47): p. 32493-506.
74. Schwarz, F. and M. Aebi, *Mechanisms and principles of N-linked protein glycosylation.* Curr Opin Struct Biol, 2011. **21**(5): p. 576-82.
75. Lund, J., et al., *Multiple interactions of IgG with its core oligosaccharide can modulate recognition by complement and human Fc gamma receptor I and influence the synthesis of its oligosaccharide chains.* J Immunol, 1996. **157**(11): p. 4963-9.
76. Rich, J.R. and S.G. Withers, *Emerging methods for the production of homogeneous human glycoproteins.* Nat Chem Biol, 2009. **5**(4): p. 206-15.
77. Wormald, M.R., et al., *Variations in oligosaccharide-protein interactions in immunoglobulin G determine the site-specific glycosylation profiles and modulate the dynamic motion of the Fc oligosaccharides.* Biochemistry, 1997. **36**(6): p. 1370-80.
78. Parekh, R.B., et al., *Association of rheumatoid arthritis and primary osteoarthritis with changes in the glycosylation pattern of total serum IgG.* Nature, 1985. **316**(6027): p. 452-7.
79. Parekh, R., et al., *Age-related galactosylation of the N-linked oligosaccharides of human serum IgG.* J Exp Med, 1988. **167**(5): p. 1731-6.
80. Mizuochi, T., et al., *Structural and numerical variations of the carbohydrate moiety of immunoglobulin G.* J Immunol, 1982. **129**(5): p. 2016-20.
81. Shikata, K., et al., *Structural changes in the oligosaccharide moiety of human IgG with aging.* Glycoconj J, 1998. **15**(7): p. 683-9.
82. Yamada, E., et al., *Structural changes of immunoglobulin G oligosaccharides with age in healthy human serum.* Glycoconj J, 1997. **14**(3): p. 401-5.
83. Gaboriaud, C., et al., *The crystal structure of the globular head of complement protein C1q provides a basis for its versatile recognition properties.* J Biol Chem, 2003. **278**(47): p. 46974-82.
84. Mimura, Y., et al., *Role of oligosaccharide residues of IgG1-Fc in Fc gamma RIIb binding.* J Biol Chem, 2001. **276**(49): p. 45539-47.
85. Krapp, S., et al., *Structural analysis of human IgG-Fc glycoforms reveals a correlation between glycosylation and structural integrity.* J Mol Biol, 2003. **325**(5): p. 979-89.
86. Mimura, Y., et al., *The influence of glycosylation on the thermal stability and*

effector function expression of human IgG1-Fc: properties of a series of truncated glycoforms. Mol Immunol, 2000. **37**(12-13): p. 697-706.
87. Barb, A.W., E.K. Brady, and J.H. Prestegard, *Branch-specific sialylation of IgG-Fc glycans by ST6Gal-I.* Biochemistry, 2009. **48**(41): p. 9705-7.
88. Lux, A. and F. Nimmerjahn, *Impact of differential glycosylation on IgG activity.* Adv Exp Med Biol, 2011. **780**: p. 113-24.
89. Duncan, A.R., et al., *Localization of the binding site for the human high-affinity Fc receptor on IgG.* Nature, 1988. **332**(6164): p. 563-4.
90. Wines, B.D., et al., *The IgG Fc contains distinct Fc receptor (FcR) binding sites: the leukocyte receptors Fc gamma RI and Fc gamma RIIa bind to a region in the Fc distinct from that recognized by neonatal FcR and protein A.* J Immunol, 2000. **164**(10): p. 5313-8.
91. Sondermann, P., et al., *The 3.2-A crystal structure of the human IgG1 Fc fragment-Fc gammaRIII complex.* Nature, 2000. **406**(6793): p. 267-73.
92. Shields, R.L., et al., *Lack of fucose on human IgG1 N-linked oligosaccharide improves binding to human Fcgamma RIII and antibody-dependent cellular toxicity.* J Biol Chem, 2002. **277**(30): p. 26733-40.
93. Shields, R.L., et al., *High resolution mapping of the binding site on human IgG1 for Fc gamma RI, Fc gamma RII, Fc gamma RIII, and FcRn and design of IgG1 variants with improved binding to the Fc gamma R.* J Biol Chem, 2001. **276**(9): p. 6591-604.
94. Boruchov, A.M., et al., *Activating and inhibitory IgG Fc receptors on human DCs mediate opposing functions.* J Clin Invest, 2005. **115**(10): p. 2914-23.
95. DiLillo, D.J. and J.V. Ravetch, *Differential Fc-Receptor Engagement Drives an Anti-tumor Vaccinal Effect.* Cell, 2015. **161**(5): p. 1035-45.
96. Biburger, M., A. Lux, and F. Nimmerjahn, *How immunoglobulin G antibodies kill target cells: revisiting an old paradigm.* Adv Immunol, 2014. **124**: p. 67-94.
97. Yuasa, T., et al., *Deletion of fcgamma receptor IIB renders H-2(b) mice susceptible to collagen-induced arthritis.* J Exp Med, 1999. **189**(1): p. 187-94.
98. Daeron, M., et al., *The same tyrosine-based inhibition motif, in the intracytoplasmic domain of Fc gamma RIIB, regulates negatively BCR-, TCR-, and FcR-dependent cell activation.* Immunity, 1995. **3**(5): p. 635-46.
99. Xiang, Z., et al., *FcgammaRIIb controls bone marrow plasma cell persistence and apoptosis.* Nat Immunol, 2007. **8**(4): p. 419-29.
100. Fukuyama, H., F. Nimmerjahn, and J.V. Ravetch, *The inhibitory Fcgamma receptor modulates autoimmunity by limiting the accumulation of immunoglobulin G+ anti-DNA plasma cells.* Nat Immunol, 2005. **6**(1): p. 99-106.
101. Thiery, J., et al., *Perforin pores in the endosomal membrane trigger the release of endocytosed granzyme B into the cytosol of target cells.* Nat Immunol, 2011. **12**(8): p. 770-7.
102. van der Heijden, J., et al., *Phenotypic variation in IgG receptors by nonclassical FCGR2C alleles.* J Immunol, 2012. **188**(3): p. 1318-24.
103. Ober, R.J., et al., *Visualizing the site and dynamics of IgG salvage by the MHC class I-related receptor, FcRn.* J Immunol, 2004. **172**(4): p. 2021-9.
104. Chaudhury, C., et al., *The major histocompatibility complex-related Fc receptor for IgG (FcRn) binds albumin and prolongs its lifespan.* J Exp Med, 2003. **197**(3): p. 315-22.
105. Dickinson, B.L., et al., *Bidirectional FcRn-dependent IgG transport in a polarized human intestinal epithelial cell line.* J Clin Invest, 1999. **104**(7): p. 903-11.
106. Gillis, C., et al., *Contribution of Human FcgammaRs to Disease with Evidence from Human Polymorphisms and Transgenic Animal Studies.* Front Immunol, 2014. **5**: p.

254.
107. Smith, K.G. and M.R. Clatworthy, *FcgammaRIIB in autoimmunity and infection: evolutionary and therapeutic implications.* Nat Rev Immunol, 2010. **10**(5): p. 328-43.
108. Ricklin, D., et al., *Complement: a key system for immune surveillance and homeostasis.* Nat Immunol, 2010. **11**(9): p. 785-97.
109. Dempsey, P.W., et al., *C3d of complement as a molecular adjuvant: bridging innate and acquired immunity.* Science, 1996. **271**(5247): p. 348-50.
110. Klos, A., et al., *The role of the anaphylatoxins in health and disease.* Mol Immunol, 2009. **46**(14): p. 2753-66.
111. Chen, N.J., et al., *C5L2 is critical for the biological activities of the anaphylatoxins C5a and C3a.* Nature, 2007. **446**(7132): p. 203-7.
112. Botto, M., et al., *Complement in human diseases: Lessons from complement deficiencies.* Mol Immunol, 2009. **46**(14): p. 2774-83.
113. Taylor, P.R., et al., *A hierarchical role for classical pathway complement proteins in the clearance of apoptotic cells in vivo.* J Exp Med, 2000. **192**(3): p. 359-66.
114. Duncan, A.R. and G. Winter, *The binding site for C1q on IgG.* Nature, 1988. **332**(6166): p. 738-40.
115. Malhotra, R., et al., *Glycosylation changes of IgG associated with rheumatoid arthritis can activate complement via the mannose-binding protein.* Nat Med, 1995. **1**(3): p. 237-43.
116. Nimmerjahn, F., R.M. Anthony, and J.V. Ravetch, *Agalactosylated IgG antibodies depend on cellular Fc receptors for in vivo activity.* Proc Natl Acad Sci U S A, 2007. **104**(20): p. 8433-7.
117. Pangburn, M.K., R.D. Schreiber, and H.J. Muller-Eberhard, *Formation of the initial C3 convertase of the alternative complement pathway. Acquisition of C3b-like activities by spontaneous hydrolysis of the putative thioester in native C3.* J Exp Med, 1981. **154**(3): p. 856-67.
118. Shohet, J.M., P. Pemberton, and M.C. Carroll, *Identification of a major binding site for complement C3 on the IgG1 heavy chain.* J Biol Chem, 1993. **268**(8): p. 5866-71.
119. Lutz, H.U. and E. Jelezarova, *Complement amplification revisited.* Mol Immunol, 2006. **43**(1-2): p. 2-12.
120. Jung, S.T., et al., *Aglycosylated IgG variants expressed in bacteria that selectively bind FcgammaRI potentiate tumor cell killing by monocyte-dendritic cells.* Proc Natl Acad Sci U S A, 2010. **107**(2): p. 604-9.
121. Boyd, P.N., A.C. Lines, and A.K. Patel, *The effect of the removal of sialic acid, galactose and total carbohydrate on the functional activity of Campath-1H.* Mol Immunol, 1995. **32**(17-18): p. 1311-8.
122. Wright, A. and S.L. Morrison, *Effect of altered CH2-associated carbohydrate structure on the functional properties and in vivo fate of chimeric mouse-human immunoglobulin G1.* J Exp Med, 1994. **180**(3): p. 1087-96.
123. Simmons, L.C., et al., *Expression of full-length immunoglobulins in Escherichia coli: rapid and efficient production of aglycosylated antibodies.* J Immunol Methods, 2002. **263**(1-2): p. 133-47.
124. Tao, M.H. and S.L. Morrison, *Studies of aglycosylated chimeric mouse-human IgG. Role of carbohydrate in the structure and effector functions mediated by the human IgG constant region.* J Immunol, 1989. **143**(8): p. 2595-601.
125. Hristodorov, D., R. Fischer, and L. Linden, *With or without sugar? (A)glycosylation of therapeutic antibodies.* Mol Biotechnol, 2013. **54**(3): p. 1056-68.
126. Beck, A. and J.M. Reichert, *Marketing approval of mogamulizumab: a triumph for*

glyco-engineering. MAbs, 2012. **4**(4): p. 419-25.
127. Parekh, R., et al., *A comparative analysis of disease-associated changes in the galactosylation of serum IgG.* J Autoimmun, 1989. **2**(2): p. 101-14.
128. Bond, A., et al., *A detailed lectin analysis of IgG glycosylation, demonstrating disease specific changes in terminal galactose and N-acetylglucosamine.* J Autoimmun, 1997. **10**(1): p. 77-85.
129. Moore, J.S., et al., *Increased levels of galactose-deficient IgG in sera of HIV-1-infected individuals.* AIDS, 2005. **19**(4): p. 381-9.
130. Ackerman, M.E., et al., *Natural variation in Fc glycosylation of HIV-specific antibodies impacts antiviral activity.* J Clin Invest, 2013. **123**(5): p. 2183-92.
131. Mehta, A.S., et al., *Increased levels of galactose-deficient anti-Gal immunoglobulin G in the sera of hepatitis C virus-infected individuals with fibrosis and cirrhosis.* J Virol, 2008. **82**(3): p. 1259-70.
132. Karsten, C.M., et al., *Anti-inflammatory activity of IgG1 mediated by Fc galactosylation and association of FcgammaRIIB and dectin-1.* Nat Med, 2012. **18**(9): p. 1401-6.
133. Kaneko, Y., F. Nimmerjahn, and J.V. Ravetch, *Anti-inflammatory activity of immunoglobulin G resulting from Fc sialylation.* Science, 2006. **313**(5787): p. 670-3.
134. Scallon, B.J., et al., *Higher levels of sialylated Fc glycans in immunoglobulin G molecules can adversely impact functionality.* Mol Immunol, 2007. **44**(7): p. 1524-34.
135. Geijtenbeek, T.B., A. Engering, and Y. Van Kooyk, *DC-SIGN, a C-type lectin on dendritic cells that unveils many aspects of dendritic cell biology.* J Leukoc Biol, 2002. **71**(6): p. 921-31.
136. Anthony, R.M., et al., *Identification of a receptor required for the anti-inflammatory activity of IVIG.* Proc Natl Acad Sci U S A, 2008. **105**(50): p. 19571-8.
137. Sondermann, P., et al., *General mechanism for modulating immunoglobulin effector function.* Proc Natl Acad Sci U S A, 2013. **110**(24): p. 9868-72.
138. Yu, X., et al., *Dissecting the molecular mechanism of IVIg therapy: the interaction between serum IgG and DC-SIGN is independent of antibody glycoform or Fc domain.* J Mol Biol, 2013. **425**(8): p. 1253-8.
139. Schwab, I., et al., *Broad requirement for terminal sialic acid residues and FcgammaRIIB for the preventive and therapeutic activity of intravenous immunoglobulins in vivo.* Eur J Immunol, 2014. **44**(5): p. 1444-53.
140. Imbach, P., et al., *High-dose intravenous gammaglobulin therapy of refractory, in particular idiopathic thrombocytopenia in childhood.* Helv Paediatr Acta, 1981. **36**(1): p. 81-6.
141. Imbach, P., et al., *High-dose intravenous gammaglobulin for idiopathic thrombocytopenic purpura in childhood.* Lancet, 1981. **1**(8232): p. 1228-31.
142. Gelfand, E.W., *Intravenous immune globulin in autoimmune and inflammatory diseases.* N Engl J Med, 2012. **367**(21): p. 2015-25.
143. Prins, C., E.W. Gelfand, and L.E. French, *Intravenous immunoglobulin: properties, mode of action and practical use in dermatology.* Acta Derm Venereol, 2007. **87**(3): p. 206-18.
144. AG, C.B., *Immune Globulin Intravenous (Human), 10 % Liquid, Privigen*, in *Clean Package Insert (218a38)_Version 33.0*. 2013, CSL Behring AG.
145. Gelfand, E.W., *Differences between IGIV products: impact on clinical outcome.* Int Immunopharmacol, 2006. **6**(4): p. 592-9.
146. Lunemann, J.D., F. Nimmerjahn, and M.C. Dalakas, *Intravenous immunoglobulin in*

neurology--mode of action and clinical efficacy. Nat Rev Neurol, 2015. **11**(2): p. 80-9.
147. Vassilev, T.L., et al., *Inhibition of cell adhesion by antibodies to Arg-Gly-Asp (RGD) in normal immunoglobulin for therapeutic use (intravenous immunoglobulin, IVIg).* Blood, 1999. **93**(11): p. 3624-31.
148. Svenson, M., et al., *Antibody to granulocyte-macrophage colony-stimulating factor is a dominant anti-cytokine activity in human IgG preparations.* Blood, 1998. **91**(6): p. 2054-61.
149. Ross, C., et al., *High avidity IFN-neutralizing antibodies in pharmaceutically prepared human IgG.* J Clin Invest, 1995. **95**(5): p. 1974-8.
150. Le Pottier, L., et al., *Intravenous immunoglobulin and cytokines: focus on tumor necrosis factor family members BAFF and APRIL.* Ann N Y Acad Sci, 2007. **1110**: p. 426-32.
151. Rossi, F. and M.D. Kazatchkine, *Antiidiotypes against autoantibodies in pooled normal human polyspecific Ig.* J Immunol, 1989. **143**(12): p. 4104-9.
152. Shoenfeld, Y., et al., *Efficacy of IVIG affinity-purified anti-double-stranded DNA anti-idiotypic antibodies in the treatment of an experimental murine model of systemic lupus erythematosus.* Int Immunol, 2002. **14**(11): p. 1303-11.
153. von Gunten, S., et al., *Intravenous immunoglobulin contains a broad repertoire of anticarbohydrate antibodies that is not restricted to the IgG2 subclass.* J Allergy Clin Immunol, 2009. **123**(6): p. 1268-76 e15.
154. Basta, M., et al., *F(ab)'2-mediated neutralization of C3a and C5a anaphylatoxins: a novel effector function of immunoglobulins.* Nat Med, 2003. **9**(4): p. 431-8.
155. Debre, M., et al., *Infusion of Fc gamma fragments for treatment of children with acute immune thrombocytopenic purpura.* Lancet, 1993. **342**(8877): p. 945-9.
156. Nagelkerke, S.Q., et al., *Inhibition of FcgammaR-mediated phagocytosis by IVIg is independent of IgG-Fc sialylation and FcgammaRIIb in human macrophages.* Blood, 2014. **124**(25): p. 3709-18.
157. Tackenberg, B., et al., *Impaired inhibitory Fcgamma receptor IIB expression on B cells in chronic inflammatory demyelinating polyneuropathy.* Proc Natl Acad Sci U S A, 2009. **106**(12): p. 4788-92.
158. Samuelsson, A., T.L. Towers, and J.V. Ravetch, *Anti-inflammatory activity of IVIG mediated through the inhibitory Fc receptor.* Science, 2001. **291**(5503): p. 484-6.
159. Hansen, R.J. and J.P. Balthasar, *Intravenous immunoglobulin mediates an increase in anti-platelet antibody clearance via the FcRn receptor.* Thromb Haemost, 2002. **88**(6): p. 898-9.
160. Kondo, N., et al., *Intravenous immunoglobulins suppress immunoglobulin productions by suppressing Ca(2+)-dependent signal transduction through Fc gamma receptors in B lymphocytes.* Scand J Immunol, 1994. **40**(1): p. 37-42.
161. Anthony, R.M., et al., *Intravenous gammaglobulin suppresses inflammation through a novel T(H)2 pathway.* Nature, 2011. **475**(7354): p. 110-3.
162. Mollnes, T.E., et al., *Inhibition of complement-mediated red cell lysis by immunoglobulins is dependent on the IG isotype and its C1 binding properties.* Scand J Immunol, 1995. **41**(5): p. 449-56.
163. Bayry, J., et al., *Inhibition of maturation and function of dendritic cells by intravenous immunoglobulin.* Blood, 2003. **101**(2): p. 758-65.
164. De Groot, A.S., et al., *Activation of natural regulatory T cells by IgG Fc-derived peptide "Tregitopes".* Blood, 2008. **112**(8): p. 3303-11.
165. Anthony, R.M., et al., *Recapitulation of IVIG anti-inflammatory activity with a recombinant IgG Fc.* Science, 2008. **320**(5874): p. 373-6.

166. Othy, S., et al., *Sialylation may be dispensable for reciprocal modulation of helper T cells by intravenous immunoglobulin.* Eur J Immunol, 2014. **44**(7): p. 2059-63.
167. Campbell, I.K., et al., *Therapeutic effect of IVIG on inflammatory arthritis in mice is dependent on the Fc portion and independent of sialylation or basophils.* J Immunol, 2014. **192**(11): p. 5031-8.
168. von Gunten, S., et al., *Immunologic and functional evidence for anti-Siglec-9 autoantibodies in intravenous immunoglobulin preparations.* Blood, 2006. **108**(13): p. 4255-9.
169. Vassilev, T., et al., *Antibodies to the CD5 molecule in normal human immunoglobulins for therapeutic use (intravenous immunoglobulins, IVIg).* Clin Exp Immunol, 1993. **92**(3): p. 369-72.
170. Viard, I., et al., *Inhibition of toxic epidermal necrolysis by blockade of CD95 with human intravenous immunoglobulin.* Science, 1998. **282**(5388): p. 490-3.
171. Modiano, J.F., et al., *Posttranscriptional regulation of T-cell IL-2 production by human pooled immunoglobin.* Clin Immunol Immunopathol, 1997. **83**(1): p. 77-85.
172. Ritter, C., et al., *IVIG regulates BAFF expression in patients with chronic inflammatory demyelinating polyneuropathy (CIDP).* J Neuroimmunol, 2014. **274**(1-2): p. 225-9.
173. Takei, S., Y.K. Arora, and S.M. Walker, *Intravenous immunoglobulin contains specific antibodies inhibitory to activation of T cells by staphylococcal toxin superantigens [see comment].* J Clin Invest, 1993. **91**(2): p. 602-7.
174. Bussel, J.B., et al., *Intravenous anti-D treatment of immune thrombocytopenic purpura: analysis of efficacy, toxicity, and mechanism of effect.* Blood, 1991. **77**(9): p. 1884-93.
175. Teeling, J.L., et al., *Therapeutic efficacy of intravenous immunoglobulin preparations depends on the immunoglobulin G dimers: studies in experimental immune thrombocytopenia.* Blood, 2001. **98**(4): p. 1095-9.
176. Kaneko, Y., et al., *Pathology and protection in nephrotoxic nephritis is determined by selective engagement of specific Fc receptors.* J Exp Med, 2006. **203**(3): p. 789-97.
177. Basta, M., et al., *High-dose intravenous immunoglobulin modifies complement-mediated in vivo clearance.* Blood, 1989. **74**(1): p. 326-33.
178. Basta, M. and M.C. Dalakas, *High-dose intravenous immunoglobulin exerts its beneficial effect in patients with dermatomyositis by blocking endomysial deposition of activated complement fragments.* J Clin Invest, 1994. **94**(5): p. 1729-35.
179. Spahn, J.D., et al., *Mechanisms of glucocorticoid reduction in asthmatic subjects treated with intravenous immunoglobulin.* J Allergy Clin Immunol, 1999. **103**(3 Pt 1): p. 421-6.
180. Laughlin, R.S., et al., *Incidence and prevalence of CIDP and the association of diabetes mellitus.* Neurology, 2009. **73**(1): p. 39-45.
181. Dalakas, M.C. and Medscape, *Advances in the diagnosis, pathogenesis and treatment of CIDP.* Nat Rev Neurol, 2011. **7**(9): p. 507-17.
182. Hattori, N., et al., *Age of onset influences clinical features of chronic inflammatory demyelinating polyneuropathy.* J Neurol Sci, 2001. **184**(1): p. 57-63.
183. Hughes, R.A., et al., *Pathogenesis of chronic inflammatory demyelinating polyradiculoneuropathy.* J Peripher Nerv Syst, 2006. **11**(1): p. 30-46.
184. Tackenberg, B., et al., *Classifications and treatment responses in chronic immune-mediated demyelinating polyneuropathy.* Neurology, 2007. **68**(19): p. 1622-9.
185. Rotta, F.T., et al., *The spectrum of chronic inflammatory demyelinating*

polyneuropathy. J Neurol Sci, 2000. **173**(2): p. 129-39.
186. Dyck, P.J., et al., *Chronic inflammatory polyradiculoneuropathy.* Mayo Clin Proc, 1975. **50**(11): p. 621-37.
187. McCombe, P.A., J.D. Pollard, and J.G. McLeod, *Chronic inflammatory demyelinating polyradiculoneuropathy. A clinical and electrophysiological study of 92 cases.* Brain, 1987. **110 (Pt 6)**: p. 1617-30.
188. Magy, L. and J.M. Vallat, *Evidence-based treatment of chronic immune-mediated neuropathies.* Expert Opin Pharmacother, 2009. **10**(11): p. 1741-54.
189. Dyck, P.J., et al., *Prednisone improves chronic inflammatory demyelinating polyradiculoneuropathy more than no treatment.* Ann Neurol, 1982. **11**(2): p. 136-41.
190. Vermeulen, M., et al., *Intravenous immunoglobulin treatment in patients with chronic inflammatory demyelinating polyneuropathy: a double blind, placebo controlled study.* J Neurol Neurosurg Psychiatry, 1993. **56**(1): p. 36-9.
191. Hughes, R., et al., *Randomized controlled trial of intravenous immunoglobulin versus oral prednisolone in chronic inflammatory demyelinating polyradiculoneuropathy.* Ann Neurol, 2001. **50**(2): p. 195-201.
192. Hughes, R.A., et al., *Intravenous immune globulin (10% caprylate-chromatography purified) for the treatment of chronic inflammatory demyelinating polyradiculoneuropathy (ICE study): a randomised placebo-controlled trial.* Lancet Neurol, 2008. **7**(2): p. 136-44.
193. Dyck, P.J., et al., *Plasma exchange in chronic inflammatory demyelinating polyradiculoneuropathy.* N Engl J Med, 1986. **314**(8): p. 461-5.
194. Dyck, P.J., et al., *A plasma exchange versus immune globulin infusion trial in chronic inflammatory demyelinating polyradiculoneuropathy.* Ann Neurol, 1994. **36**(6): p. 838-45.
195. Hahn, A.F., et al., *Plasma-exchange therapy in chronic inflammatory demyelinating polyneuropathy. A double-blind, sham-controlled, cross-over study.* Brain, 1996. **119 (Pt 4)**: p. 1055-66.
196. Vallat, J.M., C. Sommer, and L. Magy, *Chronic inflammatory demyelinating polyradiculoneuropathy: diagnostic and therapeutic challenges for a treatable condition.* Lancet Neurol, 2010. **9**(4): p. 402-12.
197. Simmons, Z., J.J. Wald, and J.W. Albers, *Chronic inflammatory demyelinating polyradiculoneuropathy in children: II. Long-term follow-up, with comparison to adults.* Muscle Nerve, 1997. **20**(12): p. 1569-75.
198. Mygland, A., P. Monstad, and C. Vedeler, *Onset and course of chronic inflammatory demyelinating polyneuropathy.* Muscle Nerve, 2005. **31**(5): p. 589-93.
199. Mahad, D.J., S.J. Howell, and M.N. Woodroofe, *Expression of chemokines in cerebrospinal fluid and serum of patients with chronic inflammatory demyelinating polyneuropathy.* J Neurol Neurosurg Psychiatry, 2002. **73**(3): p. 320-3.
200. Misawa, S., et al., *Serum levels of tumor necrosis factor-alpha in chronic inflammatory demyelinating polyneuropathy.* Neurology, 2001. **56**(5): p. 666-9.
201. Kieseier, B.C., et al., *Chemokines and chemokine receptors in inflammatory demyelinating neuropathies: a central role for IP-10.* Brain, 2002. **125**(Pt 4): p. 823-34.
202. Rentzos, M., et al., *Proinflammatory cytokines in serum and cerebrospinal fluid of CIDP patients.* Neurol Res, 2012. **34**(9): p. 842-6.
203. Dalakas, M.C. and W.K. Engel, *Immunoglobulin and complement deposits in nerves of patients with chronic relapsing polyneuropathy.* Arch Neurol, 1980. **37**(10): p. 637-40.

204. Yan, W.X., et al., *Passive transfer of demyelination by serum or IgG from chronic inflammatory demyelinating polyneuropathy patients.* Ann Neurol, 2000. **47**(6): p. 765-75.
205. Diamond, B., et al., *Losing your nerves? Maybe it's the antibodies.* Nat Rev Immunol, 2009. **9**(6): p. 449-56.
206. Querol, L., et al., *Neurofascin IgG4 antibodies in CIDP associate with disabling tremor and poor response to IVIg.* Neurology, 2014. **82**(10): p. 879-86.
207. Querol, L., et al., *Antibodies to contactin-1 in chronic inflammatory demyelinating polyneuropathy.* Ann Neurol, 2013. **73**(3): p. 370-80.
208. McCombe, P.A., J.D. Pollard, and J.G. McLeod, *Absence of antimyelin antibodies and serum demyelinating factors in most patients with chronic inflammatory demyelinating polyradiculoneuropathy.* Clin Exp Neurol, 1988. **25**: p. 53-60.
209. Connolly, A.M., et al., *High-titer selective serum anti-beta-tubulin antibodies in chronic inflammatory demyelinating polyneuropathy.* Neurology, 1993. **43**(3 Pt 1): p. 557-62.
210. Connolly, A.M., et al., *Serum IgM monoclonal autoantibody binding to the 301 to 314 amino acid epitope of beta-tubulin: clinical association with slowly progressive demyelinating polyneuropathy.* Neurology, 1997. **48**(1): p. 243-8.
211. Smith, K.A., *Louis pasteur, the father of immunology?* Front Immunol, 2012. **3**: p. 68.
212. Baxter, A.G., *The origin and application of experimental autoimmune encephalomyelitis.* Nat Rev Immunol, 2007. **7**(11): p. 904-12.
213. Stuart, G. and K.S. Krikorian, *A fatal neuro paralytic accident of antirabies treatment.* Lancet, 1930. **1**: p. 1123-1125.
214. Stuart, G. and K.S. Krikorian, *Neuroparalytic Accidents Complicating Antirabic Treatment.* Br Med J, 1933. **1**(3768): p. 501-4.
215. Toro, G., I. Vergara, and G. Roman, *Neuroparalytic accidents of antirabies vaccination with suckling mouse brain vaccine. Clinical and pathologic study of 21 cases.* Arch Neurol, 1977. **34**(11): p. 694-700.
216. Rivers, T.M., D.H. Sprunt, and G.P. Berry, *Observations on Attempts to Produce Acute Disseminated Encephalomyelitis in Monkeys.* J Exp Med, 1933. **58**(1): p. 39-53.
217. Rivers, T.M. and F.F. Schwentker, *Encephalomyelitis Accompanied by Myelin Destruction Experimentally Produced in Monkeys.* J Exp Med, 1935. **61**(5): p. 689-702.
218. Schwentker, F.F. and T.M. Rivers, *The Antibody Response of Rabbits to Injections of Emulsions and Extracts of Homologous Brain.* J Exp Med, 1934. **60**(5): p. 559-74.
219. Zamvil, S., et al., *T-cell clones specific for myelin basic protein induce chronic relapsing paralysis and demyelination.* Nature, 1985. **317**(6035): p. 355-8.
220. Zamvil, S.S. and L. Steinman, *The T lymphocyte in experimental allergic encephalomyelitis.* Annu Rev Immunol, 1990. **8**: p. 579-621.
221. Bourquin, C., et al., *Selective unresponsiveness to conformational B cell epitopes of the myelin oligodendrocyte glycoprotein in H-2b mice.* J Immunol, 2003. **171**(1): p. 455-61.
222. Gold, R., C. Linington, and H. Lassmann, *Understanding pathogenesis and therapy of multiple sclerosis via animal models: 70 years of merits and culprits in experimental autoimmune encephalomyelitis research.* Brain, 2006. **129**(Pt 8): p. 1953-71.
223. Miceli, M.C. and J.R. Parnes, *The roles of CD4 and CD8 in T cell activation.* Semin Immunol, 1991. **3**(3): p. 133-41.
224. Leung, S., et al., *The cytokine milieu in the interplay of pathogenic Th1/Th17 cells*

and regulatory T cells in autoimmune disease. Cell Mol Immunol, 2010. **7**(3): p. 182-9.
225. Yu, D. and C.G. Vinuesa, *Multiple checkpoints keep follicular helper T cells under control to prevent autoimmunity.* Cell Mol Immunol, 2010. **7**(3): p. 198-203.
226. Nurieva, R.I. and Y. Chung, *Understanding the development and function of T follicular helper cells.* Cell Mol Immunol, 2010. **7**(3): p. 190-7.
227. Wan, Y.Y., *Regulatory T cells: immune suppression and beyond.* Cell Mol Immunol, 2010. **7**(3): p. 204-10.
228. Mendel, I., N. Kerlero de Rosbo, and A. Ben-Nun, *A myelin oligodendrocyte glycoprotein peptide induces typical chronic experimental autoimmune encephalomyelitis in H-2b mice: fine specificity and T cell receptor V beta expression of encephalitogenic T cells.* Eur J Immunol, 1995. **25**(7): p. 1951-9.
229. Hofstetter, H.H., C.L. Shive, and T.G. Forsthuber, *Pertussis toxin modulates the immune response to neuroantigens injected in incomplete Freund's adjuvant: induction of Th1 cells and experimental autoimmune encephalomyelitis in the presence of high frequencies of Th2 cells.* J Immunol, 2002. **169**(1): p. 117-25.
230. Chen, X., et al., *Pertussis toxin as an adjuvant suppresses the number and function of CD4+CD25+ T regulatory cells.* Eur J Immunol, 2006. **36**(3): p. 671-80.
231. Matthieu, J.M. and P. Amiguet, *Myelin/oligodendrocyte glycoprotein expression during development in normal and myelin-deficient mice.* Dev Neurosci, 1990. **12**(4-5): p. 293-302.
232. Amiguet, P., et al., *Purification and partial structural and functional characterization of mouse myelin/oligodendrocyte glycoprotein.* J Neurochem, 1992. **58**(5): p. 1676-82.
233. Pagany, M., et al., *Myelin oligodendrocyte glycoprotein is expressed in the peripheral nervous system of rodents and primates.* Neurosci Lett, 2003. **350**(3): p. 165-8.
234. Kuerten, S., et al., *MP4- and MOG:35-55-induced EAE in C57BL/6 mice differentially targets brain, spinal cord and cerebellum.* J Neuroimmunol, 2007. **189**(1-2): p. 31-40.
235. Meyer zu Horste, G., H.P. Hartung, and B.C. Kieseier, *From bench to bedside--experimental rationale for immune-specific therapies in the inflamed peripheral nerve.* Nat Clin Pract Neurol, 2007. **3**(4): p. 198-211.
236. Bruhns, P., et al., *Colony-stimulating factor-1-dependent macrophages are responsible for IVIG protection in antibody-induced autoimmune disease.* Immunity, 2003. **18**(4): p. 573-81.
237. Mendell, J.R., et al., *Randomized controlled trial of IVIg in untreated chronic inflammatory demyelinating polyradiculoneuropathy.* Neurology, 2001. **56**(4): p. 445-9.
238. van Swieten, J.C., et al., *Interobserver agreement for the assessment of handicap in stroke patients.* Stroke, 1988. **19**(5): p. 604-7.
239. Huang, W., et al., *Chemoenzymatic glycoengineering of intact IgG antibodies for gain of functions.* J Am Chem Soc, 2012. **134**(29): p. 12308-18.
240. Lux, A., et al., *Impact of immune complex size and glycosylation on IgG binding to human FcgammaRs.* J Immunol, 2013. **190**(8): p. 4315-23.
241. Washburn, N., et al., *Controlled tetra-Fc sialylation of IVIg results in a drug candidate with consistent enhanced anti-inflammatory activity.* Proc Natl Acad Sci U S A, 2015. **112**(11): p. E1297-306.
242. Stadlmann, J., et al., *A close look at human IgG sialylation and subclass distribution after lectin fractionation.* Proteomics, 2009. **9**(17): p. 4143-53.
243. Kuenzle, S., et al., *Pathogen specificity and autoimmunity are distinct features of*

antigen-driven immune responses in neuroborreliosis. Infect Immun, 2007. **75**(8): p. 3842-7.
244. Dale, R.C., et al., *Antibodies to MOG have a demyelination phenotype and affect oligodendrocyte cytoskeleton.* Neurol Neuroimmunol Neuroinflamm, 2014. **1**(1): p. e12.
245. Holers, V.M., *Complement and its receptors: new insights into human disease.* Annu Rev Immunol, 2014. **32**: p. 433-59.
246. Jorgensen, S.H., et al., *Intravenous immunoglobulin ameliorates experimental autoimmune encephalomyelitis and reduces neuropathological abnormalities when administered prophylactically.* Neurol Res, 2005. **27**(6): p. 591-7.
247. Fiebiger, B.M., et al., *Protection in antibody- and T cell-mediated autoimmune diseases by antiinflammatory IgG Fcs requires type II FcRs.* Proc Natl Acad Sci U S A, 2015. **112**(18): p. E2385-94.
248. von Pawel-Rammingen, U., B.P. Johansson, and L. Bjorck, *IdeS, a novel streptococcal cysteine proteinase with unique specificity for immunoglobulin G.* EMBO J, 2002. **21**(7): p. 1607-15.
249. Brostoff, S.W. and D.W. Mason, *Experimental allergic encephalomyelitis: successful treatment in vivo with a monoclonal antibody that recognizes T helper cells.* J Immunol, 1984. **133**(4): p. 1938-42.
250. O'Connor, R.A., et al., *Cutting edge: Th1 cells facilitate the entry of Th17 cells to the central nervous system during experimental autoimmune encephalomyelitis.* J Immunol, 2008. **181**(6): p. 3750-4.
251. McNally, J.P., et al., *Eliminating encephalitogenic T cells without undermining protective immunity.* J Immunol, 2014. **192**(1): p. 73-83.
252. Bettelli, E., et al., *Myelin oligodendrocyte glycoprotein-specific T cell receptor transgenic mice develop spontaneous autoimmune optic neuritis.* J Exp Med, 2003. **197**(9): p. 1073-81.
253. Achiron, A., et al., *Intravenous immunoglobulin treatment of experimental T cell-mediated autoimmune disease. Upregulation of T cell proliferation and downregulation of tumor necrosis factor alpha secretion.* J Clin Invest, 1994. **93**(2): p. 600-5.
254. Williams, J.L., et al., *Memory cells specific for myelin oligodendrocyte glycoprotein (MOG) govern the transfer of experimental autoimmune encephalomyelitis.* J Neuroimmunol, 2011. **234**(1-2): p. 84-92.
255. Clynes, R., et al., *Modulation of immune complex-induced inflammation in vivo by the coordinate expression of activation and inhibitory Fc receptors.* J Exp Med, 1999. **189**(1): p. 179-85.
256. Park, S.Y., et al., *Resistance of Fc receptor- deficient mice to fatal glomerulonephritis.* J Clin Invest, 1998. **102**(6): p. 1229-38.
257. Boross, P., et al., *The inhibiting Fc receptor for IgG, FcgammaRIIB, is a modifier of autoimmune susceptibility.* J Immunol, 2011. **187**(3): p. 1304-13.
258. Nakamura, A., et al., *Fcgamma receptor IIB-deficient mice develop Goodpasture's syndrome upon immunization with type IV collagen: a novel murine model for autoimmune glomerular basement membrane disease.* J Exp Med, 2000. **191**(5): p. 899-906.
259. Bolland, S. and J.V. Ravetch, *Spontaneous autoimmune disease in Fc(gamma)RIIB-deficient mice results from strain-specific epistasis.* Immunity, 2000. **13**(2): p. 277-85.
260. Clynes, R. and J.V. Ravetch, *Cytotoxic antibodies trigger inflammation through Fc receptors.* Immunity, 1995. **3**(1): p. 21-6.

261. Hobday, P.M., et al., *Fcgamma receptor III and Fcgamma receptor IV on macrophages drive autoimmune valvular carditis in mice.* Arthritis Rheumatol, 2014. **66**(4): p. 852-62.
262. Duits, A.J., et al., *Skewed distribution of IgG Fc receptor IIa (CD32) polymorphism is associated with renal disease in systemic lupus erythematosus patients.* Arthritis Rheum, 1995. **38**(12): p. 1832-6.
263. Song, Y.W., et al., *Abnormal distribution of Fc gamma receptor type IIa polymorphisms in Korean patients with systemic lupus erythematosus.* Arthritis Rheum, 1998. **41**(3): p. 421-6.
264. Wu, J., et al., *A novel polymorphism of FcgammaRIIIa (CD16) alters receptor function and predisposes to autoimmune disease.* J Clin Invest, 1997. **100**(5): p. 1059-70.
265. Nieto, A., et al., *Involvement of Fcgamma receptor IIIA genotypes in susceptibility to rheumatoid arthritis.* Arthritis Rheum, 2000. **43**(4): p. 735-9.
266. Floto, R.A., et al., *Loss of function of a lupus-associated FcgammaRIIb polymorphism through exclusion from lipid rafts.* Nat Med, 2005. **11**(10): p. 1056-8.
267. Kyogoku, C., et al., *Fcgamma receptor gene polymorphisms in Japanese patients with systemic lupus erythematosus: contribution of FCGR2B to genetic susceptibility.* Arthritis Rheum, 2002. **46**(5): p. 1242-54.
268. Siriboonrit, U., et al., *Association of Fcgamma receptor IIb and IIIb polymorphisms with susceptibility to systemic lupus erythematosus in Thais.* Tissue Antigens, 2003. **61**(5): p. 374-83.
269. Li, X., et al., *A novel polymorphism in the Fcgamma receptor IIB (CD32B) transmembrane region alters receptor signaling.* Arthritis Rheum, 2003. **48**(11): p. 3242-52.
270. International Consortium for Systemic Lupus Erythematosus, G., et al., *Genome-wide association scan in women with systemic lupus erythematosus identifies susceptibility variants in ITGAM, PXK, KIAA1542 and other loci.* Nat Genet, 2008. **40**(2): p. 204-10.
271. Su, K., et al., *A promoter haplotype of the immunoreceptor tyrosine-based inhibitory motif-bearing FcgammaRIIb alters receptor expression and associates with autoimmunity. I. Regulatory FCGR2B polymorphisms and their association with systemic lupus erythematosus.* J Immunol, 2004. **172**(11): p. 7186-91.
272. Blank, M.C., et al., *Decreased transcription of the human FCGR2B gene mediated by the -343 G/C promoter polymorphism and association with systemic lupus erythematosus.* Hum Genet, 2005. **117**(2-3): p. 220-7.
273. Baerenwaldt, A., et al., *Fcgamma receptor IIB (FcgammaRIIB) maintains humoral tolerance in the human immune system in vivo.* Proc Natl Acad Sci U S A, 2011. **108**(46): p. 18772-7.
274. Horton, H.M., et al., *Antibody-mediated coengagement of FcgammaRIIb and B cell receptor complex suppresses humoral immunity in systemic lupus erythematosus.* J Immunol, 2011. **186**(7): p. 4223-33.
275. Kikuchi-Taura, A., et al., *Monocyte CD64 expression as a novel biomarker for the disease activity of systemic lupus erythematosus.* Lupus, 2015.
276. Madia, F., et al., *pSTAT1, pSTAT3, and T-bet as markers of disease activity in chronic inflammatory demyelinating polyradiculoneuropathy.* J Peripher Nerv Syst, 2009. **14**(2): p. 107-17.
277. Marzo, M.E., et al., *Chronic inflammatory demyelinating polyneuropathy during treatment with interferon-alpha.* J Neurol Neurosurg Psychiatry, 1998. **65**(4): p. 604.

278. Meriggioli, M.N. and J. Rowin, *Chronic inflammatory demyelinating polyneuropathy after treatment with interferon-alpha.* Muscle Nerve, 2000. **23**(3): p. 433-5.
279. Anthoney, D.A., I. Bone, and T.R. Evans, *Inflammatory demyelinating polyneuropathy: a complication of immunotherapy in malignant melanoma.* Ann Oncol, 2000. **11**(9): p. 1197-200.
280. Hirotani, M., et al., *Chronic inflammatory demyelinating polyneuropathy after treatment with interferon-alpha.* Intern Med, 2009. **48**(5): p. 373-5.
281. Khiani, V., et al., *Acute inflammatory demyelinating polyneuropathy associated with pegylated interferon alpha 2a therapy for chronic hepatitis C virus infection.* World J Gastroenterol, 2008. **14**(2): p. 318-21.
282. Kato-Motozaki, Y., et al., *Polyethylene glycol interferon alpha-2b-induced immune-mediated polyradiculoneuropathy.* Intern Med, 2009. **48**(7): p. 569-72.
283. Shiga, K., et al., *Chronic inflammatory demyelinating polyneuropathy due to the administration of pegylated interferon alpha-2b: a neuropathology case report.* Intern Med, 2012. **51**(2): p. 217-21.
284. Tanaka, M., et al., *Activation of Fc gamma RI on monocytes triggers differentiation into immature dendritic cells that induce autoreactive T cell responses.* J Immunol, 2009. **183**(4): p. 2349-55.
285. Brownlie, R.J., et al., *Distinct cell-specific control of autoimmunity and infection by FcgammaRIIb.* J Exp Med, 2008. **205**(4): p. 883-95.
286. Takai, T., *Roles of Fc receptors in autoimmunity.* Nat Rev Immunol, 2002. **2**(8): p. 580-92.
287. Leontyev, D., Y. Katsman, and D.R. Branch, *Mouse background and IVIG dosage are critical in establishing the role of inhibitory Fcgamma receptor for the amelioration of experimental ITP.* Blood, 2012. **119**(22): p. 5261-4.
288. Crow, A.R., et al., *IVIg-mediated amelioration of murine ITP via FcgammaRIIB is independent of SHIP1, SHP-1, and Btk activity.* Blood, 2003. **102**(2): p. 558-60.
289. Park-Min, K.H., et al., *FcgammaRIII-dependent inhibition of interferon-gamma responses mediates suppressive effects of intravenous immune globulin.* Immunity, 2007. **26**(1): p. 67-78.
290. Latov, N., et al., *Timing and course of clinical response to intravenous immunoglobulin in chronic inflammatory demyelinating polyradiculoneuropathy.* Arch Neurol, 2010. **67**(7): p. 802-7.
291. Ravetch, J.V. and S. Bolland, *IgG Fc receptors.* Annu Rev Immunol, 2001. **19**: p. 275-90.
292. Belostocki, K., et al., *FcgammaRIIa is a target for modulation by TNFalpha in human neutrophils.* Clin Immunol, 2005. **117**(1): p. 78-86.
293. Clarkson, S.B., et al., *Blockade of clearance of immune complexes by an anti-Fc gamma receptor monoclonal antibody.* J Exp Med, 1986. **164**(2): p. 474-89.
294. Schwab, I., et al., *IVIg-mediated amelioration of ITP in mice is dependent on sialic acid and SIGNR1.* Eur J Immunol, 2012. **42**(4): p. 826-30.
295. Leontyev, D., et al., *Sialylation-independent mechanism involved in the amelioration of murine immune thrombocytopenia using intravenous gammaglobulin.* Transfusion, 2012. **52**(8): p. 1799-805.
296. Rombouts, Y., et al., *Anti-citrullinated protein antibodies acquire a pro-inflammatory Fc glycosylation phenotype prior to the onset of rheumatoid arthritis.* Ann Rheum Dis, 2015. **74**(1): p. 234-41.
297. Rook, G.A., et al., *Changes in IgG glycoform levels are associated with remission of arthritis during pregnancy.* J Autoimmun, 1991. **4**(5): p. 779-94.
298. van de Geijn, F.E., et al., *Immunoglobulin G galactosylation and sialylation are*

associated with pregnancy-induced improvement of rheumatoid arthritis and the postpartum flare: results from a large prospective cohort study. Arthritis Res Ther, 2009. **11**(6): p. R193.
299. Rahman, A. and D. Isenberg, *Does it take sugar? A clinical role for measuring the glycosylation of IgG?* Ann Rheum Dis, 1995. **54**(9): p. 689-91.
300. Espy, C., et al., *Sialylation levels of anti-proteinase 3 antibodies are associated with the activity of granulomatosis with polyangiitis (Wegener's).* Arthritis Rheum, 2011. **63**(7): p. 2105-15.
301. Wong, A.H., et al., *Sialylated IgG-Fc: a novel biomarker of chronic inflammatory demyelinating polyneuropathy.* J Neurol Neurosurg Psychiatry, 2015.
302. Nose, M. and H. Wigzell, *Biological significance of carbohydrate chains on monoclonal antibodies.* Proc Natl Acad Sci U S A, 1983. **80**(21): p. 6632-6.
303. Ito, K., et al., *Lack of galactosylation enhances the pathogenic activity of IgG1 but Not IgG2a anti-erythrocyte autoantibodies.* J Immunol, 2014. **192**(2): p. 581-8.
304. van de Geijn, F.E., et al., *Mannose-binding lectin polymorphisms are not associated with rheumatoid arthritis--confirmation in two large cohorts.* Rheumatology (Oxford), 2008. **47**(8): p. 1168-71.
305. van de Geijn, F.E., et al., *Mannose-binding lectin does not explain the course and outcome of pregnancy in rheumatoid arthritis.* Arthritis Res Ther, 2011. **13**(1): p. R10.
306. Idusogie, E.E., et al., *Mapping of the C1q binding site on rituxan, a chimeric antibody with a human IgG1 Fc.* J Immunol, 2000. **164**(8): p. 4178-84.
307. Ahmed, A.A., et al., *Structural characterization of anti-inflammatory immunoglobulin G Fc proteins.* J Mol Biol, 2014. **426**(18): p. 3166-79.
308. Trouw, L.A., et al., *Genetic variants in the region of the C1q genes are associated with rheumatoid arthritis.* Clin Exp Immunol, 2013. **173**(1): p. 76-83.
309. Vlam, L., et al., *Complement activity is associated with disease severity in multifocal motor neuropathy.* Neurol Neuroimmunol Neuroinflamm, 2015. **2**(4).
310. Klos, A., et al., *International Union of Basic and Clinical Pharmacology. [corrected]. LXXXVII. Complement peptide C5a, C4a, and C3a receptors.* Pharmacol Rev, 2013. **65**(1): p. 500-43.
311. Zhou, W., *The new face of anaphylatoxins in immune regulation.* Immunobiology, 2012. **217**(2): p. 225-34.
312. Hashimoto, M., et al., *Complement drives Th17 cell differentiation and triggers autoimmune arthritis.* J Exp Med, 2010. **207**(6): p. 1135-43.
313. Peng, Q., et al., *Dendritic cell synthesis of C3 is required for full T cell activation and development of a Th1 phenotype.* J Immunol, 2006. **176**(6): p. 3330-41.
314. Liu, J., et al., *IFN-gamma and IL-17 production in experimental autoimmune encephalomyelitis depends on local APC-T cell complement production.* J Immunol, 2008. **180**(9): p. 5882-9.
315. Gutzmer, R., et al., *Human monocyte-derived dendritic cells are chemoattracted to C3a after up-regulation of the C3a receptor with interferons.* Immunology, 2004. **111**(4): p. 435-43.
316. Williams, T.J. and P.J. Jose, *Mediation of increased vascular permeability after complement activation. Histamine-independent action of rabbit C5a.* J Exp Med, 1981. **153**(1): p. 136-53.
317. Fischer, E., et al., *Human eosinophils express CR1 and CR3 complement receptors for cleavage fragments of C3.* Cell Immunol, 1986. **97**(2): p. 297-306.
318. Rotshenker, S., *Microglia and macrophage activation and the regulation of complement-receptor-3 (CR3/MAC-1)-mediated myelin phagocytosis in injury and*

disease. J Mol Neurosci, 2003. **21**(1): p. 65-72.
319. Jack, R.M., B.A. Lowenstein, and A. Nicholson-Weller, *Regulation of C1q receptor expression on human polymorphonuclear leukocytes.* J Immunol, 1994. **153**(1): p. 262-9.
320. Steinberger, P., et al., *Identification of human CD93 as the phagocytic C1q receptor (C1qRp) by expression cloning.* J Leukoc Biol, 2002. **71**(1): p. 133-40.
321. Wagner, C., et al., *The complement receptor 3, CR3 (CD11b/CD18), on T lymphocytes: activation-dependent up-regulation and regulatory function.* Eur J Immunol, 2001. **31**(4): p. 1173-80.
322. Merle, N.S., et al., *Complement System Part II: Role in Immunity.* Front Immunol, 2015. **6**: p. 257.
323. Harre, U., et al., *Glycosylation of immunoglobulin G determines osteoclast differentiation and bone loss.* Nat Commun, 2015. **6**: p. 6651.
324. Pashov, A., et al., *Normal immunoglobulin G protects against experimental allergic encephalomyelitis by inducing transferable T cell unresponsiveness to myelin basic protein.* Eur J Immunol, 1998. **28**(6): p. 1823-31.
325. Ephrem, A., et al., *Expansion of CD4+CD25+ regulatory T cells by intravenous immunoglobulin: a critical factor in controlling experimental autoimmune encephalomyelitis.* Blood, 2008. **111**(2): p. 715-22.
326. Iruretagoyena, M.I., et al., *Activating and inhibitory Fcgamma receptors can differentially modulate T cell-mediated autoimmunity.* Eur J Immunol, 2008. **38**(8): p. 2241-50.
327. Rahman, Z.S., et al., *Expression of the autoimmune Fcgr2b NZW allele fails to be upregulated in germinal center B cells and is associated with increased IgG production.* Genes Immun, 2007. **8**(7): p. 604-12.
328. Andersen, J.T., et al., *Cross-species binding analyses of mouse and human neonatal Fc receptor show dramatic differences in immunoglobulin G and albumin binding.* J Biol Chem, 2010. **285**(7): p. 4826-36.
329. Covell, D.G., et al., *Pharmacokinetics of monoclonal immunoglobulin G1, F(ab')2, and Fab' in mice.* Cancer Res, 1986. **46**(8): p. 3969-78.
330. Langrish, C.L., et al., *IL-23 drives a pathogenic T cell population that induces autoimmune inflammation.* J Exp Med, 2005. **201**(2): p. 233-40.
331. Stromnes, I.M. and J.M. Goverman, *Passive induction of experimental allergic encephalomyelitis.* Nat Protoc, 2006. **1**(4): p. 1952-60.
332. Roy, E., et al., *Therapeutic efficacy of high-dose intravenous immunoglobulin in Mycobacterium tuberculosis infection in mice.* Infect Immun, 2005. **73**(9): p. 6101-9.
333. Othy, S., et al., *Intravenous gammaglobulin inhibits encephalitogenic potential of pathogenic T cells and interferes with their trafficking to the central nervous system, implicating sphingosine-1 phosphate receptor 1-mammalian target of rapamycin axis.* J Immunol, 2013. **190**(9): p. 4535-41.
334. Steinbach, K., et al., *Neutrophils amplify autoimmune central nervous system infiltrates by maturing local APCs.* J Immunol, 2013. **191**(9): p. 4531-9.
335. von Gunten, S., et al., *Siglec-9 transduces apoptotic and nonapoptotic death signals into neutrophils depending on the proinflammatory cytokine environment.* Blood, 2005. **106**(4): p. 1423-31.
336. Aoyama-Ishikawa, M., et al., *Intravenous immunoglobulin-induced neutrophil apoptosis in the lung during murine endotoxemia.* Surg Infect (Larchmt), 2014. **15**(1): p. 36-42.
337. Tangye, S.G., et al., *Identification of functional human splenic memory B cells by*

expression of CD148 and CD27. J Exp Med, 1998. **188**(9): p. 1691-703.
338. Ziegler-Heitbrock, H.W., et al., *The novel subset of CD14+/CD16+ blood monocytes exhibits features of tissue macrophages.* Eur J Immunol, 1993. **23**(9): p. 2053-8.
339. Almeida, J., et al., *Comparative analysis of the morphological, cytochemical, immunophenotypical, and functional characteristics of normal human peripheral blood lineage(-)/CD16(+)/HLA-DR(+)/CD14(-/lo) cells, CD14(+) monocytes, and CD16(-) dendritic cells.* Clin Immunol, 2001. **100**(3): p. 325-38.
340. Jung, K., W. Cho, and F.E. Regnier, *Glycoproteomics of plasma based on narrow selectivity lectin affinity chromatography.* J Proteome Res, 2009. **8**(2): p. 643-50.
341. Wu, A.M., et al., *Differential affinities of Erythrina cristagalli lectin (ECL) toward monosaccharides and polyvalent mammalian structural units.* Glycoconj J, 2007. **24**(9): p. 591-604.
342. Shibuya, N., et al., *The elderberry (Sambucus nigra L.) bark lectin recognizes the Neu5Ac(alpha 2-6)Gal/GalNAc sequence.* J Biol Chem, 1987. **262**(4): p. 1596-601.
343. Dalziel, M., I. McFarlane, and J.S. Axford, *Lectin analysis of human immunoglobulin G N-glycan sialylation.* Glycoconj J, 1999. **16**(12): p. 801-7.
344. Gagnon, P., C.W. Cheung, and P.J. Yazaki, *Reverse calcium affinity purification of Fab with calcium derivatized hydroxyapatite.* J Immunol Methods, 2009. **342**(1-2): p. 115-8.
345. Cho, M.S., H. Yee, and S. Chan, *Establishment of a human somatic hybrid cell line for recombinant protein production.* J Biomed Sci, 2002. **9**(6 Pt 2): p. 631-8.
346. Warnock, D., et al., *In vitro galactosylation of human IgG at 1 kg scale using recombinant galactosyltransferase.* Biotechnol Bioeng, 2005. **92**(7): p. 831-42.
347. Lee-MacAry, A.E., et al., *Development of a novel flow cytometric cell-mediated cytotoxicity assay using the fluorophores PKH-26 and TO-PRO-3 iodide.* J Immunol Methods, 2001. **252**(1-2): p. 83-92.
348. Holmes, K.L., et al., *Alleles of the Ly-17 alloantigen define polymorphisms of the murine IgG Fc receptor.* Proc Natl Acad Sci U S A, 1985. **82**(22): p. 7706-10.
349. Miller, S.D. and W.J. Karpus, *Experimental autoimmune encephalomyelitis in the mouse.* Curr Protoc Immunol, 2007. **Chapter 15**: p. Unit 15 1.

Abbreviations:

AAL	*Aleuria aurantia* lectin
ADCC	Antibody-dependent cell-mediated cytotoxicity
ADCP	Antibody-dependent cell-mediated phagocytosis
AID	Activation-induced deaminase
APC	Antigen presenting cell
β1,4GalT	β1,4 galactosyltransferase-1
B6 mice	C57BL/6 mice
BCR	B cell receptor
C	Cytosine
CCR	CC chemokine receptor
CD	Cluster of differentiation
CDC	Complement-dependent cytotoxicity
CDR	Complementary determining region
cDNA	Complementary DNA
CHO	Chinese hamster ovary
CIDP	Chronic inflammatory demyelinating polyneuropathy
C_L	Constant region, light chain
CNS	Central nervous system
C_H	Constant region, heavy chain
CFA	Complete Freund's adjuvant
CR	Complement receptor
CTL	Cytotoxic T lymphocyte
DC-SIGN	DC-specific intercellular adhesion molecule-3-grabbing non-integrin
dLNs	Draining lymph nodes
DNA	Deoxyribonucleic acid
EAE	Experimental autoimmune encephalomyelitis
EC_{50}	Half maximal effective concentration
ECL	*Erythrina cristagalli* lectin
ELISA	Enzyme-linked Immunosorbent Assay
EndoS	Endoglycosidase from *Streptococcus pyogenes*
FCS	Fetal calf serum
H	Histidine
hu8-18C5	Humanized 8-18C5 antibody
N-glycan	Asparagine-glycan
ER	Endoplasmatic reticulum

HC	Heavy chain
HEK293T	Human embryonic kidney cells containing the SV40 Large T-antigen
DC	Dendritic cell
F	Phenylalanine
Fab	Fragment antigen binding
$F(ab')_2$	Fragment antigen binding (disulfide-linked dimer)
FACS	Fluorescence-activated cell sorting
Fc	Fragment crystallizable
FcγR	Fcγ receptor
FcRn	Neonatal Fc receptor
FSC	Forward scatter
FSC-A	FSC-area
FCS-H	FSC-height
Fuc	Fucose
Gal	Galactose
GlcNAc	N-acetylglucosamine
GM-CSF	Granulocyte-macrophage colony stimulating factor
I	Isoleucine
i.p.	intraperitoneal
Ig	Immunoglobulin
IgA	Immunoglobulin A
IgD	Immunoglobulin D
IgE	Immunoglobulin E
IgG	Immunoglobulin G
IgM	Immunoglobulin M
IFN	Interferon
IL	Interleukin
ITAM	Immunoreceptor tyrosin-based activation motif
ITIM	Immunoreceptor tyrosin-based inhibitory motif
ITP	Idiopathic thrombocytopenic purpura
IU	International units
IVIG	Intravenous Immunoglobulin
LC	Light chain
LCA	*Lens culinaris* agglutinin
LN	Lymph node
mRNA	Messenger RNA
Man	Mannose

MBL	Mannose-binding lectin
MBP	Myelin basic protein
MFI	Median fluorescence intensity
MHC	Major histocompatibility complex
MMN	Multifocal motor neuropathy
MOG	Myelin oligodendrocyte glycoprotein
N	Asparagine
NK	Natural killer cell
PAMP	Pathogen associated molecular patterns
PBMC	Peripheral blood mononuclear cells
PBS	Phosphate buffered saline
PAGE	Polyacrylamide gel electrophoresis
PMA	Phorbol myristate acetate
Q	Glutamine
R	Arginine
RA	Rheumatoid arthritis
RNA	Ribonucleic acid
rpm	Rotations per minute
RTX	Rituximab
SDS	Sodium dodecyl sulfate
SEM	Standard error of the mean
SHM	Somatic hypermutation
SIGLEC	Sialic acid-binding immunoglobulin-type lectins
SLE	Systemic lupus erythematosus
SNA	*Sambucus nigra* agglutinin
SNP	Single-nucleotide polymorphism
ST6Gal1	α2,6-sialyltransferase
SSC-A	Side scatter area
T	Threonine (proteins)
T	Thymidine (DNA)
TBS	Tris buffered saline
TCR	T cell receptor
Tregs	Regulatory T cells
U	Uracil
V(D)J	Variable, diversity and joining elements
V_H	Variable region, heavy chain
V_L	Variable region, light chain

Declaration

Herewith I declare that I have written this thesis myself and only used the stated references.

Further,

I declare that I have performed all the experiments myself, with assistance from Christian Keller (C1q deposition assays), Patrick Weber (cloning, flow cytometry, protein purification, animal experiments) Flavio Cueni (FcγR expression in CIDP patients) and Miguel Maurer (protein purification, cloning) and with the exception of 2-AB HPLC-FL which was performed by Biswa Pronab Choudhury and colleagues

Zürich, 16.07.2015

.....

Isaak Josef Quast, Zürich, Switzerland

Curriculum vitae

PERSONAL DATA

Name:	
Address:	Hofwiesenstrasse 234, CH-8057, Zürich, Switzerland
Cell phone:	+41 77 4531229
E-mail address:	isaak.quast@uzh.ch
Nationality:	Austria
Date of birth:	24th February, 1985

EDUCATION

2010 - present	PhD at the Institute of Experimental Immunology, University of Zürich, Switzerland, Group Jan Lünemann
2003 - 2009	Master studies in Biology (specialization Genetics/Microbiology), University of Vienna, Austria
1999 – 2003	Grammar school: Oberstufenrealgymnasium Perg (Austria)

RESEARCH EXPERIENCE

06. 2010 - present: **PhD Graduate Student**
PhD under supervision of Prof. Jan Lünemann
Institute of Experimental Immunology
University of Zürich, Zürich, Switzerland
Project: FcγRIIb and IgG-Fc sialylation in autoimmune neuroinflammation

11. 2009 - 01. 2010: **Visiting Graduate Student**
Research associate within the 6th European Marie-Curie Framework Program (MRTN-CT-2005-019248) under supervision of Prof. Hartmut Hengel
Institute for Virology
Heinrich-Heine University, Düsseldorf, Germany
Project: Establishment of an *in vitro* cell culture system for human cytomegalovirus in human endothelial cells

06. 2008 - 09. 2009: **Undergraduate Student**
Master thesis under supervision of Prof. Erhard Hofer
Department of Vascular Biology and Thrombosis Research
Medical University of Vienna, Vienna, Austria
Project: “Characterization of CD94/NKG2 receptors on cytotoxic lymphocytes”

02. 2008 - 05. 2008: **Undergraduate Student**
Internship under supervision of Prof. Ernst Müllner
Department for Medical Biochemistry
Medical University of Vienna, Vienna, Austria
Project: Contribution to the elucidation of a size-sensing mechanisms in dividing mammalian cells

PUBLICATIONS

Quast I., Keller CW., Maurer MA, Giddens JP., Tackenberg B., Wang L-X., Münz C., Nimmerjahn F., Dalakas M., Lünemann JD. IgG Fc-sialylation impairs complement-dependent cytotoxicity
Under review

Quast I., Cueni F., Nimmerjahn F., Tackenberg B., Lünemann JD. Deregulated Fcg Receptor Expression in Patients with CIDP
Neurology: Neuroimmunology & Neuroinflammation. Accepted June 2015

Quast I, Lünemann JD. Fc glycan-modulated immunoglobulin G effector functions. J Clin Immunol. 2014 Jul;34 Suppl 1:S51-5. doi: 10.1007/s10875-014-0018-3. Epub 2014 Apr 24.

Maurer MA, Rakocevic G, Leung CS, **Quast I**, Lukačišin M, Goebels N, Münz C, Wardemann H, Dalakas M, Lünemann JD. Rituximab induces sustained reduction of pathogenic B cells in patients with peripheral nervous system autoimmunity. J Clin Invest. Apr 2, 2012; 122(4): 1393–1402.

TEACHING EXPERIENCE

2013	Organization and supervision of “Comprehensive course in flow cytometry” (1 week)
2011 - 2013	Tutor at the “Immunology I” block course (2 weeks) at ETH Zürich
01. 2011 - 01. 2012	Master-student supervision

FELLOWSHIPS & PRICES

2011 - present	DOC PhD fellowship of the Austrian Academy of Sciences (ÖAW)
November 2014	Travel Grant from the German Society for Immunology (DGfI) for the “44th Australasian Society for Immunology Annual Scientific Meeting”, Wollongong, Australia
August 2013	Travel Grant from the European Federation of Immunological Societies (EFIS) for the “15th International Congress of Immunology”, Milan, Italy
September 2011	Young Investigator Award; Second International Forum on Immunoglobulin Research (IFIR 2011), Barcelona, Spain

Appendix